SHOCK WAVE STRUCTURE IN GAS MIXTURES AND PLASMAS

by

S.R.M. Sinclair

Manuscript received Jan 30, 1968.

MAY 1968

UTIAS REPORT NO. 130
AFOSR 68-057€

ACKNOWLEDGEMENTS

I would like to express my sincere thanks to Dr. J.H. deLeeuw for providing the opportunity to conduct this research under his supervision. His guidance has been invaluable.

I am indebted to many fellow students and friends at the Institute for their contributions, both direct and indirect to this work. In particular I would like to thank Dr. A.A. Sonin for many conversations and suggestions concerning the plasma shock wave problem which was our common interest.

The computer time required for this study was generously provided by the Institute of Computer Science, University of Toronto.

To my wife, Helen, who typed the original copy of this report and to Mrs. J.V. Dublack who typed the master sheets, I extend my thanks for their patience in performing these arduous tasks. Mr. Collin Edge of the Department of Mechanical Engineering, Royal Military College produced the final drafted figures.

This research was supported by the Defence Research Board of Canada and by the United States Air Force Office of Scientific Research under grant AFOSR 276-66.

TABLE OF CONTENTS

NOTATION

Some symbols which have been defined locally and used only within a single section of the report do not appear in this table.

A_1, A_2	defined in Eq. 8 of Sec. 4.1
a	$\sqrt{k/mT}$
B	constant appearing in the Mott-Smith shock structure solution (see page 10).
b	collisional impact parameter
$\bar{C}$	$\bar{c}/c_m$
$\bar{c}$	random molecular velocity about the species mean
c_m	most probable random speed of a Maxwellian distribution
D	diffusion coefficient
E	(part 2) electric field strength (induced by charge separation in the ionized shock)
e	(part 2) electrostatic charge
e	base of natural logarithms
erf(Z)	$\frac{1}{2\pi}\int_0^{\infty} e^{-Z^2} dZ$
f	(part 1) distribution function of molecular velocities
	(part 2) concentration in units of its upstream value
$\bar{G}$	centre of mass velocity of a colliding pair of molecules
$\bar{g}$	relative velocity between a colliding pair
$\hat{i}$	unit vector pointing in the flow direction.
κ	signifies the complete elliptic integral of its argument
K	force constant in the inverse fifth power repulsion molecular interaction (Maxwellian molecules)
k	Boltzmann's constant
M_D	downstream infinity Mach number
M	upstream infinity Mach number
M_1	$m_1/(m_1+ m_2)$

M_2		$m_2/(m_1+ m_2)$
m, m_1, m_2		molecular mass
m_o		$m_1 + m_2$
N		molecular number density in units of the upstream infinity value
n		molecular number density
$\hat{n}$		unit vector along the line of centres at the point of closest approach in a binary molecular collisions
P(Z)		probability distribution associated with event Z
P_{ij}	=	$p_{ij} - \delta_{ij}p$
p_{ij}		pressure tensor
p		hydrostatic pressure
$\bar{q}$		heat flux vector
R, R_1, R_2, R_3		numbers selected from the random number generator
r		hard sphere molecular radius
$\mathscr{r}$		radius of influence for colliding hard spheres (e.g. for He-A collision $= r_{He} + r_A$)
Sc		(part 1) hard sphere collision cross-section
Sc_1		(part 2) ambipolar Schmidt number defined on page 43
$\mathscr{S}$	=	mu^2/kT
T		temperature
T"		temperature based on the one-one pressure tensor component ($T" = p_{11}/nk$)
$T^{\perp}$	=	$(p_{22} + p_{23})/2nk$
t		time
$\hat{t}$		unit vector perpendicular to the line of centres at the point of closest approach and in the collision plane as viewed in centre of mass coordinates
$\bar{u}$		mean flow velocity
$u_{\alpha\beta}$		velocity ratio across a normal shock
$\bar{v}$		molecular velocity
$\bar{w}$		diffusion velocity (species mean velocity relative to the overall gas mean velocity)

x	flow-direction coordinate
$\underline{dv}$	elemental volume in velocity spece e.g. $\underline{dv} = dv_1 dv_2 dv_3$ in cartesian velocity coordinates
$\underline{dc}$	similar to $\underline{dv}$ but with the origin of velocity coordinates at the mean flow velocity ($\bar{c} = \bar{v} - \bar{u}$)

Greek Symbols

γ	ratio of specific heats
δ_{ij}	$= 1$ for $i = j$ $= 0$ for $i \neq j$
λ	thermal conductivity
λ_1	upstream mean free path (for mutual collisions between light gas pairs)
μ	viscosity coefficient
η	friction coefficient for momentum transfer between diffusing species
ρ	density
ω	molecular mass ratio m_{heavy}/m_{light}
Δ	shock wave thickness based on the maximum slope of the density profile
$\Delta(\Phi(\bar{v}))$	collisional contribution to change in $\Phi(\bar{v})$
$\Phi(\bar{v})$	polynomial function of the molecular velocity

Subscripts

i,j,K,ℓ	indicate vector components
e,i	in part 2 refer to electrons and ions respectively

Superscripts

$''$	parallel to the direction of mean flow
$\perp$	perpendicular to the direction of mean flow

1. INTRODUCTION

Shock wave structure studies are to some extent the result of the proverbial "mountain climber" motivation. The shock is there. It structure could be ignored for most practical purposes, however, it is certainly not a true surface discontinuity in the gas and the question naturally presents itself - How thick is the shock and how severe are the gradients within the compression region? On the other hand, these studies do indirectly serve a very important and fundamental purpose. The plane gas dynamic shock wave is a one-dimensional transition flow problem (in the sense that significant flow changes take place over a distance scale of the order of a mean free path) with simple boundary conditions and no gas-surface interactions. It is an ideal, though rather severe, test of the kinetic theory methods used for solving non-equilibrium problems in rarefied gasdynamics.

The quantitative description of the shock transition has been the subject of a large volume of theoretical and experimental work, particularly in the last decade, although the pioneering papers appeared much earlier under the names of Becker, Thomas, Mott-Smith et al (Refs. 1, 2 and 3). Concurrent with this accumulation of knowledge about the structure of shock waves in single component gases, there has developed an interest in the study of shock transitions in gas mixtures with emphasis on mixtures of inert gases, since they are generally easier to handle both experimentally and theoretically. There have been two major contributions to this subject. The first of these, a paper published by Sherman in 1960 (Ref. 4), has been the stimulus for much of the work which followed. Sherman used Navier-Stokes equations for the over-all gas combined with a diffusion equation which is sometimes referred to as Fick's law of diffusion. This combination corresponds to the Chapman-Enskog second approximation solution of the Boltzmann equations for the binary mixture. From this system of differential equations Sherman calculated, numerically, the density profiles for the species shock compressions and the overall gas temperature profiles for various combinations of equilibrium concentration and mass ratio. The interesting result was an unexpected prediction for the density profile of a small concentration of heavy species (argon) in a predominantly light gas (helium) shock. Sherman's calculations predicted an initial pre-expansion of the argon before it compressed. The controversy over this result has not been completely resolved.

The second important contributer is Oberai (Ref. 5) who has solved the binary shock problem using an extension of Mott-Smith's famous bimodal solution for single component shock waves. The method does not reproduce the unusual result found by the Chapman-Enskog method but predicts, for all mixtures regardless of concentration ratio and mass ratio, monotonic density profiles. However, this method is based on mathematical approximations the severity of which is as difficult to evaluate as is the penalty for the approximations of the Chapman-Enskog expansion.

The main topic under consideration in this report is shock wave structure in binary mixtures with a small concentration of heavy species. In Section III, an attempt is made to isolate the origin of Sherman's result. In Section IV a Monte Carlo solution for this problem is outlined. In Section V a number of moment solutions are compared in detail with the Monte Carlo solution. Section VI concerns a different physical problem - shock structure in a weakly ionized gas with elevated electron temperature. This section contains its own introduction to the specific plasma shock problem which is considered therein, however it should be noted here that the ionized gas shock waves considered in Section VI are characterized by significant diffusive

broadening of the compression zone similar to that observed for the neutral binary mixtures with widely disparate masses.

Some of the solutions for single component shock structure are outlined in Section II. This is not a comprehensive review of that topic but a collection of those fundamental methods which will be used directly or referred to in the discussion of shock waves in gas mixtures.

II. SINGLE COMPONENT SHOCK WAVE THEORIES

The list of important contributions to the subject of plane shock wave theory is quite long; however, only a small number of fundamentally different methods have been used to attack this transition flow problem. It will be necessary to refer to some of these methods in detail in later sections. Although the multi-component shock structure problem differs in many respects from the single component case, the main feature, namely, significant changes in flow properties over the distance of a mean free path, is common to both. Moreover, for the problems treated in this report, one species is present in very small quantities with the result that the dominant species shock is essentially one-component in nature. A collection of some of the fundament ideas of the one-component solutions will serve as an introduction to shock wave theory as well as a review of some of the more important approximate solution methods for the Boltzmann equation. The following methods will be reviewed: the Chapman-Enskog expansion method, the moment equation approximation and BGK modelling of the Boltzmann collision term. (Readers familiar with this material should turn to the binary mixture considerationsof Section III.)

2.1 Navier-Stokes Shock Structure

An important contribution to the shock structure theory is based on the Navier-Stokes equations of continuum fluid flow. Although the general shock structure problem with its strong flow gradients on a mean free path scale violates the basic assumptions of the continuum theory, experimental evidence confirms that Navier-Stokes (N.S.) shock wave theory is a reasonable description for low Mach numbers ($M < 2$). Since the equations themselves are universally familiar to fluid-dynamicists, this is an instructive introduction to shock structure as well as being historically the starting point for the subject.

The Navier-Stokes equations are usually derived, in their continuum context, as macroscopic balance equations for the conservation of mass, momentum, and energy of the fluid in conjunction with the classical Fourier law of heat conduction and a linear relation between shear stress and rate of deformation. It is known, however, that the N.S. equations correspond to the second approximation in the Chapman-Enskog (C.-E.)solution for the Boltzmann kinetic equation. The flow variables, such as number density and mean velocity, are defined in kinetic theory as moments of the distribution function $f(\bar{v},\bar{x},t)$ where f is the probable number density in six-dimensional $(\bar{v},\bar{x})$ - space (-probable in the sense that it is conceived to represent an average over a large number of replications of the same macroscopic problem with different microscopic boundary or initial conditions for the individual particles in the flow.) The symbol for local number density, $n(\bar{x},t)$ then represents a probable number density since

$$n(\bar{x},t) = \int f(\bar{v},\bar{x},t)\ \underline{dv} \qquad (1)$$

where $\underline{dv}$ represents an infinitesimal "volume" element in velocity space e.g. $\underline{dv} = dv_1 dv_2 dv_3$ in a cartesian coordinate frame.

This distribution function must satisfy the Boltzmann integro-differential equation (B E) for conservation of mass in phase space. For the one-dimensional steady shock problem the B E has the form

$$v_x \frac{df}{dx} = \iiint \left(f(\bar{v}')\ f(\bar{v}_1') - f(\bar{v})\ f(\bar{v}_1) \right) |\bar{v} - \bar{v}_1|\ b\,db\,d\epsilon\,d\underline{v}_1 = \left(\frac{\partial f}{\partial t}\right)_{coll} \qquad (2)$$

where b and ϵ are the impact parameter and collision orientation angle shown below

$\bar{v}$ is the velocity of the observed group before collision

$\bar{v}_1$ is the velocity of the collision partner group before collision

The primed velocities are the resultant velocities of the two groups after collision

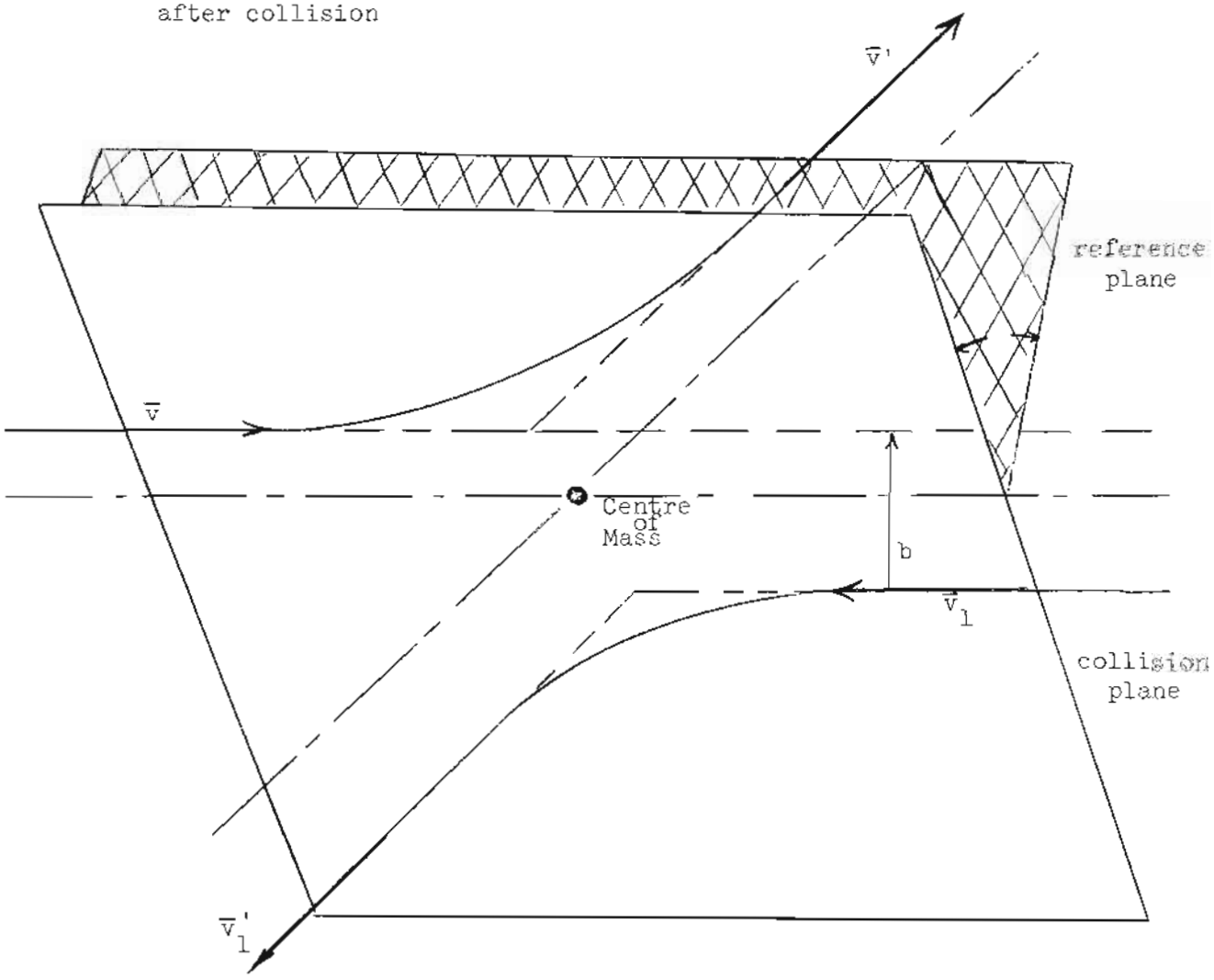

The Chapman-Enskog scheme looks for solutions to the B.E. for which the distribution function is expanded as a series of correction terms,

$$f = f^{0} + f^{1} + f^{2} + \ldots, \tag{3}$$

and where f^{0} is a local Maxwellian

$$f^{0} = \frac{n}{(2\pi k/m\Gamma)^{3/2}} \; e^{-\frac{m}{2kT} c_K c_K} \tag{4}$$

(the rectangular cartesian tensor notation $c_K c_K = c_1^2 + c_2^2 + c_3^2$ is used)

$n = \int f \, \underline{dv}$ is the local mean number density

$u_i = \frac{1}{n} \int v_i \, f \, \underline{dv}$ the local mean velocity

$c_i = v_i - u_i$ the particle random velocity component

$p = \frac{m}{3} \int c_K c_K \, f \, \underline{dc}$ the kinetic pressure

$T = p/nk$ the temperature, by definition.

The formalism for setting up and solving the approximate equations for the $f^1, f^2, \ldots$ in order is elaborated in Chapter 7 of Ref. 6 and will not be reproduced here in detail. The exact conservation equations are derived by multiplying Eq. 2 by m, mv_i, $mv_K v_K/2$, in turn and integrating over all of velocity space. The collisional term on the R.H.S. contributes nothing to these moment equations since, for a single component gas, mass, momentum and energy of the species are conserved in each collision. The resulting moment equations are then:

$$\frac{d}{dx}(nu) = 0 \tag{5}$$

$$u \frac{du}{dx} + \frac{1}{\rho} \frac{dp_{11}}{dx} = 0 \tag{6}$$

$$\frac{3}{2} u \frac{dp}{dx} + \frac{3}{2} p \frac{du}{dx} + p_{11} \frac{du}{dx} + \frac{dq_1}{dx} = 0 \tag{7}$$

$$p_{11} = m \int c_1^2 \, f \, \underline{dc}$$

$$q_1 = \frac{m}{2} \int c_1 c^2 f \, \underline{dc}$$

The influence of the collision term shows up only indirectly in the expressions for p_{11}, q_1.

At each stage the approximate equation is solved for f^i and the distribution function approximated by all terms up to and including f^i is used to derive approximate values of q_1 p_{11}. In this solution method the successive correction terms for f are represented in terms of the three basic flow quantities n,u,T and their gradients. The conservation equations with the approximate forms of

q_1, p_{11} represent a closed system of differential equations which can be, theoretically at least, solved for the appropriate boundary conditions.

In first approximation

$$f \simeq f^0$$

$$(p_{11})^0 = p$$

$$q_1{}^0 = 0$$

To this approximation the flow equations are the non-dissipitive Euler equations;

$$\frac{d}{dx}(nu) = 0 \tag{8}$$

$$u\frac{du}{dx} + \frac{1}{\rho}\frac{dp}{dx} = 0 \tag{9}$$

$$\frac{5}{2}u\frac{dp}{dx} + \frac{3}{2}p\frac{du}{dx} = 0 \tag{10}$$

The second approximation yields

$$f \simeq f^0 + f^1$$

$$(p_{11})^1 = p - \frac{4}{3}\mu\frac{du}{dx}$$

$$(q_1)^1 = -\lambda\frac{dT}{dx}$$

The second approximation (N.S.) equations are

$$\frac{d}{dx}(nu) = 0 \tag{11}$$

$$u\frac{du}{dx} + \frac{1}{\rho}\frac{dp}{dx} - \frac{4}{3}\frac{1}{\rho}\frac{d}{dx}\left(\mu\frac{du}{dx}\right) = 0 \tag{12}$$

$$\frac{5}{2}u\frac{dp}{dx} + \frac{3}{2}p\frac{du}{dx} - \frac{4}{3}\mu\left(\frac{du}{dx}\right)^2 - \frac{d}{dx}\left(\lambda\frac{dT}{dx}\right) = 0 \tag{13}$$

where μ, λ are respectively the coefficients of viscosity and heat conduction. Values for these coefficients can be derived for any specific molecular collision model or may be specified from empirical data. (See Appendix B.)

This set of coupled differential equations must be solved with the plane shock wave boundary conditions.

$$\frac{d}{dx} \to 0 \qquad \text{as } x \to \pm\infty$$

$$\rho, T, u \to \rho_1, T_1, u_1 \text{ as } x \to -\infty \tag{14}$$

Integrated once with respect to x the N.S. conservation equations become:

$$\rho u = \text{constant} = \rho_1 u_1 \tag{15}$$

$$p + \rho u^2 - \mu \frac{du}{dx} = p_1 + \rho_1 u_1^2 \tag{16}$$

$$\rho u \left(\frac{5}{2} p/\rho + u^2/2 \right) - u \mu \frac{du}{dx} - \lambda \frac{dT}{dx} = \rho_1 u_1 \left(\frac{5}{2} \frac{p_1}{\rho_1} + u_1^2/2 \right) \tag{17}$$

The pair of first order ordinary differential equations, Eqs. 16 and 17, must be integrated numerically, incorporating in the solution a specific temperature dependence for the transport coefficients μ, λ. Gilbarg and Paolucci (Ref.7) have summarized the results from a number of different choices for this temperature dependence. Their paper is an extension of the early works of Becker and Thomas, who first treated the detailed shock structure using N.S. equations.

Some interesting features of this second approximation solution can be observed from the phase space (velocity, temperature) diagram for N.S. shock structure sketched in Fig. 1. The equilibrium points X_1 and X_2 correspond to the $x = -\infty$ and $x = +\infty$ physical coordinates respectively. Roots of the characteristic equation for the system show that X_2 is a saddle point and X_1 is nodal. The stable nature of integration procedures which proceed along the integral curves toward the nodal point is illustrated in Figure 1. The solid line represents the integral curve corresponding to the shock wave boundary conditions at X_1. The dashed lines represent solutions to this set of differential equations which do not pass through the downstream equilibrium point. All solutions converge toward the nodal point. The stable direction for numerically integrating the system is, then, from downstream to upstream i.e. from X_2 to X_1. This is a peculiar feature of the C.E. equations. Other methods used for solving the shock structure problem integrate stably from upstream to downstream. The envelope curves (a) and (b) correspond to $\mu = 0$ and $\lambda = 0$ respectively. There is a continuous N.S. solution to the shock structure problem for zero heat conduction or zero viscosity but not for both $\mu = 0, \lambda = 0$.

Since the Navier-Stokes solution assumes implicitly that gradients on a mean free path scale are small it might be anticipated that the solution could be improved by including further terms in the expansion. Shock structure calculations have been made using the next higher order set of equations in this sequence however, the third approximation equations (Burnett equations), unlike the N.S. equations, do not give solutions to the shock wave problem for Mach numbers greater than about 2.2.

2.2 Moment Equation Methods

Unlike the Chapman-Enskog method in which a series solution of the Boltzmann equation is attempted a different method consists of replacing the Boltzmann equation by a system of velocity moments of that equation. These so-called moment equations are derived by multiplying the entire BE by a sequence of particle velocity component polynomials and, for each member of the sequence, integrating over the entire range of velocity space.

For instance, if $\Phi(\bar{v})$ is one of a sequence of velocity polynomials

$$(\Phi = m,\ mv_i,\ mv^2, \ldots)$$

the corresponding moment equation is

$$\int \Phi(\bar{v}) \left[\frac{\partial f}{\partial t} + v_i \frac{\partial f}{\partial x_i} + \frac{F_i}{m} \frac{\partial f}{\partial v_i} = \left(\frac{\partial f}{\partial t}\right)_{coll} \right] \underline{dv} \qquad (1)$$

The dependent variables of this system of equations are the moments of the distribution function resulting from the integration indicated in the general moment equation i.e.

$$n = \int f \, \underline{dv}$$

$$u_i = \frac{1}{n} \int v_i f \, \underline{dv}$$

and where $c_i = v_i - u_i$

$$p_{ij} = m \int c_i c_j f \, \underline{dc}$$

$$P_{ij} = m \int \left(c_i c_j - \frac{1}{3} c^2 \delta_{ij}\right) f \underline{dc}$$

(p_{ij} is the complete pressure tensor; P_{ij} is formed from p_{ij} by subtracting the trace from each diagonal term i.e. $P_{ij} = p_{ij} - \delta_{ij} p$ where $p = \frac{m}{3} \int c^2 f \, \underline{dc}$, the so-called hydrostatic pressure).

In this way, the single Boltzmann integro-differential equation can be replaced by a set of coupled partial differential equations. However, no finite group of moment equations, in the general case, will form a closed set. The essential step in the moment method is to prescribe the form of the distribution function in terms of a finite number of its moments. The number of independent variables in the moment equations will then be limited to the number used to describe f and this same number of moment equations will necessarily form a closed set.

The most famous example of the moment method is the Grad 13-moment solution to the BE. The 13-moment equations have been used to solve a wide range of kinetic theory problems including shock structure for a limited set of low Mach number cases. In this approximate solution the distribution function is expanded about a local equilibrium state in terms of Hermite velocity polynomials keeping the first thirteen terms (Ref. 8,9):

$$f = \frac{n}{(2\pi k/mT)^{3/2}} e^{-\frac{mc^2}{2kT}} \left\{1 + \frac{P_{ij}}{2nkT}\left(\frac{c_i c_j}{k/m\ T}\right)\right.$$

$$\left. + \frac{q_i c_i}{nkT\ k/mT}\left(1 - \frac{c^2}{5k/mT}\right)\right\} \qquad (2)$$

The 13 unknown flow variables in this case are:

$$n(\text{or } \rho),\ u_i,\ T\ (\text{or } p),\ P_{ij},\ q_i$$

The 13-moment equations are derived by choosing

$$\phi = m,\ mc_i,\ mc^2,\ m(c_i c_j - \tfrac{1}{3}\delta_{ij} c^2),\ m\, c_i c^2$$

and the equations then can be written:

$$\frac{\partial \rho}{\partial t} + \frac{\partial}{\partial x_K}(\rho u_K) = 0 \qquad (3)$$

$$\frac{\partial u_i}{\partial t} + u_K \frac{\partial u_i}{\partial x_K} + \frac{1}{\rho}\frac{\partial P_{iK}}{\partial x_K} = 0 \qquad (4)$$

$$\frac{\partial p}{\partial t} + \frac{\partial}{\partial x_K}(pu_K) + \frac{2}{3} P_{iK}\frac{\partial u_i}{\partial x_K} + \frac{2}{3}\frac{\partial q_K}{\partial x_K} = 0$$

$$\frac{\partial p_{ij}}{\partial t} + \frac{\partial}{\partial x_K}(u_K p_{ij}) + \frac{2}{5}\left(\frac{\partial q_i}{\partial x_i} + \frac{\partial q_i}{\partial x_j} - \frac{2}{3}\delta_{ij}\frac{\partial q_K}{\partial x_K}\right)$$

$$+ p_{iK}\frac{\partial u_j}{\partial x_K} + p_{jK}\frac{\partial u_i}{\partial x_K} - \frac{2}{3}\delta_{ij}\, p_{K\ell}\frac{\partial u_K}{\partial x_\ell}$$

$$+ p\left(\frac{\partial u_i}{\partial x_i} + \frac{\partial u_i}{\partial x_i} - \frac{2}{3}\delta_{ij}\frac{\partial u_K}{\partial x_K}\right) = \left(\overline{\Delta p_{ij}}\right)_{coll} \qquad (5)$$

$$\frac{\partial q_i}{\partial t} + \frac{\partial}{\partial x_K}(u_K q_i) + \frac{7}{5} q_K \frac{\partial u_i}{\partial x_K} + \frac{2}{5} q_i \frac{\partial u_K}{\partial x_i} + \frac{2}{5} q_i \frac{\partial u_K}{\partial x_K}$$

$$+ \frac{k}{m} T \frac{\partial p_{iK}}{\partial x_K} + \frac{7}{2} p_{iK}\frac{k}{m}\frac{\partial T}{\partial x_K} - \frac{p_{iK}}{\rho}\frac{\partial P_{K\ell}}{\partial x_\ell}$$

$$+ \frac{5}{2} p \frac{\partial}{\partial x_i}(k/m\ T) = (\overline{\Delta q_i})_{coll} \qquad (6)$$

$(\overline{\Delta p_{ij}})_{coll}$, $(\overline{\Delta q_i})_{coll}$ are the collisional contributions to stress and heat flux equations and depend upon the molecular collision model. This set of 13 first order partial differential equations is hyperbolic, that is, the system will propagate disturbances at a set of finite characteristic speeds. This feature of moment equation solutions has been discussed by Grad (Ref. 10) and Holway (Ref. 11) and will be dealt with in connection with the binary shock problem in Sec. V. However, at this point it should be noted that the fastest characteristic speed of the system represents an upper limit on the shock speed for which these equations can give a continuous unique solution. The characteristic speeds for the 13-moment equations are:

$$\tau = 0, \quad \pm \sqrt{4.54\ k/mT} \ , \quad \pm \sqrt{.661\ k/mT}$$

These equations are incapable of describing the structure of shock waves travelling at Mach numbers greater than M = 1.65

(M = 1.65 corresponds to the fast characteristic speed, $\tau = \sqrt{4.54\ k/mT} = 1.65\sqrt{\frac{\gamma kT}{m}}$)

A second moment method, much simpler but very well suited for the particular problem of steady plane shock structure is the solution first proposed by Mott-Smith* As in the previous case, a form for the distribution function is assumed, this time a so-called "bimodal" Maxwellian is chosen rather than an expansion about a local equilibrium state. The bimodal distribution has the following form:

$$f = n_1(x)\ f_1^{\,o} + n_2(x)\ f_2^{\,o} \tag{7}$$

where

$$f_\alpha^o = \left(\frac{m}{2\pi kT_\alpha}\right)^{3/2} \exp\left\{ - \frac{m}{2kT_\alpha} \ (\bar{v} - \bar{u}_\alpha)^2 \right\}$$

$$\bar{u}_\alpha = \hat{i}\ u_\alpha \qquad (\alpha = 1, 2)$$

where $\hat{i}$ is the 1-D flow-direction unit vector

and (u_1,T_1), (u_2,T_2) are respectively the upstream infinity and downstream infinity values of the mean velocity and temperature. For given initial conditions (u_1,T_1) the Rankine-Hugoniot values for (u_2,T_2) are given by the moment equations for the conserved quantities - mass, momentum and energy.

(1) $\Phi = 1$

$$u_1 \frac{d\ n_1}{dx} + u_2 \frac{d\ n_2}{dx} = 0 \qquad \text{i.e.} \quad n_1u_1 + n_2u_2 = n_{1_0}u_1 \tag{8}$$

(2) $\Phi = v_x$

$$(u_1^2 + a_1^2) \frac{d\ n_1}{dx} + (u_2^2 + a_2^2) \frac{d\ n_2}{dx} = 0 \tag{9}$$

$$a_i^2 = k/m\ T_i$$

(3) $\Phi = v^2$

$$u_1(u_1^2 + 5a_1^2) \frac{d\ n_1}{dx} + u_2\ (u_2^2 + 5a_2^2) \frac{d\ n_2}{dx} = 0 \tag{10}$$

The boundary conditions on the two dependent variables $n_1(x)$, $n_2(x)$ are:

*Mott-Smith (M.S.)

$$
\begin{aligned}
&n_1(x) \to n_{1_0} \quad \text{as } x \to -\infty \\
&n_2(x) \to 0 \\
&\\
&n_1(x) \to 0 \quad \text{as } x \to \infty \\
&n_2(x) \to u_1/u_2
\end{aligned}
\tag{11}
$$

Equations (9) and (10) give the Ranke-Hugoniot relations:

$$u_1^2 + a_1^2 = u_1/u_2 \,(u_2^2 + a_2^2)$$

$$u_1^2 + 5a_1^2 = u_2^2 + 5a_2^2$$

Equation (8) gives $n_2(x)$ in terms of $n_1(x)$.

One further moment equation is required for the determination of the spatial dependence of $n_1(x)$. Usually the equation corresponding to $\Phi = v_x^2$ is used.

$$u_1(u_1^2 + 3a_1^2)\frac{dn_1}{dx} + u_2(u_2^2 + 3a_2^2)\frac{dn_2}{dx} = (\overline{\Delta v_x^2})_{coll} \tag{12}$$

where

$(\overline{\Delta v_x^2})_{coll}$ is the total collisional contribution

$$\int\int\int (v'^2_x - v_x^2)\, f(\bar{v})\, f(\bar{v}_1)\, |\bar{v} - \bar{v}_1|\, b\, db\, d\epsilon\, \underline{dv}\, \underline{dv_1}$$

(see sketch on page 3)

This integral was evaluated for hard spheres and the Sutherland collision model by Mott-Smith. (The necessary integrations are reproduced in Appendix A for hard spheres and Maxwellian molecules.)

The solution of Eq. 12 is:

$$n_1(x) = \frac{n_{1_0}}{1 + e^{Bx/\lambda_1}}$$

where B is a function of the shock Mach number derived from the collision integral and can be found in tabular form for various molecular models in the literature (Ref. 3, 11). The quantity λ_1 is the upstream equilibrium mean free path and the distance scaling parameter for the problem.

This simple solution is, perhaps unexpectedly, a very good approximation for the structure of high Mach number shocks ($M > 2$). In these cases the shock region is relatively thin, in the range of 2 to 4 upstream mean free paths. It is, then, reasonable to assume that at any point in the compression region, the distribution function contains contributions from both the bounding Maxwellians which have not suffered collisions in the compression zone. This is especially true of the upstream cold Maxwellian which is streaming into the shock. The Mott-Smith distribution function reproduces this feature of the high Mach number shocks in detail. It is not surprising that this solution

becomes less accurate (on the basis of density profile thickness comparisons with experimental values) at very low Mach numbers where the shock wave represents a much more gradual change involving many collisions, on the average, per particle. The distribution function in these cases evolves with only minor distortions from local Maxwellian and does not develop the two stream nature.

Many modifications have been made to these two basic moment methods. Ziering et al tried to improve the simple Mott-Smith solution by using a 3-mode Maxwellian distribution: (Ref. 12)

$$f = n_1(x) f_1^{\,o} + n_2(x) f_2^{\,o} + n_3(x) \quad \frac{(v_x - u_3)}{k/m\, T_3} \quad f_3^{\,o}$$

(The first two terms are the same as in Mott-Smith's solution. Term 3 is a modified intermediate Maxwellian.)

Holway produced results giving similar agreement with experimental results over a large Mach number range by modifying the "downstream Maxwellian" part of the M.S. distribution function. His method can be described as an expansion of the distribution function less the upstream streaming portion, i.e. $(f - n_1(x) f_1^{\,o})$, in ellipsoidal polynomials. In reference 11 Holway has carried out the solution keeping only the first term of the expansion i.e.

$$f = \frac{n_1(x)}{(2\pi k/m T_1)^{3/2}} \; e^{-\frac{m}{2kT_1}(\bar{v} - \hat{i}\, u_1)^2}$$

$$= \frac{n_2(x)}{(2\pi k/m)^{3/2}} \quad \frac{1}{\lambda_{21}^{\frac{1}{2}}} \quad \frac{1}{\lambda_{22}} \; e^{-\frac{m}{2k\lambda_{21}}(v_x - u_2)^2} \; e^{-\frac{m}{2k\lambda_{22}}(v_2^{\,2} + v_3^2)}$$

u_1, T_1 are the upstream disturbed mean velocity and temperature, $u_2(x)$, $\lambda_{21}(x)$, $\lambda_{22}(x)$ are additional flow variables to be determined from the moment equations along with $n_1(x)$, $n_2(x)$. The quantities λ_{21}, λ_{22} are temperatures of the expanded portion of the distribution in the flow and perpendicular directions. The downstream boundary conditions are then

$$u_2(x) \to u_2$$

$$\lambda_{21},\ \lambda_{22} \to T_2$$

where u_2, T_2 are the downstream equilibrium mean velocity and temperature.

The extra freedom of this solution also produces more agreeable low Mach number results.

2.3 BGK Model Equation

The two previous methods sought approximate solutions to the exact Boltzmann equation. A basically different approach seeks exact solutions to an approximate form of the Boltzmann equation which uses a simplified model for the collision integral. Solutions to the BGK modelled B.E. (Ref. 13) for plane shock boundary conditions are of this type.

The BGK equation is not to be considered a substitute for the B.E. It will, at best, give a reasonable qualitative indication of the important effects or trends in a gas kinetic problem. However, because of its simplicity and its proven performance in many other problems, the BGK shock wave solution is of some interest. In particular, it shows that the distribution function in high Mach number shocks is in fact strongly bimodal as the Mott-Smith solution presupposes.

The BGK equation for the one-dimensional flow problem has the following form:

$$v_x \frac{df}{dx} = nK[F-f] \tag{1}$$

where F has a Maxwellian form with local mean velocity and temperature.

The complicated integral on the right hand side of the B.E. has been replaced by a relaxation model. Molecules are disappearing from the $\bar{v}$-group at a rate

$$L = n\,K\,f \tag{2}$$

If K were considered to be a function of the molecular velocity $\bar{v}$, this "LOSS" contribution to the collisional change in f would have the same form as the exact Boltzmann expression i.e.

$$\begin{aligned} L_B &= nf \int f_1 |\mathbf{v}-\mathbf{v_1}| b\, db\, d\epsilon\, \underline{dv_1} \\ &= n\,f\,K_B(\bar{v}) \end{aligned} \tag{3}$$

As a simplification, K is usually taken to be some mean collision frequency dependent upon the local mean flow properties but independent of the velocity group being considered. The "GAIN" collision term is much more severely modelled. The function F is a Maxwellian distribution with mean velocity and temperature equal to the true local values of these quantities. The molecules redistributed by collisions are assumed to reappear, fully Maxwellianized, about the mean flow velocity.

The model can only be judged critically on the basis of its results. However, it is interesting to notice that the two main assumptions in the modelled collision term find some support in the actual collisional behaviour of two extreme collision models - hard elastic spheres and Maxwellian (5th power law repulsive) molecules. For Maxwellian molecules the collision frequency is independent of molecular velocity as assumed in the collisional loss term of the BGK equation. On the other hand, in a collision between hard elastic spheres the probability of scattering the relative velocity vector in any direction about the centre of mass velocity is proportional to the solid angle into which the scattering occurs and is independent of direction i.e. the scattering pattern

is symmetrical about the centre of mass velocity (see Sec. 4.3). The BGK "GAIN" term requires the scattering to be not only symmetrical but the velocity distribution to be Maxwellian.

The Boltzmann integro-differential equation has been replaced, then, by the much simpler first order differential equation, Eq. 1, the solution to which can be written:

$$f_{\pm}(v_x \gtrless 0,\ v_y, v_z, x) = \int_{\pm\infty}^{x} \frac{nK}{v_x} F \exp\left\{-\int_{x'}^{x} \frac{nK}{v_x}\, dx''\right\} dx' \qquad (4)$$

where

$$F = \frac{n}{(2\pi k/mT)^{3/2}}\, e^{-\frac{m}{2kT}(\bar{v}-\hat{i}u)^2}$$

$$n = \int f(\bar{v},x)\, \underline{dv} \qquad (5)$$

$$u = \frac{1}{n}\int v_x\, f(\bar{v},x)\, \underline{dv} \qquad (6)$$

$$T = \frac{m}{3nk}\int (\bar{v}-\hat{i}u)^2\, f(\bar{v},x)\, \underline{dv} \qquad (7)$$

It is evident that an initial approximation to the spatial dependence of the three moments n, u, T through the shock wave is sufficient to start an iterative solution procedure for the set of equations 4, 5, 6 and 7. These initial estimates can be used in the R.H.S. of Eq. 4 to determine $f_{\pm}$ (1st approx.) at a set of discrete points in the phase space. This discrete representation of f is then used in equations 5, 6 and 7 to derive new number density, velocity and temperature profiles. The procedure is repeated to convergence, giving final profiles for the BGK shock wave solution. The problem as stated appears to be straight-forward; however it entails truncated numerical integrations over the infinite velocity space as well as the single physical space coordinate. Such procedures require very great care to ensure acceptable accuracy for reasonable computation times. Chahine and Narasimha (Ref. 14) have performed these computations, integrating as many as 15 times when required. Their results for inverse shock thickness based on the maximum slope of the density profile are plotted in Fig. 2 along with results for the other solutions described in this section. The most interesting feature of the BGK results is the predicted shape of the distribution function within high Mach number shock waves. Starting with the N.S. approximation as the zeroth iterate, the distribution function develops a pronounced double-maximum form similar to the Mott-Smith distribution. This can be seen in Fig. 3. The BGK distribution function at an intermediate point in a Mach 10 shock is plotted as a function of the flow direction random velocity component for a series of perpendicular velocities. The double-maximum shape is very pronounced for small values of the perpendicular velocity component. This is a strong indication that the Mott-Smith solution gives a reasonable microscopic picture as well as accurate mean flow profiles.

All theories described in the previous sections are based on mathematical approximations, the implications of which can only be accurately determined empirically. Such comparison is possible in the single component case because there exists a sufficient volume of independent experimental determinations of shock density profiles. The range of experimentally observed shock density thicknesses is indicated in Fig. 1.

All of the curves of Fig. 1 have the same basic shape starting from inverse thickness equal zero at Mach 1. (This corresponds to an infinitely thick shock. The ordinate of this plot is λ_1/Δ where λ_1 is the upstream mean free path and Δ is the maximum slope density thickness of the shock.) The various methods predict a maximum in the neighbourhood of M = 3 and a very gradual decrease towards an asymtotic value at higher Mach numbers. It is important to note the dependence of absolute shock thickness on Prandtl number referring to the Navier-Stokes curves. A good deal of caution is required when comparing experimental results with the calculations for a specific molecular model. When the theoretical analysis is of the Navier-Stokes type, the Prandtl number and the viscosity-temperature dependence can be matched with the experimental value. For other kinetic theory methods a correspondence between the theoretical model of the gas and the actual gas collision properties is not so easily attained.

III. THE ANOMALOUS PRE-ACCELERATION OF THE CHAPMAN-ENSKOG SOLUTION

Sherman (Ref. 4) has shown that the Chapman-Enskog second approximation shock solution for a helium-argon mixture with an equilibrium molecular fraction of 2% argon at a shock Mach number of 2, predicts a pre-expansion of the heavy gas before its eventual shock compression to the downstream Rankine-Hugoniot value (see Fig. 4 and 5 of Ref. 4). Predictably, since this result defies intuitive explanation, Dr. Sherman's paper has been followed by a number of others, each presenting a point of view about the origin of this usual behaviour. Certainly much of the interest in this solution is academic; nevertheless, it is important to determine whether it is a real physical phenomenon or a mathematical anomaly.

Liu (Ref. 15) in a short note, has made some important observations regarding the pre-acceleration. He has shown, first of all, that the initial expansion of the heavy gas is not caused by the nonlinear effects of strong shock waves but occurs, in the C.-E. solution, even for limiting weak shocks. He has also shown why the Burnett stresses, i.e. the correction terms associated with the third approximation, are too small to account for the anomaly.

Oberai, (Ref. 5) as noted earlier, has recalculated the troublesome cases using an extension of the single component shock structure solution proposed by Mott-Smith. For binary mixtures the distribution function for each of the two species in Oberai's solution has the same bimodal form,

$$f^i = n_1(x)\, f_1^i + n_2(x)\, f_2^i \qquad (1)$$

where

$$f_\alpha{}^i = \left(\frac{m_i}{2\pi k T_\alpha}\right)^{3/2} \exp\left\{ - \frac{m_i}{2kT_\alpha} (\bar{v} - \hat{1}\, u_\alpha)^2 \right\}$$

As in the single component solution, u_1, T_1 are common to both species and are the upstream equilibrium values of mean velocity and temperature. The values of u_2, T_2 vary with position but at any position are common to both species. They are chosen to satisfy the overall conservation of momentum and energy within the shock. It is obvious that for the cases of interest here where one species dominates the flow, u_2, T_2 will not vary much from the downstream equilibrium mean velocity and temperature since in the limit as $\frac{n_{heavy}}{n_{light}} \to 0$ they take on these constant values exactly. The distribution function for the argon is, then, even more sharply double-peaked than the helium distribution. Oberai has selected the v_x^2-moment equations for each species to solve the problem for a Maxwellian molecular collision approximation. The density profiles calculated from this solution are monotonic.

Oberai's solution is a very interesting addition to the theory of binary shock structure. However, it is something less than a completely satisfactory contradiction of the C.-E. result. The moment solution is not an exact solution to the problem and it is difficult to assess the consequences of the assumptions on which it is based. For example, the argon distribution function is forced to be similar to the helium distribution at all points (but with sharper peaks because of the smaller random speed of the heavy argon molecules.) It will be shown rather conclusively in the next section that the argon distribution function evolves in a very different way from this. Still it is the contention of this report that Oberai's solution is qualitatively correct, although the rigidity imposed on the distribution function causes it to err in detail.

The Chapman-Enskog solution for the binary mixture gas flow problem is described in detail in Chapter VIII of Chapman and Cowling's book (Ref. 6). The distribution function for each species, f^i, satisfies a Boltzmann equation for that species including a collision term for cross-collisions with the second type molecules. Each of these distribution functions is expanded in a sequence of correction terms with the first approximation term being a Maxwellian with mean velocity and temperature equal to the local flow mean values i.e.

$$f^i = f_o^i + f_1^i + f_2^i + \ldots . \qquad (2)$$

where

$$f_o^i = \frac{n_i}{(2\pi k/m_i T)^{3/2}} \exp\left\{ - \frac{m_i}{2kT} (\bar{v} - \bar{u})^2 \right\}$$

$\bar{u}, T$ are the overall flow mean velocity and temperature.

This point is important and it can be emphasized in terms of the specific problem under consideration. If the argon is present only in trace quantities, the helium dominates the flow and $\bar{u}$ and T of the overall flow will be very nearly equal to the helium mean velocity and temperature. If is a different story for the trace of argon. The cross-collisions between helium and argon atoms do not communicate energy or momentum difference efficiently because of the large difference in mass between the two types of particles. The argon mean velocity may be substantially different from the overall mean flow within the shock. It would seem more reasonable to expand the distribution function of each species about the local mean velocity and mean random energy of that species, however such a modification does not fit into the C.-E. formal solution.

In the C-E. method, a sequence of specific approximations are made based essentially on the assumption that diffusion velocities are small and thermal contact between the species is good. In the context of this formal solution it is difficult to identify any particular one approximation as the cause of the anomalous pre-expansion. However, Fick's law of diffusion (which is equivalent to the C.E. diffusion equation disregarding thermal diffusion) can be derived from a different kinetic theory point of view - one which clarifies the implications of the C.E. approximations.

For the sake of the illustration, consider the limiting case as $n_A/n_{He} \to 0$. The helium shock is then described by a single component shock structure theory. The diffusion equation to determine the behaviour of the argon can be derived from the argon momentum equation. For the one-dimensional shock problem this equation is: (See Chapman and Cowling, Sec. 3.13.)

$$\left[u \frac{d}{dx} (\rho_A w_A) + 2 \rho_A w_A \frac{du}{dx} + \frac{d}{dx} \left(P^*_{A_{11}} - \frac{\rho_A}{\rho} P^*_{11} \right) \right]$$

$$+ \frac{d\, p^*_A}{dx} - \frac{\rho_A}{\rho} \frac{dp^*}{dx} = \eta \quad n_A n_{He} (u_{He} - u_A) \qquad (3)$$

where $w_A = u_A - u$

the starred quantities signify that these random velocity moments for the argon are defined about the overall gas mean velocity u.

i.e.

$$p^*_A = \frac{m_A}{3} \int c^*_K c^*_K f \, dc^*_K \qquad (4)$$

$$c^*_K = (v_x - u)$$

The pressure tensor terms $P^*_{A_{11}}$ and P^*_{11} for argon and total flow are similarly defined. Neglecting the terms in square brackets, this is the C.-E. second approximation diffusion equation without thermal diffusion (see Chapman and Cowling pg. 408). It is immediately obvious from this equation that the first term in the square bracket is not necessarily small - in fact in the strong diffusion shock problem it will be relatively important at the upstream end of the shock where dw_A/dx may be of the same order as du/dx since it is anticipated that the helium will compress first in the exact solution. (On the basis of the C.-E. theory predictions,

$$\left| \frac{dw_A}{dx} \right| = \left| \frac{du}{dx} \right| + \left| \frac{du_A}{dx} \right|$$

at the upstream end of the shock since the overall gas begins to decelerate while the argon initially accelerates. If this were in fact the case, the neglected term would be even more important). Roughly speaking, the C.E. diffusion equation approximates the acceleration term in the heavy particle momentum equation by the overall gas acceleration. The following calculation makes it clear that this approximate treatment of the heavy particle acceleration term is the cause of a pre-expansion anomaly: consider as a demonstration the shock wave structure in a mixture of predominantly helium with a very small concentration of argon. For this limiting case the single component Mott-Smith shock solution (see Sec. 2 .2) is a reasonable approximation for the behaviour of the helium. The argon compression is described by a simple version of its momentum equation -

$$\rho_A u_A \frac{du_A}{dx} + \frac{d p_A}{dx} = \eta n_A n_{He} (u_{He} - u_A) \qquad (5)$$

where the random velocity has been taken with respect to u_A

$$c_K = v_K - u_{A_K}$$

and the moments are also taken with respect to u_A

$$p_A = \frac{m_A}{3} \int c_K c_K f \, \underline{dc}$$

This momentum equation assumes a local Maxwellian distribution function about the species mean properties and a linear friction term for collisional momentum exchange. The integrated argon density profile calculated from this equation will be compared with the results obtained when the acceleration term in the above equation is replaced by the overall gas (i.e. the helium gas) acceleration in other words by equation 3 dropping the square bracketted terms.

$$\frac{d p_A^*}{dx} - \frac{\rho_A}{\rho} \frac{dp}{dx} = \eta n_A n_{He} (u_{He} - u_A) \qquad (6)$$

$$\left(u_A \frac{du_A}{dx} \text{ is replaced by } u\frac{du}{dx} \simeq \frac{1}{\rho} \frac{dp}{dx} \right)$$

In both Eqs. 5 and 6, the substitution

$$p_A = n_A k T$$

is made, where T is the overall gas mean temperature. This is not a good approximation and it will be eliminated in Section V where individual species temperatures are allowed. It is, nevertheless, consistent with the C.-E. second approximation which does not include differences in the species temperature. With no further approximations, equations 5 and 6 can be written in non-dimensional form:

$$(\theta - \mathcal{S}) \frac{dN_A}{dX} = N_A N_{He} \eta' (u_{He} - u_A) - N_A \frac{d\theta}{dx} \qquad (7)$$

and

$$\theta \frac{dN_A}{dX} = N_A N_{He} \eta' (u_{He} - u_A) - N_A \frac{d\theta}{dx} + \frac{m_A}{m_{He}} N_A \left(\frac{d\theta}{dx} + \frac{1}{N_{He}} \frac{dN_{He}}{dx} \right) \qquad (8)$$

The quantities N_A, N, u_{He}, u_A, θ are in units of their upstream equilibrium values n_{A_1}, n_1, u_{He_1}, u_{A_1}, T_1 respectively

and

$$\mathcal{S} = \frac{m_A u_A^2}{k T_1}$$

$X = x/\lambda_1$ where λ_1 is the upstream equilibrium value of the He-He mean free path

$\eta = \frac{8}{3} \sqrt{\pi} r_{12}^2 (2 k T_\mu)$ r_{12} is He-A interaction radius for hard sphere model.

$$\eta' = \frac{K \lambda_o}{n_{A_o} kT_o}$$

In each case, values of N, θ, $\frac{dN}{dX}$, $\frac{d\theta}{dX}$ are calculated from the dominant Mott-Smith helium shock. The first order ordinary differential equation in the dependent variable N_A is integrated in each case numerically. The results for the density are shown in Fig. 4. For each species the number density in units of the upstream equilibrium value for that species is plotted as a function of distance from the centre of the helium shock in units of the upstream helium mean free path. The density undershoot occurs in the solution of Eq. 8 but not for the solution of Eq. 7 in which the argon inertia term appears explicitly.

The purpose of this section has been to reduce the diffusion shock problem to as simple a formulation as possible in order to expose the exact nature of the cause of the C.E. pre-acceleration. In doing this, the argument has been based on some approximations in the derivation of the argon momentum equation which have not been fully justified. These approximations will be eliminated in Section V. However, two conclusions can be drawn here:

(1) Replacing the species acceleration by the overall flow acceleration in the simple momentum equation for the argon results directly in the appearance of a pre-expansion in the argon density profile.

(2) The C.E. diffusion equation contains, implicitly, approximations which are equivalent to this mis-representation of the diffusing species inertia. (See Eq. 3).

IV. A MONTE CARLO SOLUTION TO A MODELLED DIFFUSION SHOCK PROBLEM

There is an obvious need for an "exact" solution to the strong diffusion shock problem as a basis for evaluating the various kinetic theory solutions and as a final check on the upstream behaviour of the diffusing heavy gas. For both of these purposes the ultimate solution would be one detailing the distribution function for the heavy particles throughout the compression region. This information would not only give profiles for the moments of the distribution function to any order but would give some idea about the severity of the kinetic theory assumptions. Generally, the kinetic theory of the shock problem proceeds by restricting the shape of the distribution function in some manner (e.g. distorted Maxwellian or bimodal Maxwellian). Knowledge of the exact distribution function shape could be used to select a reasonable kinetic theory model.

There is an experimental method available for producing the complete distribution function at a point in a rarefied flow, however it has not yet been applied to this problem. It is the Doppler shift technique used by Muntz (Ref. 16).

In order to fill this gap, temporarily at least, a numerical experiment has been devised to solve a modelled diffusion shock problem. The model is this: the light gas shock is assumed to have a Mott-Smith profile

and to dominate the total momentum and energy fluxes. Hence it is considered to be undisturbed by the small concentration of heavy gas. The "exact" heavy particle flow pattern induced by this light gas shock can be built up using a test-particle Monte Carlo approach. Heavy particles are introduced into the flow far upstream of the light gas compression and their trajectories are followed collision by collision as they pass through the shock. At a number of stations in the shock region the contribution of each particle to the distribution function and its moments is accumulated to produce an acceptable average when a sufficient number of trajectories has been generated. Within the limits of statistical precision of the finite sample and the restricted nature of the modelled problem itself, this information is an exact description of the actual heavy gas behaviour. The restrictions placed on the light gas shock are not troublesome in the evaluation of various kinetic theory approaches using the Monte Carlo results as a standard since the kinetic theory can use the same model for the light gas shock. The comparison thus gives a valid indication of the seriousness of the various approximations made in the kinetic theory of diffusion shock structure.

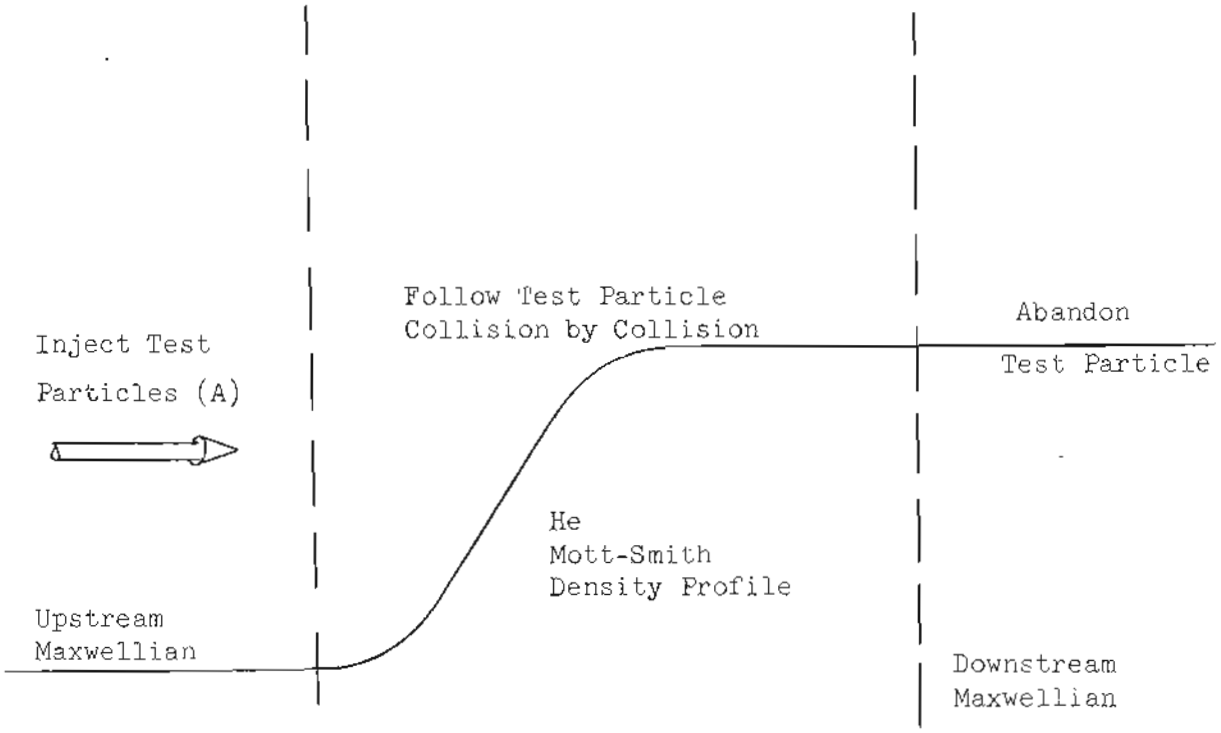

There are two types of molecular numerical experiments, the distinction between the two resting in the amount of exact knowledge available about the system to be analyzed. Gas-surface interaction studies are being carried out on large digital computers by idealizing the surface to a single perfect crystal lattice face and assuming an analytical interaction law between the impinging gas molecule and the lattice. This type of problem is completely deterministic in nature. Analytical expressions can be written for the trajectory of a particle with known velocity far above the surface. The computer's task in such an experiment is to account for a large number of impinging molecules spread over all possible initial aiming points. The second type of problem is characterized by a probabilistic description of part of the system and is popularly called a Monte Carlo method.

It is in general impossible to keep track of the exact position and velocity of each particle in a molecular gas flow problem. In place of such complete knowledge it is usual for the distribution function at any point in the flow to be known either analytically or in approximate numerical form. If a test particle is being followed along its trajectory through a gas described by a known distribution function this information does not give a deterministic answer to the location or type of its next collision with a gas molecule. The Monte Carlo technique requires that it be possible to express these essentially non-deterministic quantities, namely distance to next collision, velocity components of the colliding particle and collision parameters (direction of centres at "contact" for hard spheres or point of closest approach) by probability distributions. As the test particle passes from collision to collision the values for these quantities are chosen by selecting a number from a random group, distributed according to the inherent probability distribution associated with that quantity. (Haviland has given a thorough exposition on Monte Carlo applications to molecular flows - see Ref. 17).

4.1 Free Path Calculation for the Test Particle

In the modelled diffusion shock problem, the background gas distribution function is assumed at all points to be the Mott-Smith bimodal Maxwellian (Section 2 .2).

$$f = \frac{n_\alpha}{(2nk/m\ T_\alpha)^{3/2}}\, e^{-\frac{m}{2kT_\alpha}(\bar{v} - \hat{i}\, u_\alpha)^2} + \frac{n_\beta}{(2nk/m\ T_\beta)^{3/2}}\, e^{-\frac{m}{2kT_\beta}(\bar{v}-\hat{i}\, u_\beta)^2} \qquad (1)$$

$$n_\alpha = \frac{n_1}{(1+e^{BX})} \qquad n_\beta = \frac{n_1\, u_{\alpha\beta}}{(1+e^{-BX})}$$

X = (distance from shock centre)$/\lambda_1$

λ_1 = is the upstream mean free path

B = is the Mott-Smith coefficient, a function of Mach number

n_1 = is the upstream infinity number density of the background gas (helium)

T_α, u_α are upstream ∞ temperature and mean velocity

T_β u_β are downstream ∞ temperature and mean velocity

$u_{\alpha\beta} = u_\alpha / u_\beta$

To get a probability distribution for the distance to the next collision, consider first a large number of replications of the test particle trajectory i.e. a beam of particles with the test particle velocity moving through a gas with Maxwellian distribution function. Elementary kinetic theory texts derive the expression for the collision frequency at a point between particles and the Maxwellian gas. (See section 5.4 of reference 6). In a Maxwellian with number density n_m:

$$\nu = n_m S_c c_m \left[e^{-\frac{C}{\sqrt{\pi}}} + \left(C + \frac{1}{2C} \right) \text{erf } C \right] \tag{2}$$

c_m is the most probable speed of the background gas

C is the beam particle velocity with respect to the background mean velocity divided by c_m

S_c is the hard sphere collision cross-section for a beam-gas particle collision

For a beam passing through the Mott-Smith distribution, similar expression can be written for the beam collision frequency with each of the Maxwellian parts of the total background distribution

$$\nu_\alpha = n_1 S_c \left[\frac{1}{(1+e^{BX})} \right] c_{m\alpha} E_\alpha \tag{3}$$

$$\nu_\beta = n_1 S_c \left[\frac{u_{\alpha\beta}}{(1+e^{-BX})} \right] c_{m\beta} E_\beta \tag{4}$$

where the subscripted symbol E represents the terms in square brackets in equation (2) for the α and β-type Maxwellian backgrounds. The total collision frequency is just the sum of these

$$\nu = \nu_\alpha + \nu_\beta \tag{5}$$

These expressions are used to derive a distribution for "the probability of survival to X without collision" where X is the flow direction coordinate in units of the upstream mean free path (λ_1) for mutual collisions between light particles.

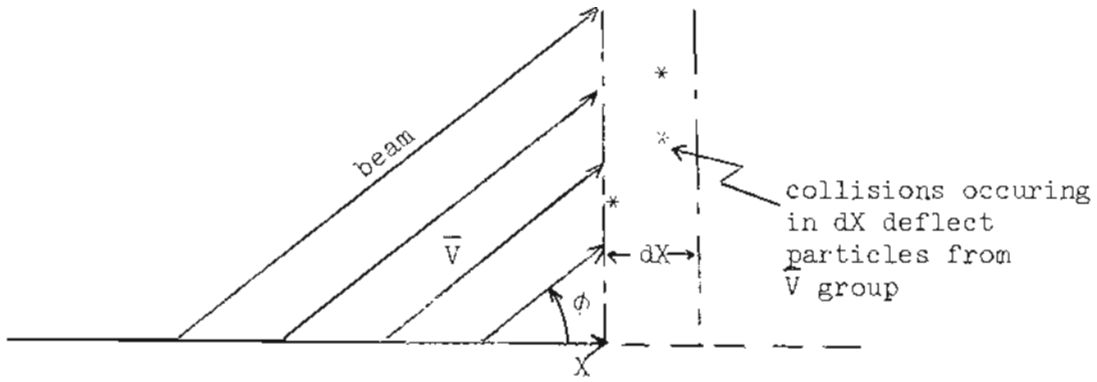

Passing from X to X + dX along the test particle path as shown in the above sketch the number of beam particles lost due to collisions with background gas molecules is

$$dn_b = - \frac{n_b \nu(X)}{V} \frac{dX}{\cos\phi} = - n_b \nu(X) dt \qquad (6)$$

where n_b is the number density of beam particles

V is beam speed

ϕ the beam angle with the flow direction

$\nu(X)$ the collision frequency of beam particles with the background at position X

dt is the time required for a beam particle to change its X-coordinate an amount dX

After integration we obtain:

$$\ell n \frac{n_b}{n_{b_o}} = - \int_{X_o}^{X} \frac{\nu(X)}{V \cos\phi} dX$$

substituting the value of $\nu(X)$ from equation (5) yields

$$\ell n \frac{n_b}{n_{b_o}} = - n_1 \frac{S_c \lambda_1}{V \cos\phi} \left[(X-X_o) - \frac{1}{B} \ell n \frac{(1+e^{BX})}{(1+e^{BX_o})} \right] c m_\beta E_\beta \qquad (7)$$

$$- n_1 \frac{S_c \lambda_1 \upsilon\alpha\beta}{V \cos\phi} \left[(X-X_o) + \frac{1}{B} \ell n \frac{(1+e^{-BX})}{(1+e^{-BX_o})} \right] c m_\beta E_\beta$$

$$\frac{n_b}{n_{b_o}} = e^{-A_1(X-X_o)} \left[\frac{1+e^{BX}}{1+e^{BX_o}} \right]^{\frac{A_1}{B}} \cdot e^{-A_2(X-X_o)} \left[\frac{1+e^{-BX}}{1+e^{-BX_o}} \right]^{-\frac{A_2}{B}} \qquad (8)$$

where

$$A_1 = \frac{n_1 S_c \lambda_1 c m_\alpha E_\alpha}{V \cos \phi}$$

$$A_2 = \frac{n_1 S_c \lambda_1 u \alpha_\beta c m_\beta E_\beta}{V \cos \phi}$$

The probability of survival from X_o to X is

$$\frac{n_b(X)}{n_b(X_o)}$$

This is the probability distribution associated with the single test particle trajectory as it leaves a collision at X_o.

Random numbers ("pseudo-random" numbers) are available on the I.B.M. 7094 in a rectangular distribution on the interval - |≤ R ≤| i.e.

$$P(R) = \begin{cases} .5 & \text{for } -1 \leq R \leq 1 \\ 0 & \text{out side this range} \end{cases}$$

where P(R)dR is the probability that the selected number will be in dR about R.

These numbers must be redistributed so that the probability of choosing R in dR is equal to the probability of collision in dX.

i.e.

$$P(R)dR = -\frac{d}{dX}\left(\frac{n_b}{n_{b_o}}\right) dX \tag{9}$$

Probability of survival to X is

$$1 - \int_{-1}^{R} P(R)dR = + \frac{n_b}{n_{b_o}}$$

$$\frac{1 - R}{2} = + \frac{n_b}{n_{b_o}}$$

or

$$e^{-A_1(X-X_o)} \left[\frac{1+e^{BX}}{1+e^{BX_o}}\right]^{\frac{A_1}{B}} e^{-A_2(X-X_o)} \left[\frac{1+e^{-BX}}{1+e^{-BX_o}}\right]^{-\frac{A_2}{B}} = \frac{1+R}{2} \tag{10}$$

For a particular choice of R from the available random number generating routine, the above is an implicit equation for the random axial coordinate of the next test particle collision, X. The equation is solved after each collision using a Newton-Ralfson convergence technique. Since the expression contains a number of exponentials and exponentiations, both relatively time-consuming operations for the computer, this can be a major contribution to the total computation

---

"pseudo-random" numbers are sequences of numbers which may be reproduced in order by starting the computer generating function at the same number for the repetition. The numbers also must satisfy randomness criteria.

time required to pass a test particle through the light gas maze. However, since the expression

e^{BZ} for Z in the range of X between the computational inlet and outlet for the heavy species

occurs repeatedly, a table of the exponentials can be stored for suitably small intervals ΔZ, to satisfy the accuracy requirements of the free path calculation. This replaces an exponential calculation by the calculation of the index associated with the exponential argument plus the selection from the table. Since the number of collision calculations is very large this is an extremely lucrative trade.

To save computation time use was made of the fact that for large values of both X and X_o (i.e. relatively far downstream in the shock front) the calculation can be simplified. In this limit the test particle is moving through a single Maxwellian gas with number density $n_1 v_{\alpha\beta}$, temperature T_β mean velocity u_β.

$$e^{-A_1(X-X_o)} \left[\frac{1+e^{BX}}{1+e^{BX_o}}\right]^{A_1/B} \rightarrow e^{-A_1(X-X_o)} e^{A_1(X-X_o)} = 1 \qquad (11)$$

and from Eq. 10

$$e^{-A_2(X-X_o)} = \frac{1+R}{2}$$

and the free path calculation is the simple logarithmic expression

$$\Delta X = -\frac{1}{A_2} \ln \frac{(1+R)}{2} \qquad (12)$$

4.2 Selection of Collision Partner Velocity

When the position of the next collision has been calculated using the exact free path expressions derived in Sec. 4.1, the next task is to select the velocity components of the light gas particle encountered by the test molecule at this position. Since, in this modelled problem, the background distribution function at a point is the sum of two Maxwellian contributions each with known properties, it is possible to decide, as an initial step, from which of the groups the target particle will be selected -

(i) select R, a random number from the rectangular random number generator . Then $\frac{R+1}{2}$ is a random number between 0 and 1.

(ii) ν_α is the total collision frequency of test particle with α-part of target maze. ν_β is the total collision frequency of test particle with β-part of target maze.

(iii) If $\frac{R+1}{2} > \frac{\nu_\alpha}{\nu_\alpha+\nu_\beta}$ the target is of the β-type, otherwise it is of the α-type.

The problem is now reduced to choosing at random a collision partner for the test particle from a Maxwellian with known properties. In the following derivation all speeds are non-dimensionalized by the most probable speed of the target Maxwellian gas (c_m). The problem can be formulated as follows:

Before collision the test and target particle velocities are sketched below

The relative probability of collision with particle at a velocity $\bar{C}$ in range dC is

$$\frac{\nu(\bar{C})}{\nu} = \frac{1}{\pi^{3/2}} \frac{C_r C^2 e^{-C^2} \sin\phi \, d\phi \, d\epsilon \, dC}{\left[\frac{e^{-V^2}}{\sqrt{\pi}} + \left(V + \frac{1}{V}\right) \operatorname{erf} V\right]} \tag{1}$$

where

$C_r = |\bar{V} - \bar{C}|$ and $[\ ]_{G(V)}$ will be denoted in the following by $G(V)$

Angles ϕ,ϵ are shown in the above sketch.

The three velocity coordinates of the target particle must be selected according to this inherent probability. Obviously, this probability is distributed uniformly over the range of ϵ so the selection of the ϵ coordinate is trivial - no redistribution is required.

$$\epsilon = \frac{R_1 + 1}{2} \cdot 2\pi \tag{2}$$

where R_1 is a random number selection from the rectangular distribution.

The probability of a (ϕ,C)-type target is found by performing the integration of equation (1) over the range of ϵ from $0 \le \epsilon \le 2\pi$ and is

$$\frac{1}{\sqrt{\pi}} \frac{\sqrt{C^2 + V^2 - 2CV\cos\phi}}{G(V)} C^2 \, d(\cos\phi) e^{-C^2} dC \tag{3}$$

First select the target particle speed C. The probability of the target particle speed C, being in the range dC about C is

$$P(C) \, dC = \left[\int_{-1}^{+1} \int_{0}^{2\pi} \frac{\nu(\bar{C})}{\nu} d\epsilon \, d\mu\right] \frac{dC}{G(V)} = F(R_2) dR_2 \tag{4}$$

where R_2, now, is a random rectangular selection, and $\mu = \cos\phi$.

Therefore integrating both sides from their corresponding initial values $\begin{cases} C = 0 \\ R_2 = -1 \end{cases}$

$$\frac{R_2+1}{2} = -\frac{2}{\sqrt{\pi}} \int_0^C \int_{-1}^{1} \sqrt{C^2 + V^2 + 2CV\mu}\; C^2 e^{-C^2}\, dC\, d\mu$$

$$= \frac{2}{\sqrt{\pi}} \frac{1}{2CV} \frac{2}{3} \int C^2 e^{-C^2} (C^2 + V^2 + 2CV\mu)^{3/2} \Big|_{\mu=1}^{\mu=-1} dC$$

If $C < V$

$$\frac{R_2+1}{2} = \frac{4}{\sqrt{\pi} G(V)} \left\{ \left(V + \frac{1}{2V} \right) \operatorname{erf} C \frac{\sqrt{\pi}}{4} - \left(\frac{1}{2} CV + \frac{1}{4} \left(1+\frac{2}{3} C^2\right) \right) e^{-C^2} \right\} \qquad (5)$$

If $C > V$

$$\frac{R_2+1}{2} = 1 - \frac{4}{G(V)\sqrt{\pi}} \left\{ \frac{1}{2} (1+C^2) e^{-C^2} + \frac{V^2}{6} e^{-C^2} \right\} \qquad (6)$$

For every randomly selected value of R_2 there is a corresponding target particle speed, C.

Rather than solve these implicit equations 5 and 6 by a numerical iterative technique, values of the quantity $R_2 = R'$ were tabulated in matrix form for a series of velocity pairs $C = C'$ and $V = V'$. When the choice of C is to be made during calculation, a random number R_2 is chosen from the generator. The column corresponding to $V' \simeq V$ is scanned to find the value of C' for which $R' \simeq R_2$. This value of C' is then the value used for C in the collision calculation. This tabulation procedure is governed by some practical considerations. The first of these is that 99.7% of all the particles in the Maxwellian have values of $C < 3$ so that the probability of collision with a target particle whose speed $C < 4$, say, can be neglected. The tabulated range for V' must be determined for each specific Mach number. Since V' is the difference between the test particle speed and the target group mean, practical limits for it will depend on the shock Mach number.

Knowing the speed of the target particle, one more random selection is required to specify the angle ϕ i.e. $\phi = \cos^{-1}\mu$

For known C

$$\int_{-1}^{R_3} P(R)dR = \frac{\int \left[\sqrt{C^2 + V^2 + 2CV\mu}\; C^2 e^{-C^2} dC\right] d\mu}{\int_{-1}^{1} \left[\sqrt{C^2+V^2+2CV_\mu} C^2 e^{-C^2} dc\right] d\mu} \qquad (7)$$

Upon integration this becomes

$$\frac{R_3+1}{2} = \frac{\{(C^2+V^2+2CV\mu)^{3/2} - |C-V|^3\}}{\{(C+V)^3 - |C-V|^3\}}$$

Solving for μ, the arcosine of the collision angle,

$$\mu = \frac{1}{2CV} \left\{ \left[\frac{R_3+1}{2} (C+V)^3 + \frac{(1-R_3)}{2} |C - V|^3 \right]^{3/2} - C^2 - V^2 \right\} \qquad (8)$$

The angle ϕ is then determined by the choice of R_3 i.e.,

$$\phi = \cos^{-1}(-\mu) \qquad (9)$$

This completes the specification of the target particle velocity.

4.3 Direction of Flight after Collision

To this point, no assumptions have been made about the intermolecular force law to be used for the collision. The two models most frequently chosen in kinetic theory calculations are based on hard elastic spheres and molecules obeying an inverse fifth power repulsive force law (Maxwellian molecules). Both of these have been used in the Monte Carlo calculation. However, only the hard sphere derivations will be shown here. The corresponding considerations for the Maxwellian molecule model are derived in Appendix B. It can be noted here that the familiar problem associated with inverse power law fields of infinite extent, namely the fact that all particles are continuously in a state of mutual collision, would render this model useless for Monte Carlo calculations if it were not possible to consider a finite cut-off point for the interparticle force. This is also considered in Appendix B.

Consider a collision between two elastic spheres, masses m_1, m_2, velocities $\bar{v}_1$, $\bar{v}_2$ before collision and represent their velocities after collision by $\bar{v}_1'$, $\bar{v}_2'$. Define

$$m_o = m_1 + m_2 \ , \quad M_1 = \frac{m_1}{m_o} \ , \quad M_2 = \frac{m_2}{m_o}$$

The centre of mass of the two molecules will move with constant velocity $\bar{G}$ defined by the equation:

$$m_o \bar{G} = m_1 \bar{v}_1 + m_2 \bar{v}_2 = m_1 \bar{v}_1' + m_2 \bar{v}_2'$$

Let $\bar{g}$ and $\bar{g}'$ represent the relative velocity of molecule "2" with respect to molecule "1" before and after collision respectively so

$$\bar{g} = \bar{v}_2 - \bar{v}_1$$

$$\bar{g}' = \bar{v}_2' - \bar{v}_1'$$

Then

$$\bar{v}_1 = \bar{G} - M_2 \bar{g}$$

$$\bar{v}_2 = \bar{G} + M_1 \bar{g}$$

$$\bar{v}_1' = \bar{G} - M_2 \bar{g}'$$

$$\bar{v}_2' = \bar{G} + M_1 \bar{g}'$$

Since the centre of mass of the two colliding molecules is unaccelerated, the collision can be viewed in an inertial frame fixed to the centre of mass. In this reference frame the collision takes place in a single plane containing the line of centres. At impact the collision looks like this:

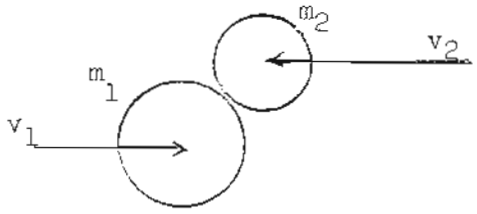

where $\hat{n}$, $\hat{t}$ are unit vectors in the collision plane parallel and perpendicular to the line of centres. For smooth spheres the tangential ($\hat{t}$) components of the two molecular velocities are conserved.

Conservation of normal ($\hat{n}$) momentum leads to:

$$m_1 v_{1_n} + m_2 v_{2_n} = m_1 v'_{1_n} + m_2 v'_{2_n}$$

Conservation of energy implies

$$m_1(v_{1_n}^2 + v_{1_t}^2) + m_2(v_{2_n}^2 + v_{2_t}^2) = m_1(v'^2_{1_n} + v'^2_{1_t}) + m_2(v'^2_{2_n} + v'^2_{2_t})$$

since tangential velocity components are conserved.

Hence

$$m_1 v_{1_n}^2 + m_2 v_{2_n}^2 = m_1 v'^2_{1_n} + m_2 v'^2_{2_n}$$

or

$$m_1(v_{1_n}^2 - v'^2_{1_n}) = m_2(v_{2_n}^2 - v'^2_{2_n})$$

i.e.

$$m_1(v_{1_n} + v'_{1_n})(v_{1_n} - v'_{1_n}) = m_2(v_{2_n} + v'_{2_n})(v_{2_n} - v'_{2_n})$$

but

$$m_1(v_{1_n} - v'_{1_n}) = m_2(v_{2_n} - v'_{2_n})$$

therefore

$$(v_{1_n} + v'_{1_n}) = (v_{2_n} + v'_{2_n})$$

The result can be written

$$v'_{1_n} = v_{1_n}\frac{(m_1 - m_2)}{m_o} + v_{2_n}\,2\,\frac{m_2}{m_o}$$

$$= -\frac{m_2}{m_o^2}(m_1 - m_2)g\cos\theta + 2\frac{m_1 m_2}{m_o^2}\,g\cos\theta$$

$$= \frac{m_2}{m_o}\,g\cos\theta = -v_{1_n}.$$

As anticipated, the collision is symmetrical about the line of centres at impact.

After collision

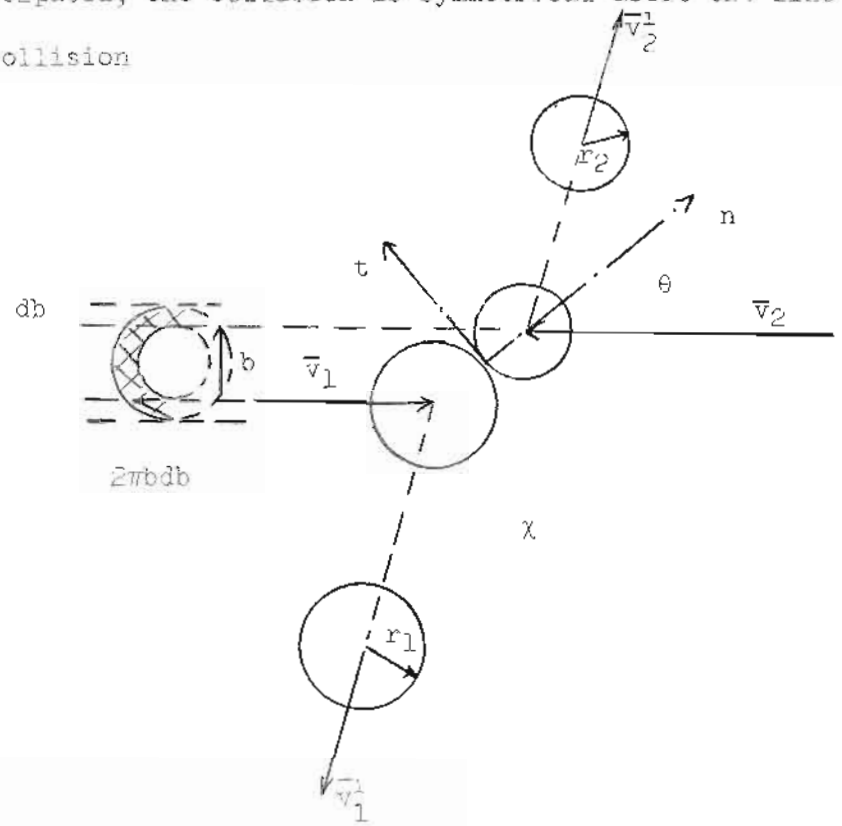

$\mathcal{R} = r_1 + r_2$
= radius of influence for collision

The rotation of relative velocity vector is 2θ

Now

$$\frac{b}{\mathcal{R}} = \sin\theta$$

The probability of the collision impact parameter being in db about b is:

$$P(b)\,db = \frac{2\pi b\,db}{\pi \mathcal{R}^2}$$

$$= 2\cos\theta\sin\theta\,d\theta$$

$$= \frac{2\pi \sin 2\theta\, d(2\theta)}{4\pi}$$

$$= \frac{2\pi \sin\chi d\chi}{4\pi}$$

$$= \frac{d\Omega}{4\pi}$$

The relative velocity vector rotates into solid angle element $d\Omega$ with probability $d\Omega/4\pi$ i.e. all solid angles are equally probable. The direction of the relative velocity vector after collision then has a random set of direction cosines. A technique for numerically selecting a set of random direction cosines, requiring selection of two random numbers is given in Haviland's report (Ref. 15) and is repeated in Appendix C.

This completes the single test particle step procedure. The position of the test particle for the succeeding step has been found and the relative velocity vector before and after collision is determined by the random procedure described above. It is a trivial algebraic step to derive from the relative velocity vectors the absolute test particle velocity after the collision.

4.4 Accumulation of the Distribution Functions and Moments

The heavy test particles are introduced at some distance upstream of the light gas compression where both gases have their cold Maxwellian properties. The random velocity components of the heavy particle can then be directly selected from a distribution of random numbers. However, care must be taken to weight the contributions of each particle according to the relative fluxes of these particles across the inlet plane. A particle having the mean flow speed, U, is treated as a single particle, weight 1, whereas a particle with flow direction velocity u, is counted to be u/U particles i.e., the probability of a particular velocity for the injected particle is the ratio of the flux of that velocity group to the total flux.

The selected particle is then followed, collision by collision as it is swept through the compression region. The downstream boundary condition is treated in a very simple-minded manner. At a distance"some number of mean free paths" downstream of the region of primary interest (this will normally be the region up to the point where the Rankine-Hugoniot compression of the heavy species is, say, 99% complete) the particle is abandoned. At this point, a portion of the heavy particles have absolute velocities in the upstream direction but their range in that direction is very small because of the high density background gas tending to sweep them downstream. This method is easy to apply but must be tested carefully at high Mach numbers. (The test procedure consists of increasing the distance of the downstream point at which the test particles are abandoned until no further effect upon the accumulated distribution in the compression region can be detected.)

As the test particle passes through the compression region it must be possible to interpret its local velocity at a number of stations in terms of the contribution it makes to the distribution function and its lower moments at these stations. For the sake of this interpretation, a time element and an element of area ΔA perpendicular to the flow direction are introduced. These two quantities have no relevance to the actual flow problem i.e. they do not correspond to any real time or area in the problem but are used to relate the results of N individual random tests to those of a continuous flux of particles.

The real constant number flux of heavy particles is nu. Consider the total sample of N particles to be injected in unit time through a cross-sectional area ΔA

therefore

$$\frac{N}{\Delta A} = n_1 u_1 \qquad (1)$$

where subscript "1" refers to upstream infinity values.

Phase space is divided into cells of volume -

$$2\pi V_p \Delta V_p \Delta u \Delta A \Delta x = \underline{\Delta V}\ \underline{\Delta x}$$

where V_p is the speed perpendicular to the flow direction

u is the flow direction speed

If $n_c(u,V_p,x)$ is the number of the N particles which are in $\underline{\Delta V}$ when they pass x then

$$\frac{n_c}{2\pi V_p \Delta V_p \Delta u \Delta A \Delta x}$$

is the number per unit time per unit volume phase space passing into and out of this phase cell.

Multiplying this quantity by the cell residence time gives the expected number in the phase cell i.e.

$$f(u,V_p,x) = \frac{n_c}{2\pi V_p \Delta V_p \Delta u \Delta A \Delta x} \cdot \frac{\Delta x}{|u|}$$

$$= \frac{n_c}{2\pi V_p \Delta V_p \Delta u} \cdot \frac{n_1 u_1}{N|u|}$$

The moments are accumulated using this formula for $f(u,V_p,x)$. The results are thus:

Number density at x

$$n \equiv \int f\ \underline{dV}$$

$$\frac{n}{n_1} = \left(\sum_N \frac{n_c}{2\pi V_p \Delta V_p u} \cdot \frac{u_1}{|u|} \cdot 2\pi V_p \Delta V_p \Delta u \right) \Big/ N$$

$$= \left(\sum n_c \frac{u_1}{|u|} \right) \Big/ N$$

Mean velocity: $\frac{u}{u_1} = \frac{n_1}{n}$

Temperatures

$$T = \frac{m_A}{3nk} \int c^2 f\ dc = \frac{m_A}{3nk} \overline{c^2}$$

$$= \frac{1}{3} \frac{m_A}{m_{He}} \cdot \gamma M^2 \left\{ \frac{n_1}{n} \left(\sum_N \frac{V^2}{|u| u_1} \right) \Big/ N - \frac{u^2}{u_1^2} \right\}$$

$$T'' = \frac{m_A \overline{c_1^2}}{n k}$$

$$= \frac{m_A}{m_{He}} \cdot \gamma M^2 \left\{ \frac{n_1}{n} \left(\sum \frac{|u|}{u_1} \right) \Big/ N - \frac{u^2}{u_1^2} \right\}$$

where M is the upstream value of the helium Mach number.

4.5 Results of the Monte Carlo Calculations

Shock profiles for the density and temperature moments have been computed for a range of Mach numbers using a hard sphere collision model and a mass ratio of the two constituents of 10. A limited number of computer runs were performed for Maxwellian molecule type collisions. However, these calculations took much more computer time. Since the main purpose of this exercise is to evaluate analytical approximations in kinetic theory, the Maxwellian molecules are used only as an occasional check that the conclusions drawn from the hard sphere calculations do not exclusively pertain to the hard sphere molecular model. The shock profiles are shown in Figures 5 to 8. In all of these figures the moments in units of their upstream equilibrium values are plotted as a function of distance from the centre of the Mott-Smith light gas shock. This distance is given in units of the upstream helium mean free path. Figures 9(a) and (b) show the detailed evolution of the distribution function of heavy particles as they pass through the compression. $N(V_x)$, the distribution function integrated over all values of the perpendicular velocity components, is plotted as a function of V_x in units of the upstream most probable random speed for the heavy gas. The important observations are these:

(i) The heavy particle density profiles are monotonics.

(ii) The 'temperature' of the heavy species associated with the flow direction random velocity, T'', rises much more rapidly than the perpendicular temperature. Both overshoot the downstream value.

(iii) The heavy particle distribution functions for M = 2 and 3 do not show the strong double maximum shape of a Mott-Smith distribution. In fact they should be reasonably well approximated by a single mode Maxwellian throughout most of the compression.

The implications of these results will be discussed in Section V, where a comparison is made with some analytical calculations.

Both Rothe (Ref. 18) and Center (Ref. 19) have investigated shock structure in He-A mixtures using the electron beam fluorescence technique. Rothe's results were difficult to interpret in terms of a one-dimensional shock wave model since the shock waves he investigated were formed in front of a shock holder placed in a free jet expansion. Three dimensional effects were important in these experiments and the results for the case of interest here, namely the case with every small argon concentration, were inconclusive. Center, on the other hand, was specifically concerned with this problem and he reports no indication of a pre-expansion of the argon at the upstream end of the shock.

Before proceeding, the three major assumptions of this solution will be restated. This Monte Carlo solution assumes a binary mixture of neutral gases with widely disparate masses (namely $m_A/m_{He} = 10$ in calculation) and a heavy species equilibrium concentration so small that its influence on the background light gas shock is negligible. This background shock is assumed to have a Mott-Smith profile. A block diagram showing the computation sequence of the Monte Carlo programs is shown on the following page.

MONTE CARLO PROGRAM SEQUENCE

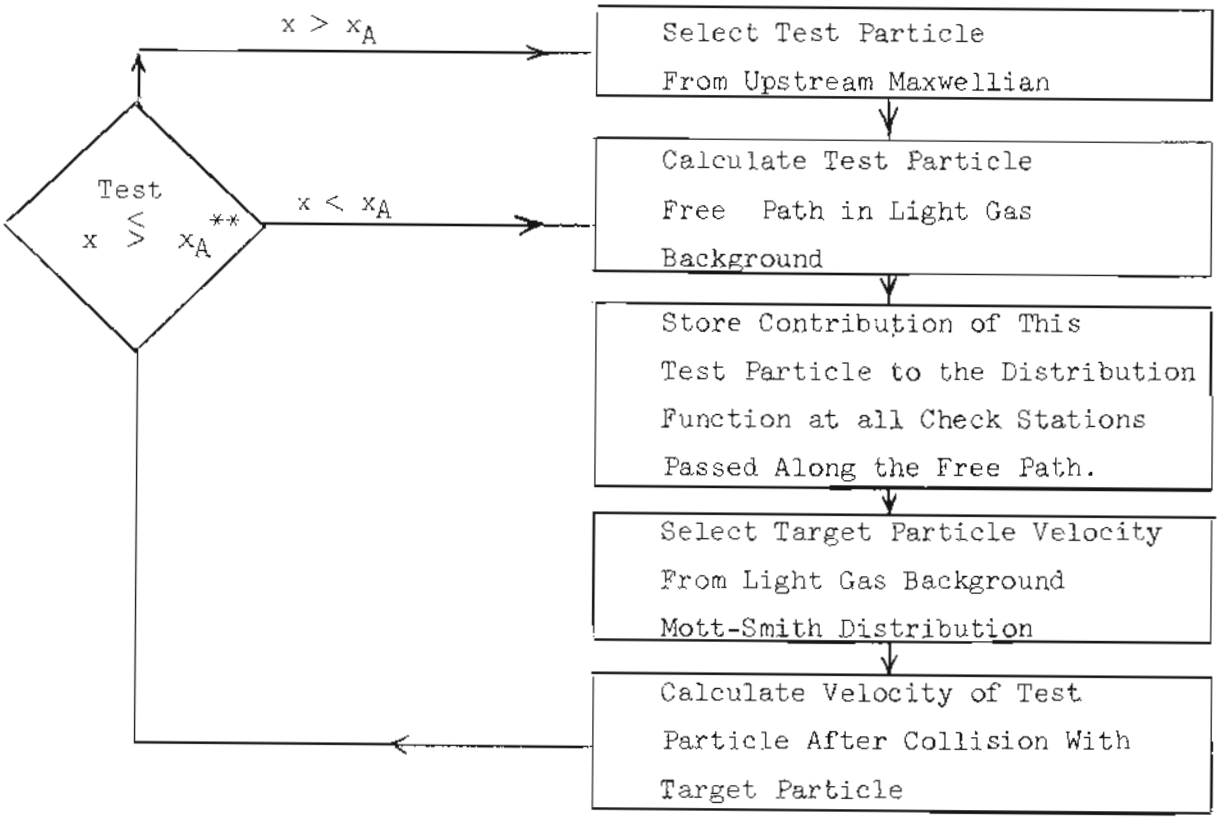

**

x Is the position coordinate of the test particle measured from the centre of the light gas shock.

x_A Is a predetermined position beyond which the test particle is abandoned (well downstream of the compression region of interest).

V. KINETIC THEORY CONSIDERATIONS FOR SHOCK WAVES IN MIXTURES WITH SMALL CONCENTRATION OF HEAVY GAS

The Monte Carlo method of solving molecular flow problems is capable of giving exact answers with finite accuracy because the behaviour of a very large number of molecules is inferred from the average behaviour of a relatively small sample. However, this type of inaccuracy yields to analysis and confidence levels can be established for solutions based on statistical calculations. The basic inexact nature of approximate kinetic theory solutions based on the Boltzmann equation is much less agreeable. As pointed out in Section II, these solutions are in general based on truncated series solutions or some initial constraints on the fundamental variable - the distribution function of random velocities. There is a good deal of educated guessing involved in setting up such a solution scheme and in some cases the solution quantities of interest are fortunately insensitive to these approximations on the microscopic level. Still, error estimates for these solutions are generally difficult to obtain. In the present situation the Monte Carlo calculations of the previous section can be used to evaluate the merit of the kinetic theory answers. The remainder of this section will outline some simple moment solutions to the modelled shock wave problem of Section IV and compare these answers with the Monte Carlo results. (Refer to Section II for description of moment solutions.)

5.1.1 Euler Equations (1-Temperature Maxwellian)

An extremely simple set of moment equations is derived by assuming the heavy particle distribution function is locally Maxwellian.

i.e.
$$f_A = \frac{n_A}{(2\,k/m_A\,T_A)^{3/2}}\, e^{-\frac{m_A}{2kT_A}(\bar{v}-\bar{u}_A)^2} \tag{1}$$

where n_A, u_A, T_A are functions of the independent variable x, the position coordinate of the one-dimensional problem, and are determined by solving the moment equations for conservation of mass momentum and energy. These are:

$$\frac{d}{dx}(n_A u_A) = 0 \qquad \text{i.e.} \quad n_A u_A = n_{A_1} u_{A_1} \tag{2}$$

$$\rho_A u_A \frac{d}{dx} u_A + \frac{dp_A}{dx} = \Delta(v_x) \tag{3}$$

$$+ 2\,\rho_A u_A^2 \frac{du_A}{dx} + 5\,\rho_A u_A \frac{k}{m_A}\frac{dT_A}{dx} = \Delta(v^2) \tag{4}$$

where the Δ's are in each case the collisional contributions to change. (The method of derivation of collision terms, Δ, is given in Appendix A).

Non-dimensionalizing the flow variables by dividing by their upstream equilibrium values, the equations can be written in matrix form:

$$\begin{pmatrix} (\theta_A - \mathcal{S}) & N_A \\ -2\mathcal{S} & 5N_A \end{pmatrix} \begin{pmatrix} dN_A/dx \\ d\theta_A/dx \end{pmatrix} = \begin{pmatrix} \Delta'(v_x) \\ \Delta'(v^2) \end{pmatrix} \qquad (5)$$

where

$$\theta_A = T_A/T_1$$

$$\mathcal{S} = \frac{m_A u_A^2}{k T_1}$$

The Δ' values are the nondimensionalized collision terms.

As in Section IV, the light gas (helium) shock is assumed to have a Mott-Smith compression profile. This fact is used in calculating the collisional interaction terms, $\Delta(v_x), \Delta(v^2)$. Equation 5 is then integrated to give shock profiles for the argon number density and temperature (Fig. 10 and 11). These results will be compared more closely with the M.C. solution later in this section. Qualitatively at least, it appears that this simple moment solution gives a reasonable picture of the shock. However, one of the striking features of this problem which cannot be simulated by the local Maxwellian distribution function is the preferential partitioning of random energy between the directions parallel and perpendicular to the flow. The M.C. temperature profile (Fig. 6) shows that the spread of the distribution of random velocities within the argon compression becomes much larger in the flow direction than in the perpendicular direction. A less restrictive form for the distribution function is required to include this effect. Nevertheless the simple Euler solution when compared with the more general solutions, will show how insensitive the lower order moments (e.g. density) are to constraints on the distribution function shape which involve its dependence on higher order moments (e.g. $T^{\perp}$, $T^{\parallel}$).

5.1.2 The Two-Temperature Maxwellian Solution

The extra freedom allowing the heavy constituent to have different temperatures in the directions parallel and perpendicular to the flow can be introduced in one of two ways: by keeping the quadratic terms in a Hermite polynomial expansion for f (Ref. 8) or by considering instead the ellipsoidal expansion proposed by Holway (Ref. 11). In the latter case only the leading term in the expansion is required since the two temperature nature of the distribution is present in the ellipsoidal exponential weight function for this series. These two choices for the 2-temperature distribution function have the form:

$$f = f_o \left(1 + \frac{(T''-T)}{T} \frac{c_u^2}{2k/mT} + \frac{(T^{\perp}-T)}{T} \frac{c_{\perp}^2}{2k/mT} \right) \qquad (1)$$

where

$$f_o = \frac{n}{(2\pi k/mT)^{3/2}} e^{-\frac{m}{2kT}(\bar{v}-\hat{i}u)^2}$$

for the Hermite expansion

and

$$f = \frac{n}{(2\pi k/m)^{3/2}} \; T''^{-\frac{1}{2}} \; \frac{1}{T^{\perp}} \; e^{-\frac{m}{2kT''}(\bar{v}_1-\bar{u})^2} \; e^{-\frac{m c_{\perp}^2}{2kT^{\perp}}} \qquad (2)$$

for the first ellipsoidal term.

Only the detailed forms of the collisional contributions to the moment equations are affected by the choice between the two alternate distributions. The left hand sides of these equations have identical forms in terms of the dependent variables $n_A, u_A, T''_A, T_A^{\perp}$. These equations are

$$\Phi = 1 \qquad \frac{d}{dx}(n_A u_A) = 0 \qquad (3)$$

$$\Phi = v_x \qquad n_A u_A \frac{du_A}{dx} + n_A \frac{k}{m_A} \frac{dT''_A}{dx} + T''_A \frac{k}{m_A} \frac{dn_A}{dx} = \Delta_2(v_x) \qquad (4)$$

$$\Phi = v^2 \qquad 2\, n_A u_A^2 \frac{du_A}{dx} + 3\, n_A u_A \frac{k}{m_A} \frac{dT''_A}{dx} + 2\, n_A u_A \frac{k}{m_A} \frac{dT_A^{\perp}}{dx} = \Delta_2(v^2) \qquad (5)$$

$$\Phi = v_x^2 \qquad 2\, n_A u_A^2 \frac{du_A}{dx} + 3\, n_A\, u_A \frac{k}{m_A} \frac{dT_A}{dx} = \Delta_2(v_x^2) \qquad (6)$$

where $\Delta_2(v_x)$, $\Delta_2(v^2)$, $\Delta_2(v_x^2)$ are the 2-temperature single mode collision calculations (Appendix A).

Solution of these equations for a light gas shock Mach number 3, mass ratio 10 (He-A) is shown for comparison with the local Maxwellian result in Figures 11 and 12. This 2-temperature solution is also plotted with the Monte Carlo curves in Fig. 5 to 8. Obviously restrictions placed on the higher moments by oversimplifying the distribution function have only small effects on the number density profile through the shock. The 1-temperature density profile deviates only slightly from the 2-temperature result, even though the 1-temperature distribution erroneously restricts the thermal energy to be equally partitioned in all directions. On the other hand, Figures 5 and 7 confirm that the 2-temperature density profiles compare quite favourably with the Monte Carlo results for M = 2 and 3. The temperature profiles compare well with the one standard deviation error bars of the Monte Carlo solution.

The process of increasing the number of moment variables is, of course, a never-ending one. Before considering the possibility of increasing the order of these single mode expansions, one very serious difficulty with these solutions must be dealt with. The problem concerns the behaviour of the solution at isolated points where the matrix of coefficients of the set of differential equations becomes singular.

5.1.3 Singular Points of the Coefficient Matrix

The inversion of the systems of equations of Sections 5.1.1 and 5.1.2 have singular points where the determinant of the coefficient matrix goes to zero.

For the Euler equations:

$$\begin{vmatrix} (\theta - \xi) & N \\ -2\xi & 5N \end{vmatrix} = 0 \qquad (1)$$

i.e. $$5\theta = 3\xi$$

$$\frac{u^2}{\frac{5}{3}\, k/mT} = 1$$

The singular point for this set of equations corresponds to a local Mach number of unity for the heavy species. In a similar way it can be shown that the 2-temperature equations are singular when

$$\frac{u^2}{3\ k/mT} \rightarrow 1 \qquad (2)$$

i.e. the "critical" speed for this solution is

$$u = \sqrt{3\ k/mT} \qquad (3)$$

Because the heavy species thermal speed is small compared to that of the light gas, the small trace of heavy gas remains "supercritical" throughout the entire compression for low Mach number light gas shocks ($u > \sqrt{3\ k/mT} > \sqrt{5/3\ k/mT}$ throughout for helium shock Mach number 3). However with increasing shock Mach number the temperature ratio across the shock becomes very large and these critical points move upstream into the shock wave. For example, for a helium shock Mach number of 10 the temperature ratio across the shock is:

$$T_{21} = \frac{(M^2+3)(5M^2-1)}{16\ M^2} = 32.2 \qquad (4)$$

the velocity ratio is

$$u_{21} = \frac{M^2+3}{4M^2} = 0.258 \qquad (5)$$

the downstream helium Mach number is $\frac{5 \times .258}{\sqrt{32.2}} = .246$

and the downstream argon Mach number is $\sqrt{10}\ M_{He} = .78$

In such cases, the finite difference solution must pass through conditions where the coefficient matrix becomes singular. (This condition sets in at much lower shock Mach numbers because the temperature overshoots T_{21} at an intermediate value.)

It is well known that the Euler equations for a one-component gas are incapable, in the general case, of describing a smooth steady transonic flow. In the Euler approximation, the resulting shock wave takes the form of a discontinuity separating a region of subsonic from a region of supersonic flow. The 1-temperature equations described in Section 5.1.1 are just the Euler equations for the argon gas with inhomogeneous terms resulting from the collisional interaction with the background helium gas. Mathematically this problem is similar to the classical problem of 1-dimensional pipe flow with frictional force and heat transfer from the walls. The solution requires physical gradients to become infinite as a decelerating supersonic flow approaches the critical condition, $M = 1$. A density and temperature discontinuity satisfying conservation of energy and momentum at the "shock" station is required to patch the supersonic and subsonic flows. The local Maxwellian distribution function of the Euler equations is too restrictive and these equations are incapable of describing a continuous transonic flow. All single mode Maxwellian expansions exhibit this "choking" behaviour and because of this are unable to describe the heavy particle flow for the full range of Mach numbers**

This is an interesting situation. The gas being described is dominated by collisions with the light background gas - collisions between pairs of heavy particles are considered vanishingly improbable. This gas is, then, completely reactive and incapable of supporting collective effects such as wave propagation. However, the mathematical equations chosen to describe the gas (single mode moment equations) do support disturbance propagation. This wave nature is independent of the inhomogeneous collision terms, that is it does not depend upon a self collision term in the moment equations, but is a result of the assumed functional relationship among the flow variables as they appear in the distribution function.

At this point the single Maxwellian mode expansion has reached a similar impasse to the one it faced when used to describe single component shocks (see Section 2.2). In that case the bimodal expansion (Mott-Smith) rescued the moment method and produced reasonable solutions for the entire Mach number range. Two types of bimodal distribution function expansions are described below.

5.2 Bimodal Soltuions

In Section III, Oberai's bimodal solution for binary mixture shock structure was described and it was pointed out there that the form of the heavy particle distribution used in that solution would not be anticipated for the case of very small heavy species concentration. The Monte Carlo solutions of Section IV confirm this fact. The distribution function shape at various stations within the argon compression for Oberai's solution is shown in Fig. 13. These sharply double-peaked distributions can be compared with the Monte Carlo distribution functions for the same conditions shown in Fig. 14. (The curves labelled "Bimodal" in this figure are discussed later in this section.) The

---

** These systems of equations are hyperbolic, that is, in time-dependent form they support the propagation of disturbances at a set of finite speeds. It can be shown that the critical points in the steady equations correspond to local speed ratios equal to these characteristic propagation speeds of the mathematical system.

density profiles calculated from Oberai-type solutions also do not compare well quantitatively with the Monte Carlo results. This comparison is made in Fig. 15. In the modelled shock problem considered here, the light gas shock is being approximated by the simple Mott-Smith single component shock solution, therefore it is possible to allow the bimodal representation of the heavy particle distribution function to have much more freedom without increasing the analytical difficulty of the complete solution unreasonably. Two modifications of the bimodal approach are considered below.

5.2.1 Bimodal Distribution - Upstream Anchored

This solution is based on a distribution function form which looks like the one used by Oberai:

$$f = \frac{n_1}{(2\pi k/m\ T_1)^{3/2}}\ e^{-\frac{m}{2kT_1}(\bar{v}-\bar{u}_1)^2} + \frac{n_2}{(2\pi k/m\ T_2)^{3/2}}\ e^{-\frac{m}{2kT_2}(\bar{v}-\bar{u}_2)^2} \qquad (1)$$

where u_1,T_1 are constant and equal to the upstream equilibrium mean velocity and temperature. The quantities u_2,T_2 are functions of x but unlike Oberai's solution where the variation in these quantities is governed by their forced identity with similar quantities in the light gas distribution, u_2,T_2 in this solution are free to vary in a manner specified by heavy particle moment equations. The Mott-Smith light gas solution assures overall conservation of momentum and energy since this gas dominates the flow. The equations used to solve for the four dependent variables n_1,n_2,u_2,T_2 are the equations for the $1,\ v_x,\ v^2,\ v_x^2$ moments:

$\Phi = 1$

$$u_1 \frac{dn_1}{dx} + u_2 \frac{dn_2}{dx} + n_2 \frac{du_2}{dx} = 0 \qquad (2)$$

$\Phi = v_x$

$$(u_1^2 + \frac{k\ T_1}{m}) \frac{dn_1}{dx} + (u_2^2 + \frac{k\ T_2}{m}) \frac{dn_2}{dx}$$

$$+ 2\ n_2 u_2 \frac{du_2}{dx} + n_2 \frac{k}{m} \frac{dT_2}{dx} = \Delta(v_x) \qquad (3)$$

$\Phi = v^2$

$$u_1(u_1^2 + 5 \frac{k}{m} T_1) \frac{dn_1}{dx} + u_2 (u_2^2 + 5 \frac{k}{m} T_2) \frac{dn_2}{dx}$$

$$+ n_2 (3u_2^2 + 5 \frac{k}{m} T_2) \frac{du_2}{dx} + 5\ n_2 u_2 \frac{k}{m} \frac{dT_2}{dx} = \Delta(v^2) \qquad (4)$$

$\Phi = v_x^2$

$$u_1(u_1^2 + 3 \frac{k}{m} T_1) \frac{dn_1}{dx} + u_2 (u_2^2 + 3 \frac{k}{m} T_2) \frac{dn_2}{dx}$$

$$+ 3\ n_2 (u_2^2 + \frac{k}{m} T_2) \frac{du_2}{dx} + 3\ n_2 u_2 \frac{k}{m} \frac{dT^2}{dx} = \Delta(v_x^2) \qquad (5)$$

To start the integration of these equations, upstream infinity values for u_2, T_2 are needed. These are found from a set of compatibility relations for the above set of equations as $n_2 \to 0$. At upstream equilibrium:

$$\frac{dn_2}{dx} = -\frac{u_1}{u_2}\frac{dn_1}{dx} \tag{6}$$

Substituting into Eq. 3, 4 and 5 and dividing by dN_1/dx**

$$\underbrace{\left[(u_1^2 + a_1^2) - \frac{u_1}{u_2}(u_2^2 + a_2^2)\right]}_{A_1}\frac{dn_1}{dN_1} = \frac{\frac{d}{dN_1}\left\{\Delta(v_x)\right\}}{\frac{d}{dN_1}\left(\frac{dN_1}{dx}\right)} = \mathcal{B}(v_x) \tag{7}$$

$$u_1\underbrace{\left[(u_1^2 + 5a_1^2) - (u_2^2 + 5a_2^2)\right]}_{A_2}\frac{dn_1}{dN_1} = \frac{\frac{d}{dN_1}\left\{\Delta(v^2)\right\}}{\frac{d}{dN_1}\left(\frac{dN_1}{dx}\right)} = \mathcal{B}(v^2) \tag{8}$$

$$u_1\underbrace{\left[(u_1^2 + 3a_1^2) - (u_2^2 + 3a_2^2)\right]}_{A_3}\frac{dn_1}{dN_1} = \frac{\frac{d}{dN_1}\left\{\Delta(v_x^2)\right\}}{\frac{d}{dN_1}\left(\frac{dN_1}{dx}\right)} = \mathcal{B}(v_x^2) \tag{9}$$

The compatibility equations are

$$\frac{\mathcal{B}(v_x)}{A_1} = \frac{\mathcal{B}(v^2)}{A_2} = \frac{\mathcal{B}(v_x^2)}{A_3} \tag{10}$$

which can be solved for initial values of u_2, T_2 in terms of u_1, T_1 ($u_2 = u_2^o$, $T_2 = T_2^o$).

These two equations for u_2 T_2 in terms of the known initial values u_1, T_1 prescribe the starting conditions for the calculation. The equations are integrated along the stable path, from upstream to downstream, using a Gill's approximation Runge-Kutta step-by-step procedure. The collision terms give the influence of the dominant He-A encounters in hard sphere approximation. (Similar Maxwellian molecule calculations are outlined in Appendix B.) The resulting density profile is labelled "Bimodal Moment Solution" in Fig. 16. The extra freedom afforded the distribution function by this bimodal solution improves the moment description of the number density variation through the shock from the results obtained for the same cases using Oberai's approximation, but it still requires a portion of the heavy gas to remain in the upstream Maxwellian group of the distribution function as the gas approaches the downstream end of the shock. The Monte Carlo distribution, although statistically rough, does not show such a tendency and intuitively this is not expected to happen in the real flow.

** N_1 here represents the portion of the helium in the upstream part of its Mott-Smith distribution. See Eq. 7 of section 2.2. Upper case in this instance specifies the dominant species.

5.2.2 Bimodal Distribution - Downstream Anchored

A similar set of equations results if the downstream portion of the distribution function is anchored. Again

$$f = \frac{n_1}{(2\pi k/mT_1)^{3/2}} e^{-\frac{m}{2kT_1}(\bar{v} - \bar{u}_1)^2} + \frac{n_2}{(2\pi k/mT_2)} e^{-\frac{m}{2kT_2}(\bar{v}-\bar{u}_2)^2} \quad (1)$$

where, this time, $u_1 T_1$ are functions of x to be determined from the moment equations but u_2, T_2 are "anchored" at the downstream equilibrium velocity and temperature. The upstream starting values for all dependent variables are known in this case -

$$n_1(x) = n_1^o \ , \ n_2(x) = 0 \ , \ u_1(x) = u_1^o, \ T_1(x) = T_1^o$$

where superscript "o" here indicates the upstream equilibrium value of the variable. The system of equations to be solved is

$\Phi = 1$

$$u_2 \frac{dn_2}{dx} + u_1 \frac{dn_1}{dx} + n_1 \frac{du_1}{dx} = 0 \quad (2)$$

$\Phi = v_x$

$$(u_2^2 + a_2^2) \frac{dn_2}{dx} + (u_1^2 + a_1^2) \frac{dn_1}{dx} + 2 n_1 u_1 \frac{du_1}{dx} \quad (3)$$

$$+ n_1 \frac{k}{m} \frac{dT_1}{dx} = \Delta(v_x)$$

$\Phi = v^2$

$$u_2 (u_2^2 + 5a_2^2) \frac{dn_2}{dx} + u_1 (u_1^2 + 5a_1^2) \frac{dn_1}{dx}$$

$$+ n_1(3u_1^2 + 5a_1^2) \frac{du_1}{dx} + 5 n_1 u_1 \frac{k}{m} \frac{dT_1}{dx} = \Delta(v^2) \quad (4)$$

$\Phi = v_x^2$

$$u_2(u_2^2 + 3a_2^2) \frac{dn_2}{dx} + u_1(u_1^2 + 3a_1^2) \frac{dn_1}{dx} \quad (5)$$

$$+ n_1(3u_1^2 + 3a_1^2) \frac{du_1}{dx} + 3 n_1 u_1 \frac{k}{m} \frac{dT_1}{dx} = \Delta(v_x^2)$$

This set of equations has also been solved for a range of high Mach numbers and the resulting density profile for M = 5 also conforms to the curve labeled "Bimodal" in Fig. 16. Again the density comparison is acceptable. However, this solution mimics the behaviour of the distribution function of the M.C. solution somewhat more accurately (Fig. 14). In the initial stages the "upstream" portion adjusts much as a single mode solution. The distribution becomes elongated in the mid compression region and approaches the downstream shape without a residual bump at the upstream velocity.

This solution could be improved again by allowing the upstream floating Maxwellian portion to have a 2-temperature behaviour similar to the single mode solution. The distribution function, less the downstream anchored portion must be expanded in terms of Hermite polynomials or ellipsoidal polynomials. It requires one higher order moment equation for which the hard sphere collision term calculation becomes relatively laborious. The one-temperature solution above serves the present purpose i.e. it shows that, if allowed sufficient flexibility, the bimodal moment solution gives a good estimate of the diffusion shock structure.

5.3 Conclusions

The following conclusions can be drawn from these calculations for shock wave structure in binary mixtures of constituents with widely differing masses:

(i) For a hard sphere or Maxwellian molecule collision model and vanishing concentration of the heavy species the velocity overshoot (or pre-expansion) predicted by the Chapman-Enskog solution does not occur. The compression is monotonic.

(ii) For the same molecular models and gas conditions as stated in (i), the distribution function of the heavy species does not develop a strong bimodal shape. Moment solutions which facilitate this moderately distorted distribution shape agree in detail with the Monte Carlo heavy species moment profiles.

(iii) The compression of the heavy species, when it is present in very small quantities, is accompanied by a temperature overshoot as collisions randomize the energy associated with the diffusion velocity between the two species.

PART II

VI. DIFFUSIVE SEPARATION OF IONS AND ATOMS IN ELEVATED ELECTRON TEMPERATURE PLASMAS

The structure of shock waves in fully ionized plasmas has been studied exhaustively using Navier Stokes equations. The restricted nature of solutions presented in some early publications in the field was overcome by Jaffrin and Probstein (Ref. 20) who presented a solution including viscous and heat conduction effects for both species, charge separation effects within the shock and separate ion and electron temperatures for the full range of Mach number and mean free path to Debye length ratios. More recently Jaffrin has reworked the N.S. solution for partially ionized shock waves (Ref. 21). The treatment is very complete for the problem Jaffrin considers i.e. a plasma in total equilibrium at upstream infinity in the shock coordinate, with no external energy sources or sinks, and constant degree of ionization. The equations used do not correspond to the second Chapman-Enskog approximation for mixtures but are a set of N.S. equations for each species with the effects of cross collisions between species appearing as contributions to the viscosity and heat conduction coefficients as well as in the inhomogeneous collision terms. The main features of these solutions are a region of preheating of the electron gas, very small diffusion velocity between charged and uncharged species, a small separation of the ion and atom temperatures and an induced electric field which increases with degree of ionization and free-stream Mach number.

A very different partially ionized shock wave was encountered by Sonin (Ref. 22) during the course of some Langmuir probe studies in a strongly non-equilibrium plasma flow. The experiments were conducted in a steady Mach 2.2 flow of highly non-equilibrium argon plasma generated by R.F. induction in the stagnation chamber (See Fig. 17) with a stagnation temperature of the heavy species about 450°K, stagnation pressure of the order 1 torr, but degree of ionization in the neighbourhood of 10^{-4}. For the various experimental runs the free stream electron temperature ranged from 2400 to 5300°K, and in all cases the Debye length was very small compared to the thickness of the bow shock in front of the blunt body placed in the flow.

The measurements are described in detail in Ref. 22. The results indicated that (a) the electron temperature remained constant throughout the bow shock and the entire shock layer, and (b) the ion shock thicknesses obtained from the ion number density profiles were substantially larger than the accepted normal shock thickness in neutral argon at the same free stream conditions. Although it was expected that the structure of the bow shock might deviate somewhat from the one-dimensional shock idealization because of the relatively low model Reynolds numbers*, the substantially thicker ion shock was attributed primarily to the diffusive separation of the ions and atoms in the shock wave. It is shown below that such separation is substantial whenever the Schmidt number based on the amibpolar diffusion coefficient is small compared to unity, as is the case when the electron temperature is large compared to the ion temperature. (The ambipolar Schmidt number is $S_{c_1} = \frac{\mu_1}{\rho_1 D_{a_1}}$, where μ is the viscosity coefficient, ρ the flow density, D_a the ambipolar diffusion coefficient and where subscript 1 indicates the upstream infinity value of these quantities.)

* Based on free stream mass flux, viscosity at stagnation temperature and model diameter, the Reynolds number was in the range 80-100

Under these strong diffusion conditions, the simple form for the viscosity and thermal conduction coefficients used by Jaffrin must be questioned as well as the form of the collision terms used in his equations. These collision terms are, in most cases, calculated for transfer between two locally Maxwellian gases. Before attempting to perform a more elaborate solution for this problem, a simple first approximation solution is presented. The simple equations used are justified somewhat by the fact that the opposing effects of ion-atom collisions and ion electron coupling are expected to dominate the problem.

6.1 A Simple Approximate Solution

To specify the problem theoretically, a chemically frozen, slightly ionized, monatomic gas is considered with a degree of ionization so low that the charged particles make no significant contribution to the over-all transfer of momentum and energy. In this limit the neutral atom shock is unaffected by the presence of the charged species and a single-component shock structure theory can be used to determine the neutral shock profile. If it is assumed for this simple theoretical treatment that the local ion and atom temperatures are equal throughout the flow and that the thermal diffusion effect may be neglected, then only the momentum equations for the diffusing species are needed to solve the problem. These are (in approximation for small diffusion velocity):

Ion Momentum Equation:

$$-(dp_i/dx) + n_i\, e\, E + (\rho_i/\rho)(dp/dx) = \eta^{ia} n_i n_a (u_1 - u_a) \qquad (1)$$

Electron Momentum Equation:

$$-(dp_e/dx) - n_e\, e\, E + (\rho_e/\rho)(dp/dx) = \eta^{ea} n_e n_a (u_e - u_a) \qquad (2)$$

where subscripts k = i, e, a refer to ions, electrons and atoms, respectively; p_k, ρ_k, n_k, u_k are species pressure, density, number density, and mean velocity; p, ρ, n, u are the over-all flow pressure, density, number density, and mean velocity; $\eta^{k\ell}$ is the coefficient of friction between species k and ℓ; e is the magnitude of the electronic charge and E the electric field induced by charge separation.

For the nonequilibrium flow problem considered here it is also appropriate to assume that:

(a) The electron temperature T_e is constant throughout the entire flow region (as observed above).

(b) The diffusion is ambipolar, i.e.

when $|n - n_e| \ll n_i$, as is the case for Debye length $\ll$ mean free path for ions

then $u_i \simeq u_e$

(c) Momentum transfer to the neutral gas by electron impacts is negligible, i.e.

$$\eta^{ea} \ll \eta^{ia}$$

(d) The relationship between the ion-atom friction coefficient and the ion diffusion coefficient D_i is

$$\eta^{ia} = \frac{kT}{nD_i}$$

where T is the common ion-atom temperature and k is Boltzmann's constant.

Equations (1) and (2) may be combined with the above assumptions to give a single equation for the ambipolar diffusion of ions and electrons:

$$\frac{n_i n_a}{n^2}(u_i - u_a) = D_i \left[\left(1 + \frac{T_e}{T}\right)\frac{d(n_i/n)}{dx} - \frac{n_i T_e}{nT} \frac{d\ \ell n\ \rho}{dx} \right] \qquad (3)$$

When distance is nondimensionalized by the upstream value of the argon mean free path based on viscosity:

$$x' = x \Big/ \frac{16}{5}\left(\frac{\mu_1}{\rho_1 (2\pi k/m\, T_1)^{\frac{1}{2}}}\right) = \frac{x}{\lambda_1}$$

and the concentration is nondimensionalized by the undisturbed value

$$f = \left(\frac{n_i}{n}\right) \Big/ \left(\frac{n_{i1}}{n_1}\right)$$

the diffusion equation has the form:

$$\frac{df}{dx'} = (f-1)\ \frac{M\, Sc_1 \rho_1\, Da_1}{\left[\frac{5}{16}(2\pi/\gamma)^{\frac{1}{2}}\right] \rho\, D_a}$$

$$- \frac{T_e/T}{(1+T_e/T)}\ f\ \frac{d\ \ell n\ \rho}{dx'} \qquad (4)$$

where M is the Mach number of the upstream infinity flow, γ is the ratio of specific heats for argon.

This equation has been solved numerically using the single component Navier-Stokes shock solution to determine the neutral gas properties and their gradients (Ref. 16). Sutherland's model for the viscosity-temperature variation was used in the Navier-Stokes equations and the ion diffusion coefficient was determined from the mobility expression given by Chanin and Biondi (Ref. 23) for argon ions diffusing in their parent gas. This mobility expression includes the effect of ion-atom charge exchange. The number density profiles for Mach number 2.2 and stagnation temperature 450°K are shown in Fig.18.

The maximum-slope ion shock thicknesses of the experimental and theoretical ion number density profiles are compared in Fig. 19 for a range of ambipolar Schmidt numbers. The maximum slope density thickness of the ion shock waves, Δ, divided by the upstream neutral-neutral mean free path, λ_1, is

plotted as a function of the ambipolar Schmidt number. The significant feature of this diagram is the illustration that the experimental shock thickness varies with ambipolar Schmidt number in a manner similar to that predicted by the theory. It indicates that in high electron temperature plasmas the shock structure is appreciably modified by diffusive separation induced by electrical coupling of the ions with the much lighter electron gas.

The magnitude of the discrepancy between the experimental points and the predictions of this simple theory is by no means surprising. It is well known that the Navier-Stokes solution underestimates the shock thickness at higher Mach numbers. For argon at M = 2.2, available values for the measured atom shock thickness are from 20% to 50% greater than those predicted by Navier-Stokes theory (Ref. 24). Another source of theoretical error is the small diffusion velocity assumption inherent in Eqs. (1) and (2). Furthermore, the experimental points may be overestimated by up to 10% as a result of an approximation in the interpretation of the measured probe current traces (Ref. 22). In addition to these factors, the experimental simulation of one-dimensional shock conditions was obviously poor, for the bow shock and the boundary layer were on the point of merging and the shock structure was in all likelihood influenced by three-dimensional effects and by downstream gradients. The neutral density was also not known precisely since the stagnation temperature used in its determination was an average value.

6.2 Kinetic Theory Solutions

It is possible, within the moment method framework, to formulate a solution to this ionized gas shock problem. Some of the objectionable features of the previous simple solution can then be avoided. As in the neutral binary mixture solutions, the Mott-Smith single component solution will be used to describe the dominant gas shock - here, the neutral argon shock wave. It is reasonably well documented that this is a superior choice to the Navier-Stokes solution for $M > 2$. In addition, the small diffusion velocity approximations inherent in the equations of Sec. 6.1 will be eliminated. The following assumptions will be made:

(i) the diffusion is ambipolar
(ii) the electron collisional interaction is entirely long range and appears in the electromagnetic force terms of the transfer equations,
(iii) the electron-to-ion temperature ratio is large.

There is no standard with which to compare solutions for this problem in the way the results of the He-A moment solutions were compared with the M.C. results. As an initial approximation, the ion distribution function is assumed to be locally Maxwellian. The electrons, which are constrained by the electric coupling with ions to have number density equal to the ion density throughout the compression also are assumed to be locally Maxwellian with mean velocity equal to the ion velocity and constant temperature ($T_e >> T_i$). Because of the extremely high electron thermal speed, the distortion of the electron distribution function caused by the relatively small shock velocity jump will be negligible so this latter assumption is not restrictive in practice. The exact form of the ion-atom collisional interaction is calculated for a hard sphere collision model. This is a good approximation for the charge-exchange dominated $A\text{-}A^+$ collision (see Ref. 23) over a small temperature range. The available equations are then:

Ion Momentum Equation:

$$-eE + m_i n_i u_i \frac{du_i}{dx} + n_i \, k \frac{dT_i}{dx} + T_i \, k \frac{dn_i}{dx} = \Delta(m_i v_x)$$

Electron Momentum Equation:

$$-eE + m_e n_e u_e \frac{du_e}{dx} + n_e \, k \cancel{\frac{dT_e}{dx}} + T_e \, k \frac{dn_e}{dx} = \Delta(m_e v_x) \simeq 0$$

Ambipolar Momentum Equation

$$(T_i' + T_e' - \mathcal{S}) \frac{dN_i}{dx'} - N_i \frac{dT_i'}{dx'} = \frac{\Delta(m_i v_x)}{\sqrt{2}\, n_{i_1} n_{a_1} k T_1 \, \pi \lambda^2}$$

Here $T' = T/T_1$

$$\frac{dT_e}{dx} = 0 \quad \text{from observations of Sec. 6.1}$$

where $\mathcal{S} = \dfrac{u_i^2}{k/m_i \, T_1}$

$x' = \dfrac{x}{\sqrt{2}\, n_{a_1} \pi \lambda^2}$

λ is the constant radius hard sphere approximation to the argon-argon collision radius

Similarly the Ambipolar Energy Equation is:

$$-2\mathcal{S} \frac{dN_i}{dx'} + 5N_i \frac{dT_i'}{dx'} = \frac{\Delta(m_i v^2)}{\sqrt{2}\, n_{i_1} n_{a_1} \, k \, T_1 \left(k \frac{T_1}{m_i} \right)^{\frac{1}{2}} \pi \lambda^2}$$

Equations 4 and 5 are to be solved for the charged particle interaction with the M.S. neutral shock. This is not the straightforward matter it was for the He-A shock case. In fact it is found that these equations are not stable for integration in either direction between the upstream and downstream equilibrium points. Consider the matrix of coefficients and the zero of its determinant.

$$\begin{pmatrix} (T_i' + T_e' - \mathcal{S}) & N_i \\ -2\mathcal{S} & 5N_i \end{pmatrix}$$

The singular point is at the condition

$$\frac{u_i^2}{\frac{5}{3} \frac{k}{m_i} (T_e + T_i)} = 0$$

As T_e varies in this expression from zero to $T_e \gg T_i, T_a$ this singular point moves from a position somewhere in the middle of the ion compression out to the upstream end of the shock when u_{i_1} (upstream infinity ion velocity)

$< \sqrt{\frac{5}{3}\frac{k}{m_i}(T_i + T_e)}$. When this condition is fulfilled, as it will be in the high electron temperature cases considered here, the entire charged particle gas is "subsonic" with respect to the ion acoustic speed $\left(\tau_i = \sqrt{\frac{5}{3}\frac{k}{m_i}(T_e + T_i)}\right)$ and neither of the equilibrium points is nodal as is required for a simple stable numerical integration of the simultaneous differential equations. The nature of these equilibrium points will be discussed in Appendix D. However, here it will be pointed out that an iterative procedure has been successfully used to overcome this computational problem. To start this iterative solution, the ion temperature is assumed to be equal to the background atom temperature at all points in the shock. Equation 4 with $T_i = T_a$ integrates stably from downstream $x = \infty$ to $x = -\infty$ to give an initial approximation to the density variation. This information, the point by point density and density gradient, is stored in the Runge-Kutta procedure and is used to approximate N_i and dN_i/dx in equation 5. This equation has then the single dependent variable, T_i and can be integrated from $x = -\infty$ to $x = \infty$, this time storing T_i and dT_i/dx for use in the next iterate of equation 4. The iteration quickly converges. Figures 20 and 21 show the convergence of the two variables N_i and T_i for $M = 3$, T_e 20,000°K.

To make a valid comparison between this moment solution and the simple solution of the previous section, equations 6.1.1 and 6.1.2 are integrated again using Mott-Smith values for the neutral argon shock and the hard sphere approximations for the $A\text{-}A^+$ collision cross section. The $M = 2.2$ results are compared in Fig. 22. (The simple solution of section 6.1 is labelled "Chapman-Enskog". It was indicated in section 3 that the form of the diffusing species momentum equation used in equations 6.1.1 and 6.1.2 is compatible with the Chapman-Enskog second approximation solution for gas mixtures.)

The same general conclusions as those stated in section 6.1 can be repeated. Very large diffusive separations between ions and atoms occur in high electron temperature, weakly ionized plasmas in regions of strong flow gradients. This solution does not agree quantitatively any better with Sonin's experimental results than did the simple solution of the previous section. Sonin is continuing research on this problem using a shock tube facility and it is hoped that some meaningful quantitative comparisons can be made with results from these experiments.

The substantial overshoot of the downstream equilibrium value by the ion temperature is similar to the effect observed in the He-A mixtures. Just as in that problem, a 2-temperature solution using the distribution function described in Sec. 5.1.2 can be performed here, employing the iterative procedure described above. For this solution the equations for $\frac{dT''}{dx}$, $\frac{dT^{\perp}}{dx}$ are both integrated upstream-to-down in each iteration. The equations are:

$$\begin{pmatrix} (T_i'' + T_e' - \zeta) & N_i & 0 \\ -2\zeta & 3N_i & 2N_i \\ -2\zeta & 3N_i & 0 \end{pmatrix} \begin{pmatrix} \frac{dN_i}{dx} \\ \frac{dT_i''}{dx} \\ \frac{dT_i'^{\perp}}{dx} \end{pmatrix} = \begin{pmatrix} \Delta(m_i v_x) \\ \Delta(m_i v^2) \\ \Delta(m_i v_x^2) \end{pmatrix}$$

As in the neutral gas problem, the parallel and perpendicular temperatures separate very strongly within the shock but this effect does not alter the density profile significantly.

6.3 Conclusions

The following general conclusions can be drawn from the consideration of this special plasma shock structure problem:

(i) In high electron temperature plasmas the shock wave structure is substantially modified by diffusive separation induced by the electrical coupling of the ions with the much lighter electrons. The shock region is diffused by the ion compression which precedes and coalesces with the neutral atom shock.

(ii) The convergence problem of moment method solutions can be avoided, in the special case where the species described is entirely "subsonic", by an iteration scheme. The ion-electron gas can be treated in this manner in cases of extremely high electron temperature.

REFERENCES

1. Becker, R. — Stosswelle and Detonation, Zeits f. Physik, 8, 321 (1922).

2. Thomas, L.H. — Note on Becker's Theory of the Shock Front, J. Chem. Phys., Vol. 12, 11 (1944).

3. Mott-Smith, H.M. — The Solution of the Boltzmann Equation for a Shock Wave, Phys. Rev. 82, 6 (1951).

4. Sherman, F.S. — Shock Wave Structure in Binary Mixtures of Chemically Inert Perfect Gases, J. Fluid Mech. 8, 465 (1960).

5. Oberai, M.M. — A Mott-Smith Distribution to Describe the Structure of a Plane Shock Wave in a Binary Mixture, Phys. Fluids, 9, 9 (1966).

6. Chapman, S. Cowling, T.G. — The Mathematical Theory of Non-Uniform Gases, Cambridge University Press (1961).

7. Gilbarg, D. Paolucci, D. — The Structure of Shock Waves in the Continuum Theory of Fluids, J. Ratl. Mech. Anal. 2, 617 (1953).

8. Grad, H. — Note on N-Dimensional Hermite Polynomials, Comm. on Pure and Applied Math., Vol. 11, 325 (1949).

9. Grad, H. — On the Kinetic Theory of Rarefied Gases, Comm. on Pure and Applied Math., Vol. 11, 325 (1949).

10. Grad. H. — The Profile of a Steady Plane Shock Wave., Comm. on Pure and Applied Math., Vol. V, 257 (1952).

11. Holway, L.H. — Approximation Procedures for Kinetic Theory , Ph.D. Dissertation, Harvard University, Cambridge, Mass.(1963).

12. Salwen, H. Grosch, G.E. Ziering, S. — Extension of the Mott-Smith Method for a One-Dimensional Shock Wave, Phys. Fluids, 7, 2 (1964).

13. Bhatnager, P.L. Gross, E.P. Krook, M. — A Model for Collision Processes in Gases 1. Small Amplitude Processes in Charged and Neutral One-Component Systems, Phys. Rev. Vol. 94, 3 (1954).

14. Chahine, M.T. Narasimha, R. — Exact Numerical Solution of the Complete BGK Equation for Strong Shock Waves, in Rarefied Gas Dynamics, J.H. deLeeuw Ed. Academic Press (1965).

15. Liu, C.Y. — Validity of Fick's Law of Diffusion for Shock Structure Problems, Phys. Fluids 8, 6, 1190 (1965).

16. Muntz, E.P. — The Direct Measurement of Velocity Distribution Functions, in Rarefied Gas Dynamics J.H. deLeeuw, Ed., Academic Press (1965).

17. Haviland, J.K. — Monte Carlo Application to Molecular Flows, MIT Fluid Dynamics Research Laboratory Report No. 61-5 (1961) and AFCRL Scientific Report 648.

18. Rothe, D.E. — Electron Beam Studies of the Diffusive Separation of Helium-Argon Mixtures in Free Jets and Shock Waves U. of T. Institute for Aerospace Studies, UTIAS Report No. 114, July, 1966.

19. Center, R.E. — Shock Structure in Helium-Argon Mixtures, Proceedings of the American Physical Society, Stanford University, November 1966.

20. Jaffrin, M.Y. Probstein, R.F. — Structure of a Plasma Shock Wave. Phys. Fluids Vol. 7, 10 (1964).

21. Jaffrin, M.Y. — Shock Structure in a Partially Ionized Gas, Phys. Fluids Vol. 8, 4 (1965).

22. Sonin, A.A. — The Behaviour of Free Molecule Cylindrical Langmuir Probes in Supersonic Flows, and Their Application to the Study of the Blunt Body Stagnation Layer, U. of T. Institute for Aerospace Studies, UTIAS Report 109, 1965.

23. Chanin, L.M. — Temperature Dependence of Ion Mobilities in Helium, Neon, and Argon, Phys. Rev. Vol. 106, 3 (1957).

24. Camac, M. — Argon Shock Structure, in Rarefied Gas Dynamics, J.H. deLeeuw, Ed. Academic Press (1965).

APPENDIX A

Boltzmann Collision Integral

If Φ is a function of molecular velocity $\bar{v}_1$, then the total collisional contribution to change in Φ is found by multiplying the collision term in the Boltzmann equation by $\Phi(\bar{v}_1)$ and integrating over the entire $\bar{v}_1$-space. In the usual notation

$$(\overline{\Delta\Phi})_{coll} = \int \Phi(\bar{v}_1) \left[f_2' f_1' - f_2 f_1 \right] gb \; db \; d\epsilon \underline{dv}_1 \; \underline{dv}_2 \qquad (1)$$

where

b	collision impact parameter (range $0 \leq b < \infty$)
ϵ	collision plane orientation (range $0 \leq \epsilon \leq 2\pi$)
$\bar{v}_2$	collision partner velocity (range $-\infty \leq v_{2i} \leq \infty$)
$f_1 = f(\bar{v}_1)$	

prime $(')$ means after collision,

or equivalently:

$$(\overline{\Delta\Phi})_{coll} = \int \left[\Phi(\bar{v}_1') - \Phi(\bar{v}_1) \right] f_2 f_1 \; g \; b \; db \; d\epsilon \; \underline{dv}_1 \; \underline{dv}_2 \qquad (2)$$

The inside integrations for $\Phi = v_{1_x}$, $v_{1_x}^2$, v_1^2 can be represented in terms of standard "cross-sections" $S^{(\ell)}$ defined below:

$\Phi = v_{1_x}$:

$$\int_0^\infty \int_0^{2\pi} (v_{1_x}' - v_{1_x}) \, gb \, db \, d\epsilon$$

$$= M_2 \, g g_x \, S^{(1)} \qquad (3)$$

$\Phi = v_{1_x}^2$:

$$\int_0^\infty \int_0^{2\pi} (v_{1_x}'^2 - v_{1_x}^2) g \; b \, db \, d\epsilon$$

$$= 2 M_2 \, v_{1_x} \, g g_x \, S^{(1)} + 2 M_2^2 g g_x [S^{(1)} - S^{(2)}/2] + \tfrac{1}{2} M_2^2 g [g^2 - g_x^2] S^{(2)} \qquad (4)$$

$\Phi = v_1^2$:

$$\int_0^\infty \int_0^{2\pi} (v_1'^2 - v_1^2) g \; b \, db \, d\epsilon$$

$$= 2 M_2 \, S^{(1)} \left[M_2 \, g^3 + v_{1_x} \, g \, g_x + g \, g^\perp \, v_1^\perp \right] \qquad (5)$$

where $M_2 = \dfrac{m_2}{m_1 + m_2}$ and m_2 is the collision partner mass.

$$S^{(\ell)} = \int_0^{2\pi} \int_0^{\infty} (1-\cos^{\ell}\chi)\, b\,db\,d\epsilon$$

χ is the collison angle shown in Sketch B-1 of Appendix B, which represents the collision geometry

$$g = \left|\bar{v}_1 - \bar{v}_2\right|$$

$$g_x = v_{1x} - v_{2x}$$

Maxwellian Molecules

$$S^{(1)} = \frac{1}{g}\left(\frac{m_1 + m_2}{m_1 m_2} \cdot K_{12}\right)^{\frac{1}{2}} \times .422 \qquad (6)$$

$$S^{(2)} = \frac{1}{g}\left(\frac{m_1 + m_2}{m_1 m_2} \cdot K_{12}\right)^{\frac{1}{2}} \times .436 \qquad (7)$$

K_{12} is the force constant in the inverse fifth power law repulsion force $\frac{K_{12}}{r^5}$. This constant is evaluated from diffusion data and the first approximation Chapman-Enskog diffusion coefficient expression for Maxwellian molecules (see Chapman and Cowling, Chapter 12). The complete moment collision terms for Maxwellian molecules are straight forward. The integrals required are of the type

$$\frac{n_1 n_2}{(2nk)^3}\left(\frac{m_1 m_2}{T_1^{\perp} T_2^{\perp}}\right)^{3/2} \sqrt{\frac{T_1^{\perp} T_2^{\perp}}{T_1'' T''_2}} \int g_x\, e^{-\frac{c_{11}^2}{2k/m_1 T_1''}}\, e^{-\frac{c_1^{\perp 2}}{2k/m_1 T_1}\perp}\, e^{-\frac{c_{21}^2}{2k/m_2 T_2''}}\, e^{\frac{c_2^{\perp 2}}{2k/m_2 T_2}\perp}\, \underline{dc}_1 \underline{dc}_2$$

$$= n_1 n_2 (u_2 - u_1) = I(g_x) \qquad (8)$$

Similarly

$$I(g_x^2) = n_1 n_2 \left\{(u_2-u_1)^2 + \frac{kT_2''}{m_2} + \frac{kT_1''}{m_1}\right\} \qquad (9)$$

$$I(g_{\perp}^2) = 2n_1 n_2 \left\{\frac{k}{m_2} T_2^{\perp} + \frac{k}{m_1} T_1^{\perp}\right\} \qquad (10)$$

$$I(v_{11} g_x) = n_1 n_2 \left\{u_1(u_2-u_1) - \frac{k T_1''}{m_1}\right\} \qquad (11)$$

$$I(v_{\perp} g_{\perp}) = 2n_1 n_2 \left\{-\frac{kT_1^{\perp}}{m_1}\right\} \qquad (12)$$

$$I(g^2) = n_1 n_2 \left[(u_2-u_1)^2 + \left(\frac{kT_2''}{m_2} + \frac{kT_1''}{m_1}\right) + 2\left(\frac{kT_2^{\perp}}{m_2} + \frac{kT_1^{\perp}}{m_1}\right)\right] \qquad (13)$$

The total moment collision terms can be expressed in terms of these elementary integrals.

Hard Elastic Sphere Molecules

$$S^{(1)} = \pi\lambda^2 \tag{14}$$

$$S^{(2)} = \frac{2}{3}\pi\lambda^2 \tag{15}$$

where λ is the radius of interaction for the colliding hard spheres.

The complete moment collision term integrations for hard spheres are not as simply derived as those for Maxwellian molecules. Odd powers of $g = \sqrt{(v_{21}-v_{11})^2 + (v_{22}-v_{12})^2 + (v_{23}-v_{13})^2}$ appear in these integrations where even powers occurred in the Maxwellian molecules case because the cross-sections, $S^{(1)}, S^{(2)}$ etc. for the fifth power molecules were proportional to $1/g$. A change in variables is of some assistance in the hard sphere calculations, however it is still a laborious task.

Consider colliding particles designated by superscripts α,β molecule masses m^α, m^β, having come from species with mean velocities u_K^α, u_K^β, temperatures T^α, T^β. Define

$$a^\alpha = \frac{kT^\alpha}{m^\alpha} \qquad a^\beta = \frac{kT^\beta}{m^\beta}$$

The new variables G_K, g_K are defined:

$$\frac{c_K^\alpha}{a^{\alpha\frac{1}{2}}} = \left(\frac{1/a^\beta}{1/a^\alpha + 1/a^\beta}\right)^{\frac{1}{2}}\left\{\left(\frac{a^\beta}{a^\alpha}\right)^{\frac{1}{2}} G_K + g_K - \epsilon_K\right\} \tag{16}$$

$$\frac{c_K^\beta}{a^{\beta\frac{1}{2}}} = \left(\frac{1/a^\alpha}{1/a^\alpha + 1/a^\beta}\right)^{\frac{1}{2}}\left\{\left(\frac{a^\alpha}{a^\beta}\right)^{\frac{1}{2}} G_K + g_K + \epsilon_K\right\} \tag{17}$$

where

$$\epsilon_K = (u_K^\alpha - u_K^\beta)/a^{m\frac{1}{2}}$$

$$g_K - \epsilon_K = (c_K^\alpha - c_K^\beta)/a^{m\frac{1}{2}}$$

$$g_K = (v_K^\alpha - v_K^\beta)/a^{m\frac{1}{2}}$$

$$a^m = \frac{k(m^\alpha T^\beta + m^\beta T^\alpha)}{m^\alpha m^\beta}$$

The Jacobian of this transformation in velocity space is:

$$\frac{\partial(\bar{C}_1', \bar{C}_2')}{\partial(\bar{G}, \bar{g})} = Cl^3 \tag{17}$$

where

$$\bar{C}_k = \bar{C}_k \left(\frac{1/a^\alpha \; 1/a^\beta}{1/a^\alpha + 1/a^\beta} \right)^{\frac{1}{2}} \tag{18}$$

$$Cl = \frac{(1/a^\alpha \; 1/a^\beta)^{\frac{1}{2}}}{1/a^\alpha + 1/a^\beta}$$

With the change to variables $\bar{g}$, $\bar{G}$, the collision integrals are of the form

$$\frac{1}{4\pi} \; \frac{1}{(2\pi)^{3/2}} \int e^{- G^2/2 + \frac{(\bar{g}-\bar{\epsilon})^2}{2}} G_{i_1} \cdots G_{i_n} \, g_{j_1} \cdots g_{j_m} \, g \, \underline{dG} \, \underline{dg} \tag{19}$$

The G -space integrals are straightforward

$$(a) \; \frac{1}{(2\pi)^{3/2}} \int e^{- G^2/2} \, \underline{dG} = 1 \tag{20}$$

$$(b) \; \frac{1}{(2\pi)^{3/2}} \int e^{-G^2/2} \; G_i G_j \, \underline{dG} = \delta_{ij} \quad \text{(Kroneker delta)} \tag{21}$$

$$(c) \; \frac{1}{(2\pi)^{3/2}} \int G^2 \, e^{-G^2/2} \; \underline{dG} = 3 \tag{22}$$

$$(d) \; \frac{1}{(2\pi)^{3/2}} \int G_i \, G_j \, G_K \, e^{-G^2/2} \, \underline{dG} = \left\{ \delta \; \delta \right\}_{ijk} \tag{23}$$

$$(e) \; \frac{1}{(2\pi)^{3/2}} \int G^2 G_i G_j \, e^{-G^2/2} \; \underline{dG} = 5\delta_{ij} \tag{24}$$

$$(f) \; \frac{1}{(2\pi)^{3/2}} \int G^4 e^{-G^2/2} \, \underline{dG} = 15 \tag{25}$$

Define

$$I^{(1)} = \frac{1}{4\pi} \int e^{-g^2/2 + \bar{g} \cdot \bar{\epsilon}} \, g \, \underline{dg} \tag{26}$$

Then

$$\frac{1}{4\pi}\int e^{-\frac{(\vec{g}-\bar{\epsilon})^2}{2}} (g_{i_1} \cdots g_{i_n})\, g\, \underline{dg} \tag{27}$$

$$= e^{-\epsilon^2/2} \frac{\partial^n I^{(1)}}{\partial\epsilon i_1 \ldots \partial\epsilon_{i_n}}$$

To evaluate

$$I^{(1)} = \frac{1}{4\pi}\, e^{\epsilon^2/2} \int e^{-x^2/2} \left|\bar{x} - \bar{\epsilon}\right| \underline{dx}$$

where

$$x_K = g_K - \epsilon_K$$

Choosing a polar coordinate system with $\bar{\epsilon}$ along the Z-axis (pointing in flow direction)

$$I^{(1)} = \frac{1}{4\pi}\, e^{\epsilon^2/2} \int e^{-x^2/2} \left(x^2+2x\epsilon\cos\varphi+\epsilon^2\right)^{\frac{1}{2}} x^2 \sin\varphi\, d\gamma\, d\varphi\, dx$$

$$= \tfrac{1}{2}\, e^{\epsilon^2/2} \int_0^\infty e^{-x^2/2}\, x^2 dx \int_{-1}^{1} (x^2-2x\epsilon u+\epsilon^2)^{\frac{1}{2}} du$$

$$= e^{\epsilon^2/2} \int_0^\infty e^{-x^2/2}\, x^2 dx \begin{cases} \left\{\epsilon + \frac{x^2}{3\epsilon}\right\} & \text{for } x < \epsilon \\ \left\{x + \frac{\epsilon^2}{3x}\right\} & \text{for } x > \epsilon \end{cases}$$

$$= e^{\epsilon^2/2} \left\{ \epsilon\, P_1 + \frac{1}{3\epsilon} P_2 + Q_2 + \frac{\epsilon^2}{3} Q_1 \right\}$$

$$= A \tag{28}$$

where

$$P_1 = \int_0^\epsilon x^2 e^{-x^2/2}\, dx \qquad P_2 = \int_0^\epsilon x^4 e^{-x^2/2} dx$$

$$P_3 = \int_0^\epsilon x^6 e^{-x^2/2}\, dx \qquad P_4 = \int_0^\epsilon x^8 e^{-x^2/2} dx$$

$$Q_1 = \int_\epsilon^\infty x e^{-x^2/2}\, dx \qquad Q_2 = \int_\epsilon^\infty x^3 e^{-x^2/2}\, dx$$

$$Q_3 = \int_\epsilon^\infty x^5 e^{-x^2/2} dx \qquad Q_4 = \int_\epsilon^\infty x^7 e^{-x^2/2} dx$$

Differentiating we find the expressions

$$\frac{\partial I^{(1)}}{\partial \epsilon} = e^{\epsilon^2/2}\left\{ (1+\epsilon^2)P_1 + \frac{1}{3}\left(1-\frac{1}{\epsilon^2}\right) P_2 + \frac{1}{3}(\epsilon^3+2\epsilon)Q_1 + \epsilon\, Q_2 \right\} = A1 \tag{29}$$

$$\frac{\partial^2 I^{(1)}}{\partial \epsilon^2} = e^{\epsilon^2/2}\left\{ (3\epsilon+\epsilon^3)P_1 + \frac{1}{3}\left(\epsilon-\frac{1}{\epsilon}+\frac{2}{\epsilon^3}\right)P_2 + \frac{1}{3}(2+5\epsilon^2+\epsilon^4)\, Q_1 + (1+\epsilon^2)Q_2 \right\} = A2 \tag{30}$$

$$\frac{\partial^3 I^{(1)}}{\partial \epsilon^3} = e^{\epsilon^2/2}\left\{ (3+6\epsilon^2+\epsilon^4)P_1 + \frac{1}{3}\left(\epsilon^2+\frac{3}{\epsilon^2}-\frac{6}{\epsilon^4}\right) P_2 + \frac{1}{3}(12\epsilon+9\epsilon^3+\epsilon^5)Q_1 + (3\epsilon+\epsilon^3)\, Q_2 \right\} = A3 \tag{31}$$

$$\frac{\partial^4 I^{(1)}}{\partial \epsilon^4} = e^{\epsilon^2/2}\left\{ (15\epsilon+10\epsilon^3+\epsilon^5)P_1 + \frac{1}{3}\left(\frac{24}{\epsilon^5}-\frac{12}{\epsilon^3}+\frac{3}{\epsilon}+2\epsilon+\epsilon^3\right)P_2 + \frac{1}{3}(12+39\epsilon^2+14\epsilon^4+\epsilon^6)Q_1 + (3+6\epsilon^2+\epsilon^4)Q_2 - 2\, e^{-\epsilon^2/2} \right\} = A4 \tag{32}$$

Similarly, define

$$\begin{aligned} I^{(3)} &= \frac{1}{4\pi}\int e^{-g^2/2 + \bar{g}\cdot\bar{\epsilon}}\, g^3\, \underline{dg} \\ &= \tfrac{1}{2}\, e^{\epsilon^2/2}\int_0^\infty e^{-x^2/2}\, x^2 dx \int_{-1}^{1} (x^2+\epsilon^2-2x\epsilon\mu)^{3/2} d\mu \\ &= e^{\epsilon^2/2}\int_0^\infty x^2 e^{-x^2/2} dx \begin{cases} \epsilon^3 + 2x^2\epsilon + \dfrac{x^4}{5\epsilon} & \text{for } x < \epsilon \\ x^3 + 2x\epsilon^2 + \dfrac{\epsilon^4}{5x} & \text{for } x > \epsilon \end{cases} \\ &= e^{\epsilon^2/2}\left\{ \epsilon^2 P_1 + 2\epsilon P_2 + \frac{1}{5\epsilon} P_3 + \frac{\epsilon^4}{5} Q_1 + 2\epsilon^2 Q_2 + Q_3 \right\} \end{aligned} \tag{33}$$

$$= B$$

Derivatives of $I^{(3)}$ give expressions for

$$\begin{aligned} &\frac{1}{4\pi}\int e^{-\frac{(\bar{g}-\bar{\epsilon})^2}{2}} (g_{i_1}\cdots g_{i_n}) g^3 \underline{dg} \\ &\qquad = e^{-\epsilon^2/2}\, \frac{\partial^n I^{(3)}}{\partial \epsilon_{i_1}\cdots \partial \epsilon_{i_n}} \end{aligned} \tag{34}$$

$$\frac{\partial I^{(3)}}{\partial \epsilon} = e^{\epsilon^2/2}\left\{ (3\epsilon^2+\epsilon^4)P_1 + 2(1+\epsilon^2)P_2 + \frac{1}{5}\left(1-\frac{1}{\epsilon^2}\right) P_3 \right.$$

$$\left. + \frac{1}{5}(4\epsilon^3+\epsilon^5)Q_1 + 2(2\epsilon+\epsilon^3)Q_2 + \epsilon Q_3 \right\} = B1 \qquad (35)$$

$$\frac{\partial^2 I^{(3)}}{\partial \epsilon^2} = e^{\epsilon^2/2}\left\{ (6\epsilon+7\epsilon^3+\epsilon^5)P_1 + 2(3\epsilon+\epsilon^3)P_2 \right.$$

$$+ \frac{1}{5}\left(\frac{2}{\epsilon^3} - \frac{1}{\epsilon} + \epsilon\right)P_3 + \frac{1}{5}(12\epsilon^2 + 9\epsilon^4+\epsilon^6)Q_1 \qquad (36)$$

$$\left. + 2(2 + 5\epsilon^2+\epsilon^4)Q_2 + (1+\epsilon^2)Q_3 \right\} = B2$$

Again, define

$$I^{(5)} = \frac{1}{4\pi}\int e^{-g^2/2 + \bar{g}\cdot\bar{\epsilon}}\, g^5 \underline{dg}$$

$$= \frac{1}{2} e^{\epsilon^2/2}\int_0^\infty e^{-x^2/2}\, x^2 dx \int_{-1}^{1} (x^2+\epsilon^2- 2x\epsilon\mu)^{5/2}\, d\mu$$

$$= e^{\epsilon^2/2}\left\{\epsilon^5 P_1 + 5\epsilon^3 P_2 + 3\epsilon P_3 + \frac{1}{7\epsilon} P_4 \right.$$

$$\left. + \frac{\epsilon^6}{7} Q_1 + 3\epsilon^4 Q_2 + 5\epsilon^2 Q_3 + Q_4 \right\} = C_6 \qquad (37)$$

Sample Collision Term Calculations

Maxwellian molecules:

For the sake of demonstration the calculation is outlined for the special case of collisional momentum and energy transfers between two gases, subscripted 1,2 having two-temperature ellipsoidal distributions.

$$f_i = \frac{n_i}{(2\pi k/m_i)^{3/2}} \frac{1}{T''^{\frac{1}{2}}_i} \frac{1}{T_{i\perp}} e^{-\frac{m_i c_{i\parallel}^2}{2kT''_i}} e^{-\frac{m_i c_{i\perp}^2}{2kT_{i\perp}}}$$

$$(\overline{\Delta v_x})_{coll} = \Delta_2(v_x) = \frac{n_1 n_2}{(2nk)^3} \left(m_1 m_2\right)^{3/2} \frac{1}{(T''_1 T''_2)^{\frac{1}{2}}} \frac{1}{T_{1\perp} T_{2\perp}} \times$$

$$\int M_2 g_x \underbrace{g S_{12}^{(1)}}_{\text{constant}} e^{-\frac{m_1 c_{1\parallel}^2}{2kT''_1}} e^{-\frac{m_1 c_{1\perp}^2}{2kT_{1\perp}}} e^{-\frac{m_1 c_{2\parallel}^2}{2kT''_2}} e^{-\frac{m_1 c_{2\perp}^2}{2kT_{2\perp}}} \underline{dc}\ \underline{dc_1}$$

$$- M_2 g S_{12}^{(1)} n_1 n_2 (u_2 - u_1)$$

$$= M_2 (g S_{12}^{(1)}) I(g_x) \tag{38}$$

$$\Delta_2(v^2) = 2M_2 (S_{12}^{(1)} g) [M_2 I(g^2) + I(v_x g_x) + I(v_\perp g_\perp)] \tag{39}$$

Hard Sphere Molecules:

As a sample calculation for hard spheres, the collisional momentum and energy transfers are derived for collisions between two one-temperature Maxwellians.

$$f_i = \frac{n_i}{(2\pi\ k/m_i\ T_i)^{3/2}} e^{\frac{mc_i^2}{2kT_i}}$$

$$(\overline{\Delta v_x})_{coll} = \Delta_1(v_x) = c_1 M_2 S^{(1)} A1 \tag{40}$$

$$\Delta_1(v^2) = c_2 M_2 S^{(1)} \{ M_2 B + (u_1 - u_2 K_2) A1 + K_2 \epsilon A_2 \} \tag{41}$$

$$K_1 = \frac{(m_1 m_2 T_1 T_2)^{\frac{1}{2}}}{m_1 T_2 + m_2 T_1}$$

$$K_2 = -\frac{m_2 T_1}{m_1 T_2 + m_2 T_1}$$

$$C_i = \left(\frac{m_1 m_2}{k^2 T_1 T_2}\right)^{3/2} n_1 n_2 \left(k \frac{(m_1 T_2 + m_2 T_1)}{m_1 m_2}\right)^{\frac{i+7}{2}} |J|$$

where $|J|$ is the Jacobian of the transformation of velocity coordinates shown in Eq. 17 .

The extension of these ideas to the calculation of higher order moment collisional contributions and to the bimodal type distribution calculations is a straightforward task within the above framework.

APPENDIX B

Maxwellian (Inverse Fifth Power Law) Molecules

An important molecular model for theoretical considerations is a point centre of repulsive force such that the force $\bar{F}$ between two molecules of masses m_1, m_2 separated by a distance r is

$$\bar{F} = -\frac{K_{12}}{r^{\nu}}\,\hat{r} \qquad (1)$$

$\hat{r}$ is a unit vector pointing along the line of centres from molecule "1" to "2"

If the position vectors of the two molecules from some fixed origin at time t are $\bar{r}_1$, $\bar{r}_2$, the position vector $\bar{r}_{21}$ of the second from the first is $\bar{r}_2 - \bar{r}_1$. The equations of motion of the two molecules are

$$m_1\ddot{\bar{r}}_1 = -\bar{F} \qquad m_2\ddot{\bar{r}}_2 = \bar{F}$$

therefore

$$\frac{m_1 m_2}{m_1 + m_2}\,\ddot{\bar{r}}_{21} = \bar{F} \qquad (2)$$

so the motion of m_2 relative to m_1 is the same as the motion of a particle with reduced mass $\frac{m_1 m_2}{m_1 + m_2} = \mu$ about a fixed centre of force $\frac{K_{12}}{r^{\nu}}$.

The polar coordinates r, θ are taken in the plane of the orbits as shown in Sketch B-1 and the equations of conservation for angular momentum and energy have the following form

$$r^2\dot{\theta} = gb \qquad (3)$$

$$\tfrac{1}{2}\left(\dot{r}^2 + r^2\dot{\theta}^2\right) + \frac{m_o K_{12}}{m_1 m_2}\,(\nu-1)\,r^{\nu-1} = \tfrac{1}{2}g^2 \qquad (4)$$

Eliminating time from Eqs. 3 and 4 gives

$$\tfrac{1}{2}\frac{g^2b^2}{r^4}\left\{\left(\frac{dr}{d\theta}\right)^2 + r^2\right\} = \tfrac{1}{2}g^2 - \frac{m_o K_{12}}{m_1 m_2(\nu-1)r^{\nu-1}} \qquad (5)$$

which integrates to give

$$\theta = \int_r^{\infty}\left\{\frac{r^4}{b^2} - r^2 - \frac{2\,m_o K_{12} r^{5-\nu}}{m_1 m_2(\nu-1)g^2b^2}\right\}^{-\frac{1}{2}} dr \qquad (6)$$

where θ is measured from the initial asymptote of the orbit. Defining $\zeta = b/r$ and $\zeta_0 = b\left(m_1 m_2 g^2/m_o K_{12}\right)^{1/\nu-1}$ the integral is

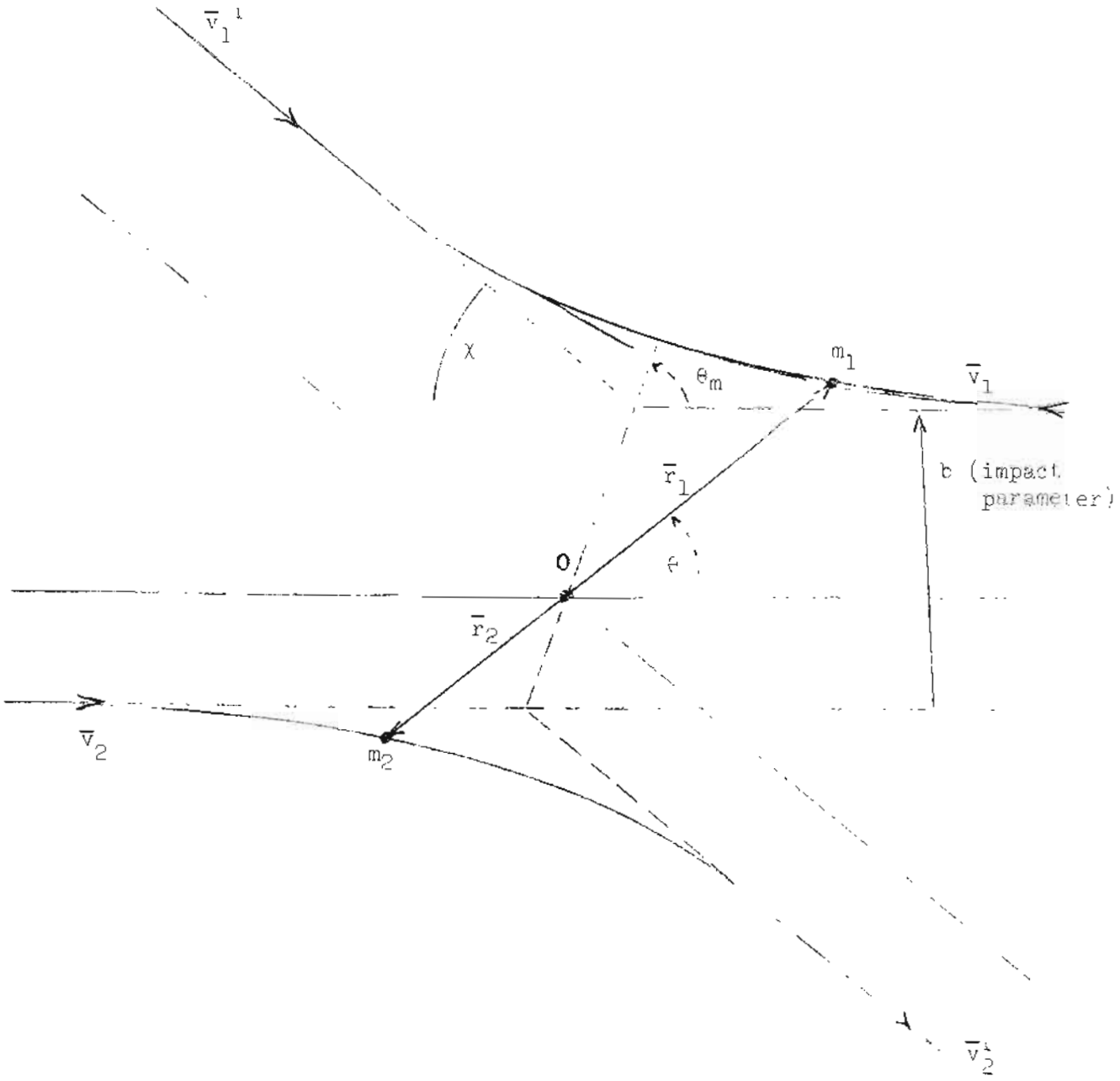

O is centre of mass

χ is deflection angle

θ_m is θ corresponding to minimum separation

SKETCH B-1: COLLISION COORDINATES

$$\theta = \int_0^{\mathcal{V}} \left\{ 1 - \mathcal{C}^2 - \frac{2}{\nu-1} \left(\frac{\mathcal{V}}{\mathcal{V}_0} \right)^{\nu-1} \right\}^{-\frac{1}{2}} d\mathcal{C} \qquad (7)$$

The apse of the orbit is given by $\frac{dr}{d\theta} = 0$ or $\frac{d\mathcal{C}}{d\theta} = 0$

i.e.

$$1 - \mathcal{C}^2 - \frac{2}{\nu-1} \left(\frac{\mathcal{V}}{\mathcal{V}_0} \right)^{\nu-1} = 0 \qquad (8)$$

For $\nu > 1$, this equation has only one real positive root, denoted by $\mathcal{C}_{00}$. The angle between the asymptotes of the orbit is twice the value of θ corresponding to $\mathcal{C} = \mathcal{C}_{00}$ and since χ, the deflection angle is the supplement of this angle,

$$\chi = \pi - 2 \int_0^{\mathcal{V}_{00}} \left\{ 1 - \mathcal{C}^2 - \frac{2}{(\nu-1)} \left(\frac{\mathcal{V}}{\mathcal{V}_{00}} \right)^{\nu-1} \right\}^{-\frac{1}{2}} d\mathcal{C} \qquad (9)$$

The integrals

$$S^{(\ell)} = \int_0^{2\pi} \int_0^{\infty} (1-\cos^{\ell}\chi)\, b\,db\,d\epsilon$$

$$= \left(\frac{m_0 K_{12}}{m_1 m_2} \right)^{2/\nu-1} g^{-\frac{4}{\nu-1}} A_{\ell}(\nu) \qquad (10)$$

where

$$A_{\ell}(\nu) = \int_0^{\infty} (1-\cos^{\ell}\chi)\, \mathcal{C}_0\, d\mathcal{C}_0$$

These constants have been evaluated numerically using the expression for χ given in equation 9. The case $\nu = 5$ is of particular interest in kinetic theory because it simplifies greatly the moment collision integrals. For $\nu = 5$, the cross sections are inversely proportional to the relative velocity g. Hypothetical molecules obeying this inverse fifth power law repulsion interaction are called Maxwellian molecules and the simplifying features of this model when applied to the moment collision integrations are pointed out in Appendix A.

Molecular interactions with infinite extent such as these inverse power law fields are not well suited to numerical experiments or Monte Carlo solutions. Although the cross-sections for transfer of molecular moments appearing in the transfer collision terms are finite for $\nu > 2$, each molecule is, theoretically, in a state of constant "collision" with all other molecules and at no time is it travelling along a straight path uninfluenced by surrounding molecules. Simply stated, these molecules do not have "free paths". The Monte Carlo technique which proposes to follow a test particle through the gaseous system is only feasible if the trajectory can be described approximately, at least, by a series of straight line "free paths" terminated by collisions which change the test particle velocity over an infinitesimal distance. Without this approximation the method becomes an impracticable dynamic simulation.

This problem is overcome by specifying a collision cut-off i.e. a rather arbitrarily chosen minimum value for the deflection angle $\chi = \chi_{min}$. A pair of particles collide if their impact parameter is smaller than that corresponding to χ_{min} ($b < b_{max}$). The mutual influence of particles with $b > b_{max}$ is neglected. The random selection of collision parameters then is quite simple

$$\epsilon = (R + 1)\pi \qquad \text{where R is a random number from the rectangular distribution on } -1 \leq R \leq 1$$

$$\frac{b}{b_{max}} = \sqrt{\frac{R+1}{2}} \tag{11}$$

giving a uniform distribution of impact points over the collision surface πb_{max}^2.

The angle θ_o between the initial asymtote and the apse line is calculated from Eq. 7

$$\theta_o = \frac{1}{(1 + 2/\xi_o^4)} \left(\frac{1}{2} - \frac{1}{2\sqrt{1+2/\xi_o^4}} \right) \tag{12}$$

where $\mathcal{K}$ symbolizes the complete elliptic integral of its argument.

One further definition: The collision frequency for Maxwellian molecules is independent of the relative speed of the colliding pairs.

$$\nu = n \left[\xi_o\right]_{max}^2 \left(\frac{K_{12}}{\mu}\right)^{\frac{1}{2}} \tag{13}$$

With these modifications the Maxwellian molecule Monte Carlo calculations follow the hard sphere program. Length is scaled in unit of the upstream "mean free path" in the light gas. Because of the long range nature of the Maxwellian molecule interaction, m.f.p. must be defined on the basis of some hard sphere analogue - for example the Chapman-Enskog first approximation to the viscosity coefficient for hard spheres is:

$$\mu_1 = \frac{5}{15\lambda^2} \left(\frac{mkT}{\pi}\right)^{\frac{1}{2}} \tag{14}$$

where $\lambda/2$ is the radius of the hard sphere molecule.

The hard sphere mean free path is: (in a Maxwellian gas)

$$\lambda = \frac{1}{\sqrt{2}\ n\ \pi\lambda^2} \tag{15}$$

or substituting for λ in terms of μ

$$\lambda_\mu = \frac{16}{5} \frac{\mu_1}{\rho\sqrt{2\pi mkT}} \tag{16}$$

For Maxwellian molecules

$$\mu_1 = \frac{kT}{3\pi A_2(5)} \left(\frac{2m}{K}\right)^{\frac{1}{2}} \tag{17}$$

therefore a viscosity mean free path for Maxwellian molecules can be defined:

$$\lambda_\mu = \frac{16}{15\pi^{3/2} n A_2(5)} \left(\frac{kT}{K}\right)^{\frac{1}{2}} \tag{18}$$

where $A_2(5) \approx .436$

K is calculated from Eq. 17 using experimental viscosity data (see Chapman and Cowling, Chapter 12).

K_{12} is calculated from the first approximation diffusion coefficient for Maxwellian molecules and experimental diffusion data. (See Chapman and Cowling, Chapter 14.)

The Maxwellian molecule Monte Carlo calculations were costly in computation time and are considered only as a check on the general nature of the hard sphere results. Good agreement between the M.C. and moment solution density profiles is shown in Fig. B-2. The extremely close agreement with the moment solution during the early stages of compression followed by a rather erratic fluctuation about that solution during the later stage was also characteristic of the hard sphere solutions with small sample size.

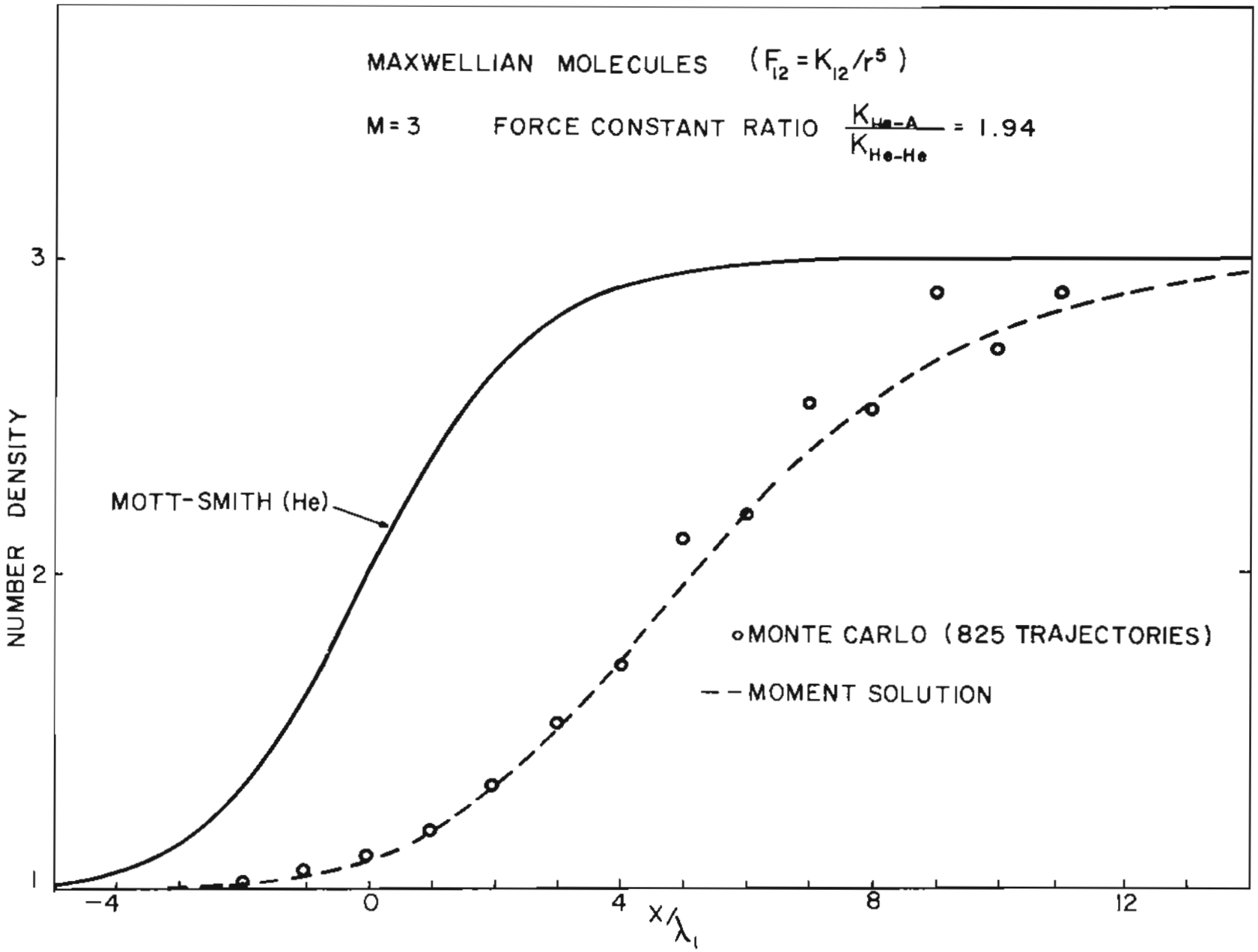

FIG B-2 NUMBER DENSITY PROFILES FOR THE MAXWELLIAN MOLECULE COLLISION MODEL

APPENDIX C

Random Direction Cosines

It was shown in Sec. 4.3 that in a hard sphere collision between molecules m_1, m_2 with initial velocity components u_1, v_1, w_1 and u_2, v_2, w_2 and relative speed g that the relative velocity vector is rotated in a centre of mass coordinate system with equal probability into equal solid angle elements without regard for direction. A set of random direction cosines, L,M,N is required to specify this random orientation (see Ref. 15). The method of specifying L,M,N with two random selections from the rectangular random number generator is illustrated in Sketch C-1. Choose a point A on a unit circle having polar coordinates (r,ϵ) by choosing two random numbers γ,δ in the rectangular distribution on -1 to +1 and rejecting the pair if A lies outside the unit circle. The spherical coordinates of B directly above A on the unit sphere are 1, ϕ, ϵ . This defines the line of centres at impact. The spherical coordinates 1, ψ,ϵ of point C are picked so $\psi = 2\phi = \pi - \chi$. This point C defines a set of random direction cosines.

Say $p(r,\epsilon)dr\ d\epsilon$ = probability of selecting r,ϵ in $dr\ d\epsilon$

$$= \frac{\text{area element } dr\ d\epsilon}{\pi}$$

$$= \frac{r\ dr\ d\epsilon}{\pi} \qquad (1)$$

Also $p(\psi,\epsilon)\ d\psi\ d\epsilon$ = probability of selecting ψ,ϵ in $d\psi\ d\epsilon$

$$= p(r,\epsilon)\ dr\ d\epsilon$$

$$= \frac{\sin\phi\ \cos\phi}{\pi}\ d\phi\ d\epsilon$$

$$= \frac{\sin\psi\ d\psi\ d\epsilon}{4\pi} = \frac{d\Omega}{4\pi}$$

$$= \frac{\text{solid angle element}}{\text{complete solid angle}} \qquad (2)$$

The direction cosines are

$$L = \cos\psi = 1 - 2r^2 \qquad (3)$$

$$M = \sin\psi\ \cos\epsilon = 2\gamma\sqrt{1-r^2} \qquad (4)$$

$$N = \sin\psi\ \sin\epsilon = 2\delta\sqrt{1-r^2}$$

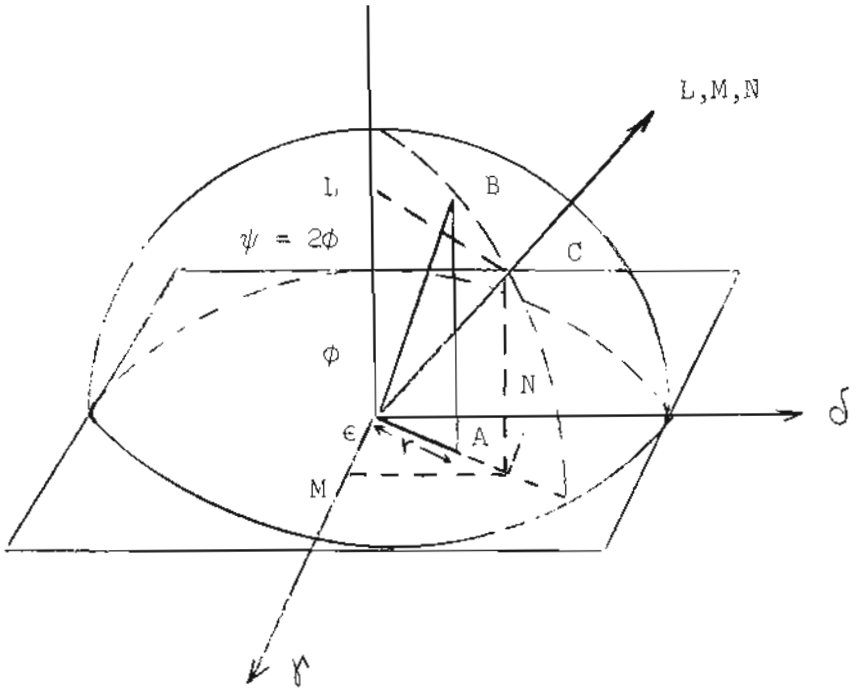

SELECTION OF RANDOM DIRECTION COSINES

APPENDIX D

Equilibrium Points of the 1-Temperature Maxwellian Diffusion Equations

The equations for the diffusing species number density and temperature behaviour must be integrated between the upstream and downstream equilibrium points. The inhomogeneous collision terms in these equations are governed by interaction between the diffusing species and a background Mott-Smith shock profile for the light gas. To demonstrate the nature of these equilibrium points the collision terms will be represented here by their Maxwellian molecule approximate forms and the characteristic equation of the set of 3 first order ordinary differential equations (including the Mott-Smith equation for the background gas) is analysed.

$$\frac{dn}{dx} = (5F - E/u) \;/\; (5T - 3\mathcal{S}) \tag{1}$$

$$\frac{dT}{dx} = \left((T-\mathcal{S})\, E/u + 2\mathcal{S}F \right) \;/\; (5T - 3\mathcal{S})n \tag{2}$$

$$\frac{dN_1}{dx} = - B(1-N_1)N_1 \tag{3}$$

where n, T are the diffusing species number density and temperature in units of their upstream equilibrium values n_1, T_1, u is the diffusing species velocity divided by $\sqrt{\frac{k}{m_1} T_1}$ and $\mathcal{S} = u^2$. (h signifies heavy species, ℓ signifies light species)

For Maxwellian molecules:

$$F = n\, N_1 \chi\, \mu\, (U_1 - u) + n\, N_2 \chi\, \mu\, (U_2 - u) \tag{4}$$

$$\begin{aligned} E = {} & 2n\, N_1 \chi\, \mu \left\{ M_\ell \left[(U_1-u)^2 + 3T_1 + \frac{3T}{m_n} \right] + u(U_1-u) - \frac{3T}{m_n} \right\} \\ & + 2n\, N_2 \chi\, \mu \left\{ M_\ell \left[(U_2-u)^2 + 3T_2 + \frac{3T}{m_n} \right] + u(U_2-u) - \frac{3T}{m_n} \right\} \end{aligned} \tag{5}$$

at upstream equilibrium

$$\begin{aligned} \frac{\partial F}{\partial n} &= N_1\, U_1 \chi\mu & \frac{\partial F}{\partial T} &= 0 \\ \frac{\partial E}{\partial n} &= 2\, N_1 \chi\mu\, u^2 & \frac{\partial E}{\partial T} &= -6\, N_1\, \mu\, M_\ell \end{aligned} \tag{6}$$

the light gas distribution function is assumed to be the simple bimodal form:

$$f = \frac{n_1}{(2\pi\, k/m_\ell T_1)^{3/2}}\, e^{-\frac{m_\ell}{2kT_1}(\bar{v}-\bar{u}_1)^2} + \frac{n_2}{(2\pi\, k/m_\ell\, T_2)^{3/2}}\, e^{-\frac{m_\ell}{2kT_2}(\bar{v}-\bar{u}_2)^2} \tag{7}$$

N_1, above, is the value of n_1 divided by the upstream equilibrium light gas number density, n_{10}, $N_2 = n_2/n_{10}$; χ is the constant part of the Maxwellian molecule collision cross section, $S^{(1)}_{\ell\text{-}h}$ for cross collisions divided by the same quantity for light-light collisions that is $= \{gS^{(1)}_{\ell\text{-}h}\}/\{gS^{(1)}_{\ell\text{-}\ell}\}$

$$\mu = \frac{m_\ell\, m_h}{m_\ell + m_h} \quad , \quad M_\ell = \frac{m_\ell}{m_\ell + m_h} \quad , \quad M_h = \frac{m_h}{m_h + m_\ell} \, , \quad U = \frac{u}{\sqrt{k/m_h T}} \qquad (8)$$

The equations are linearized about the equilibrium points where all gradients go to zero.

$$\frac{dn}{dx} = \Big\{ \underbrace{\left(5\frac{\partial F}{\partial n} - \frac{1}{u}\frac{\partial E}{\partial n}\right)}_{a_{11}} \Delta n + \underbrace{\left(5\frac{\partial F}{\partial T} - \frac{1}{u}\frac{\partial E}{\partial T}\right)}_{a_{12}} \Delta T + \underbrace{\left(5\frac{\partial F}{\partial N_1} - \frac{1}{u}\frac{\partial E}{\partial N_1}\right)}_{a_{13}} \Delta N_1 \Big\} \Big/ (5T-3S)$$

$$\frac{dT}{dx} = \Big\{ \underbrace{\left(\frac{(T-S)}{u}\frac{\partial E}{\partial n} + 2S\frac{\partial F}{\partial n}\right)}_{a_{21}} \Delta n + \underbrace{\left(\frac{(T-S)}{u}\frac{\partial E}{\partial T} + 2S\frac{\partial F}{\partial T}\right)}_{a_{22}} \Delta T + \underbrace{\left(\frac{(T-S)}{u}\frac{\partial E}{\partial N_1} + 2S\frac{\partial F}{\partial N_1}\right)}_{a_{23}} \Delta N_1 \Big\} \Big/ (5T-3S)n$$

$$\frac{dN_1}{dx} = \underbrace{\frac{\partial}{\partial n}\left(\frac{dN_1}{dx}\right)}_{a_{31}=0} \Delta n + \underbrace{\frac{\partial}{\partial T}\left(\frac{dN_1}{dx}\right)}_{a_{32}=0} \Delta T + \underbrace{\left(-B(1-2N_1)\right)}_{a_{33}} \Delta N_1 \qquad (9)$$

The characteristic equation is

$$[(a_{11}-\lambda)(a_{22}-\lambda) - a_{21}\, a_{12}]\,(a_{33}-\lambda) = 0 \qquad (10)$$

i.e.

$$(a\lambda^2 + b\lambda + c)(a_{33} - \lambda) = 0 \qquad (11)$$

One of the roots is $a_{33} = -B(1-2N_1)$ which has the value B at upstream equilibrium and -B downstream. The others are the roots of the quadratic $a\lambda^2 + b\lambda + c = 0$. Since only the qualitative nature of the equilibrium points is of interest, it is sufficient to determine the signs of these two roots.

$$a_{11} = 3\,\mu\chi\, N_1/(5T-3S) = 3\,\mu\chi\sqrt{\gamma}\, M/5\,(1-\omega M^2)$$

$$a_{12} = \frac{6\, N_1 \mu\chi M_\ell}{u(5T-3S)} = 6\,\mu\chi\, M_\ell/5\sqrt{\gamma}\, M\,(1-\omega M^2) \qquad (12)$$

$$a_{21} = 2\,T\,N_1\chi(\mu\, u/(5T-3S) = 2\,\mu\sqrt{\gamma}\, M/5\,(1-\omega M^2)$$

$$a_{22} = \frac{-6(T-S)\, N_1\chi(\mu\, M_\ell}{u(5T-3S)} = -\frac{6\chi\mu\, M_\ell(1-\omega\gamma M^2)}{5\sqrt{\gamma}\, M\,(1-\omega M^2)}$$

$$\lambda^2 - (a_{11} + a_{22})\,\lambda + a_{11}\,a_{22} - a_{12}\,a_{21} = 0$$

$$c = \frac{-\,6\chi^2\,\mu^2\,M_\ell}{5(1-\omega M^2)^2} \qquad \omega = \frac{m_h}{m_\ell} \tag{13}$$

Supersonic, $(1-\omega M^2) < 0$. Roots are same sign as -b

$$b = -\chi\mu\,\frac{(-6\,M_\ell\,(1-\omega\gamma M^2) + 3\,\gamma M^2)}{5\sqrt{\gamma}\,M\,(1-\omega M^2)} > 0 \quad \text{for } \sqrt{\omega}\ M > 1 \tag{14}$$

These two roots are negative. The third root is positive at $x = -\infty$, $\lambda_3 = B$. The equilibrium point then is a saddle point.

At the downstream point

$$\frac{\partial F}{\partial n} = N_2 U_2 \chi\mu \qquad \frac{\partial F}{\partial T} = 0$$

$$\frac{\partial F}{\partial n} = 2\,N_2\chi\mu\,\sqrt{\gamma T_2}\,M_D U_2 \quad \frac{\partial F}{\partial T} = -\,6\,N_2\,\mu\,M_\ell \tag{15}$$

$$a_{11} = 3\chi\mu\,N_2\,\sqrt{\gamma T_2}\,M_D/5\,T_2\,(1-\omega M_D^2)$$

$$a_{12} = 6\,N_2\,\mu\chi\,M_\ell/5\,\sqrt{\gamma T_2}\,M_D\,T_2\,(1-\omega M_D^2)$$

$$a_{21} = 2\chi\mu\,T_2\,\sqrt{\gamma T_2}\,M_D/5\,T_2\,(1-\omega M_D^2) \tag{16}$$

$$a_{22} = -\,\frac{6\chi\mu\,M_D\,T_2\,(1-\omega\gamma M_D^2)}{5\,\sqrt{\gamma T_2}\,T_2\,(1-\omega M_D^2)}$$

$$c = -\,\frac{6}{5}\,\frac{\chi^2\,\mu^2 M_\ell}{T_2(-\,\omega M_D^2)^2} \tag{17}$$

where ωM_D is the heavy gas downstream Mach number.

$c < 0$ for $\omega M_D^2 < 1$

$b^2 - 4\,ac > b^2$ so the roots have opposite sign and the equilibrium point is a saddle type downstream when the gas passes through M = 1. It is nodal for entirely supersonic diffusing heavy species.

For the ionized gas case of section 6, the charged species are subsonic throughout. The downstream equilibrium point is then a saddle point and not a suitable numerical integration target point.

Singular Points in 3 - D Phase Space

Consider the set of 3 first order linear ordinary differential equations which correspond to the linearized form of the flow equations about an equilibrium point.

$$\begin{aligned} \frac{dx}{dt} &= X(x,y,z,t) \\ \frac{dy}{dt} &= Y(x,y,z,t) \\ \frac{dz}{dt} &= Z(x,y,z,t) \end{aligned} \tag{18}$$

The general solution of this system has the form

$$\begin{aligned} x &= c_1\alpha_1 e^{\lambda_1 t} + c_2\alpha_2 e^{\lambda_2 t} + c_3\alpha_3 e^{\lambda_3 t} \\ y &= c_1\beta_1 e^{\lambda_1 t} + c_2\beta_2 e^{\lambda_2 t} + c_3\beta_3 e^{\lambda_3 t} \\ z &= c_1\gamma_1 e^{\lambda_i t} + c_2\gamma_2 e^{\lambda_2 t} + c_3\gamma_3 e^{\lambda_3 t} \end{aligned} \tag{19}$$

If λ_1, λ_2, λ_3 are all of the same sign, all solutions pass through (0,0,0) at either $t \to \pm\infty$. This particular condition represents a nodal point and a stable approach point for numerical integration of the set.

If two roots of the same sign (say λ_1, λ_2, $\lessgtr 0$) then there is a set of solutions passing through the origin - those for which $c_3 = 0$

$$\begin{aligned} x &= \alpha_1 p + \alpha_2 q \\ y &= \beta_1 p + \beta_2 q \\ z &= \gamma_1 p + \gamma_2 q \end{aligned} \qquad \text{where } \begin{aligned} p &= c_1 e^{\lambda_1 t} \\ q &= c_2 e^{\lambda_2 t} \end{aligned} \tag{20}$$

Solving the consistency relationship:

$$\left(\alpha_2 - \alpha_1 \frac{\gamma_2}{\gamma_1}\right)\left(x - \frac{\alpha_1}{\beta_1} y\right) = \left(\alpha_2 - \frac{\alpha_1}{\beta_1}\beta_2\right)\left(x - \frac{\alpha_1}{\gamma_1} z\right) \tag{21}$$

i.e. $F(x,y,z) = 0$ a surface passing through (0,0,0) as $t \to \mp\infty$

All solutions for which $c_3 \neq 0$ diverge as $t \to \mp \infty$. As $t \to \pm \infty$ the solutions $c_3 = 0$ diverge from the equilibrium point whereas the line solution $c_1 = c_2 = 0$, $c_3 \neq 0$ passes through (0,0,0). Both of these conditions represent 3-dimensional saddle points and are unsatisfactory numerical integration approach points.

Case - Diffusing Species Subsonic Throughout

It was stated in Sec. 6.2 that although the quilibrium points for the high electron temperature ionized gas case are both saddle points, an iterative scheme of solution converges. Under these conditions the diffusing charged species are subsonic throughout with respect to the ion acoustic speed $\sqrt{\frac{k}{m_i}(T_i + T_e)}$. The important features of the iteration scheme is that only one of the equations is integrated at each iteration - the profile of one of the variables is approximated by its value from the previous solution. The solution is started by assuming the ions to have the atom temperature for integration of the charged particle number density equation. Then, using the notation described above

$$\frac{dn}{dx} = \left(F - n \frac{dT}{dx}\right) / (\theta - \mathcal{D}) \tag{22}$$

where $\frac{dT}{dx}$ is a prescribed function of x (and hence N_1) from the previous iteration i.e.

$$\frac{dn}{dx} = (F - \phi(N_1) n) / (\theta - \mathcal{D})$$

$$\frac{\partial}{\partial n}\left(\frac{dn}{dx}\right) = \frac{\partial F}{\partial n} / (\theta - \mathcal{D}) \tag{23}$$

$$> 0 \quad \text{at both upstream and downstream}$$

$$(\theta = T_e + T_i \; ; \; (\theta - \mathcal{D}) > 0)$$

$$\frac{\partial}{\partial N_1}\left(\frac{dN_1}{dx}\right) = \overset{\text{up}}{\underset{\text{down}}{\pm}} B \quad \text{at stream}$$

The linearized equations in this case are

$$\begin{aligned} \frac{dn}{dx} &= \frac{\partial}{\partial n}\left(\frac{dn}{dx}\right)^{a_{11}} \Delta n + \frac{\partial}{\partial N_1}\left(\frac{dn}{dx}\right)^{0} \Delta N_1 \\ \frac{dN_1}{dx} &= \frac{\partial}{\partial n}\left(\frac{dN_1}{dx}\right)^{0} \Delta n + \frac{\partial}{\partial N_1}\left(\frac{dN_1}{dx}\right)^{a_{22}} \Delta N_1 \end{aligned} \tag{24}$$

The characteristic equation is:

$$(a_{11} - \lambda)(a_{22} - \lambda) = 0 \quad \text{since } a_{12} = a_{21} = 0 \tag{25}$$

Downstream, then, the roots are of opposite sign but they are both positive upstream. Therefore the direction of stable numerical integration for dn/dx is

from the downstream saddle point into upstream node.

Similarly for the diffusing species temperature integration when n is specified from the previous iteration

$$\frac{dT}{dx} = \left(\frac{E}{u} + 2\zeta \frac{dn}{dx} \right) / 5n \tag{26}$$

$$= (E/u + \psi (N_1))/5n$$

$$\frac{\partial}{\partial T} \left(\frac{dT}{dx} \right) = \frac{\partial}{\partial T} \frac{(E/u)}{5n} < 0 \tag{27}$$

$$\frac{\partial}{\partial N_1} \left(\frac{dN_1}{dx} \right) = \pm B \text{ at } \begin{matrix} up \\ down \end{matrix} stream \tag{28}$$

For this integration the roots are both negative at a downstream node and of opposing signs at an upstream saddle point. The set inegrates stably from upstream to down.

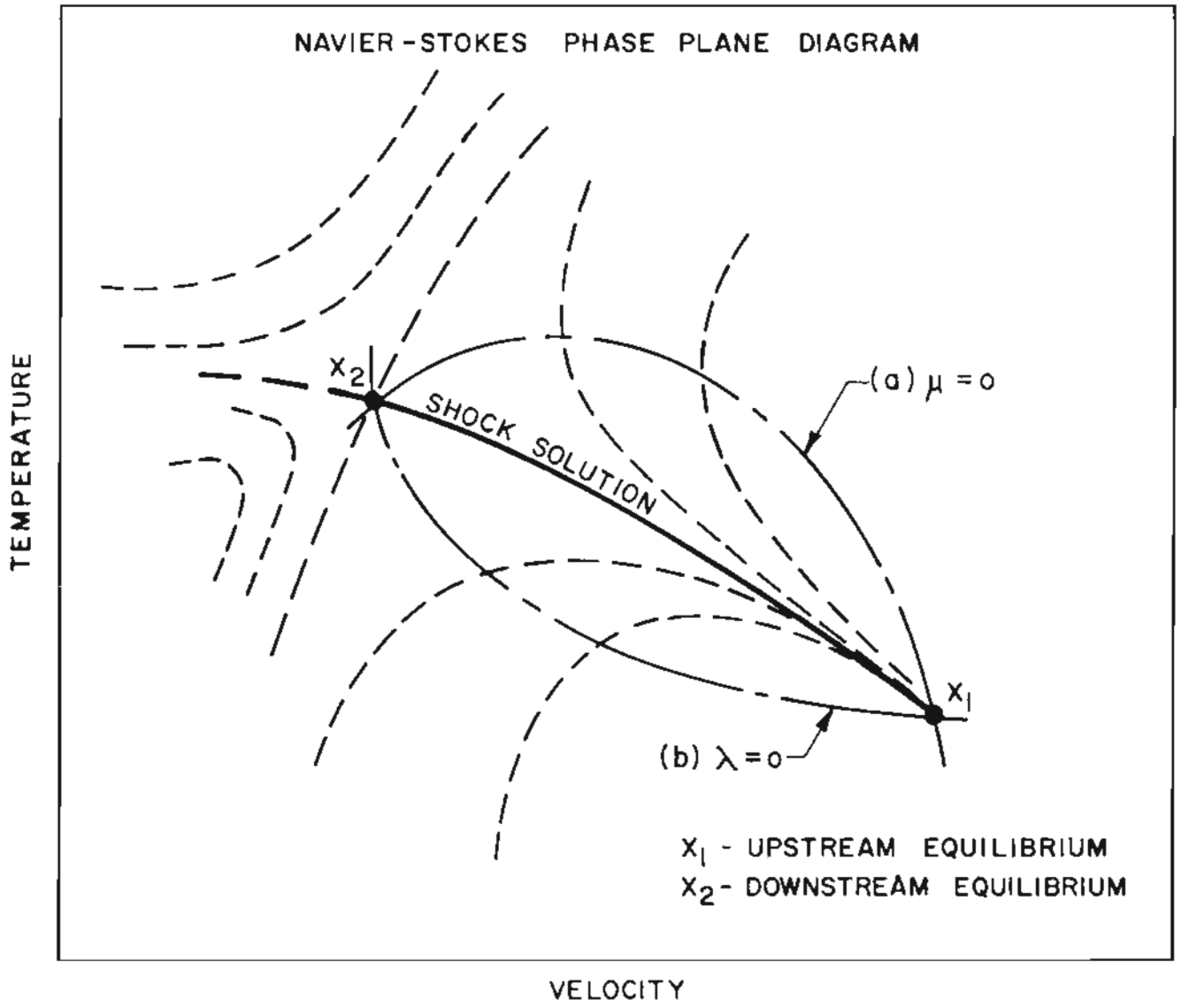

FIG. 1 PHASE PLANE REPRESENTATION OF THE NAVIER-STOKES SHOCK WAVE STRUCTURE SOLUTION

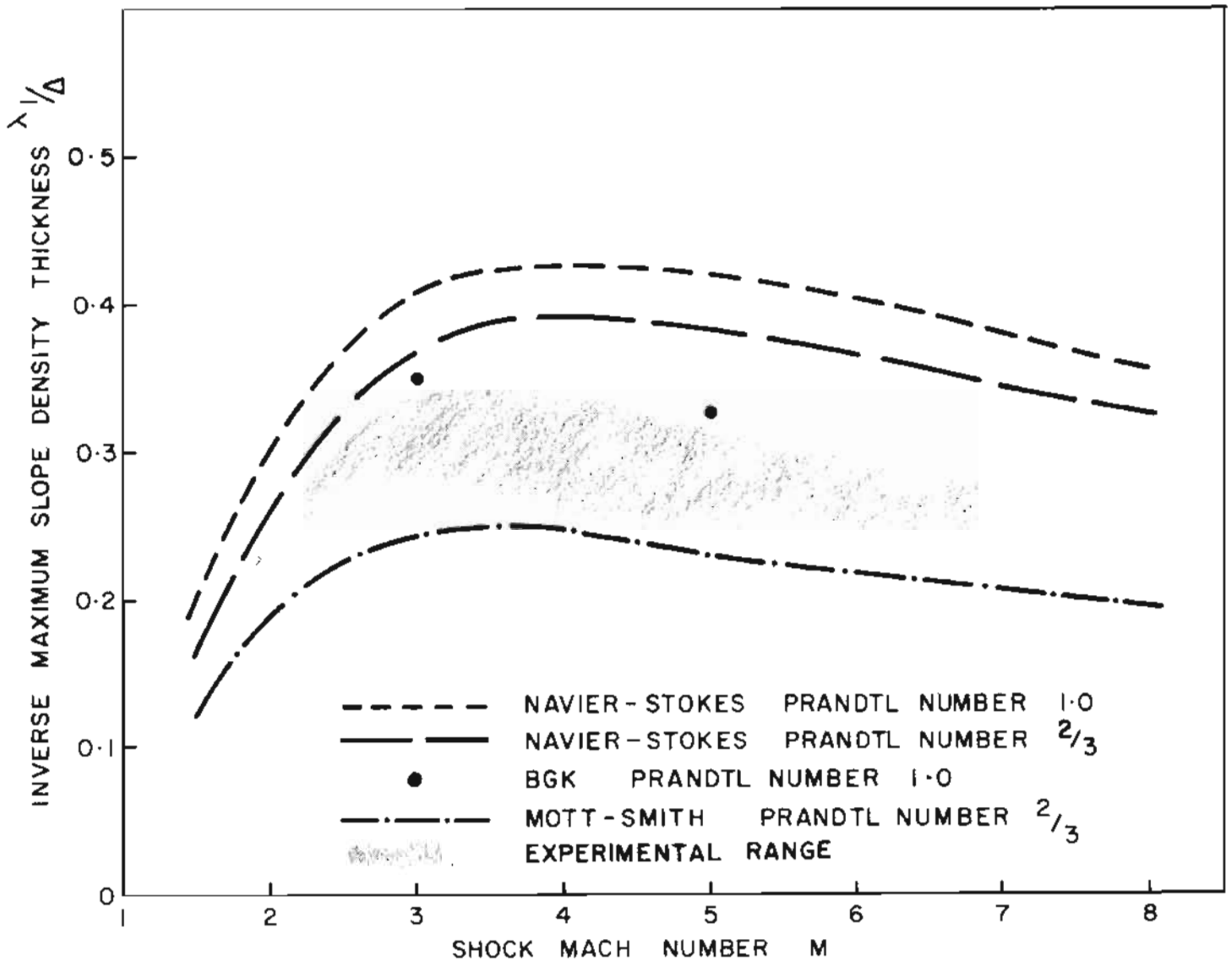

FIG. 2 SINGLE COMPONENT SHOCK WAVE THICKNESS AS A FUNCTION OF SHOCK MACH NUMBER

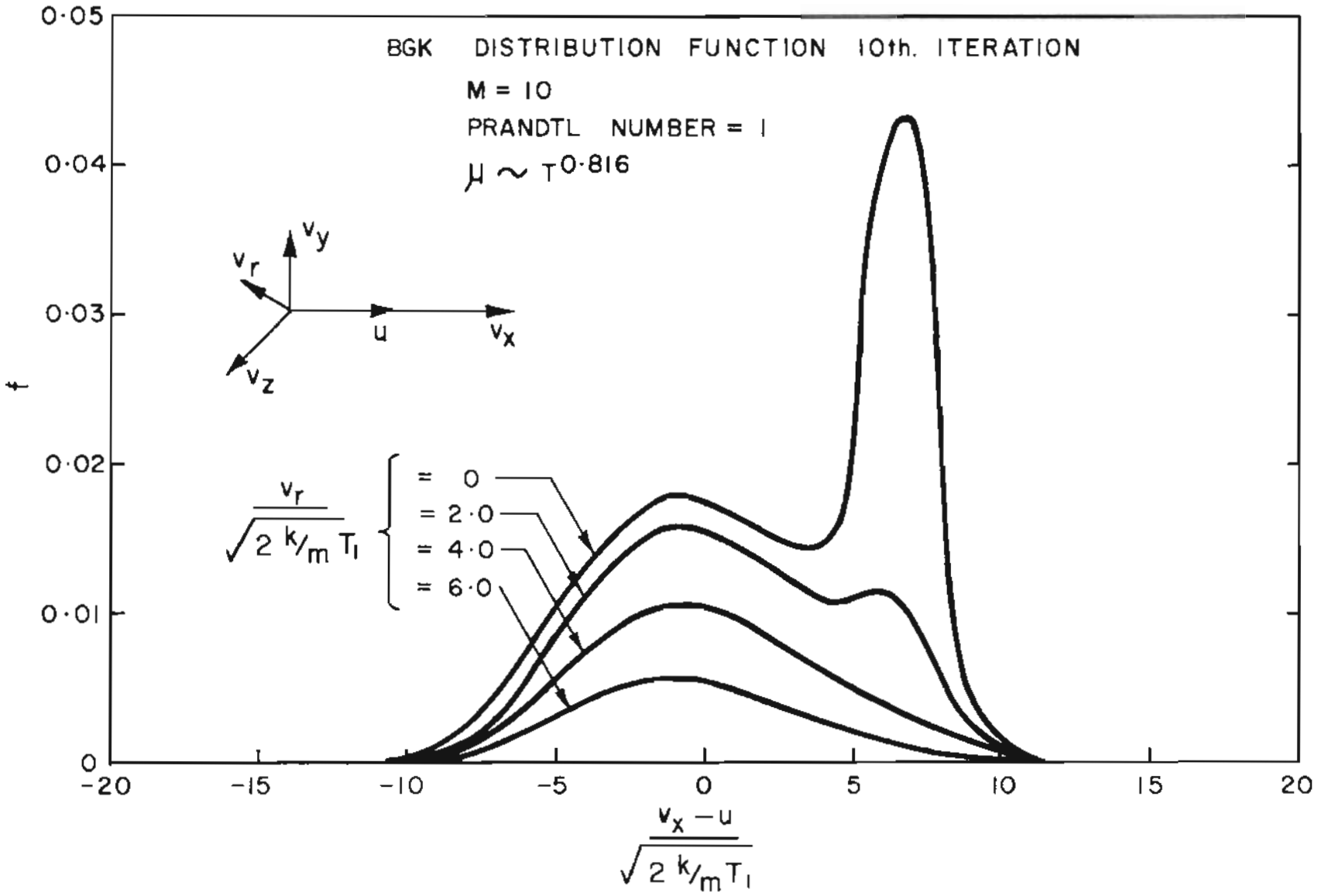

FIG. 3 DEPENDENCE OF THE BGK SOLUTION DISTRIBUTION FUNCTION ON v_x AND v_r AT A POINT WITHIN THE SHOCK.

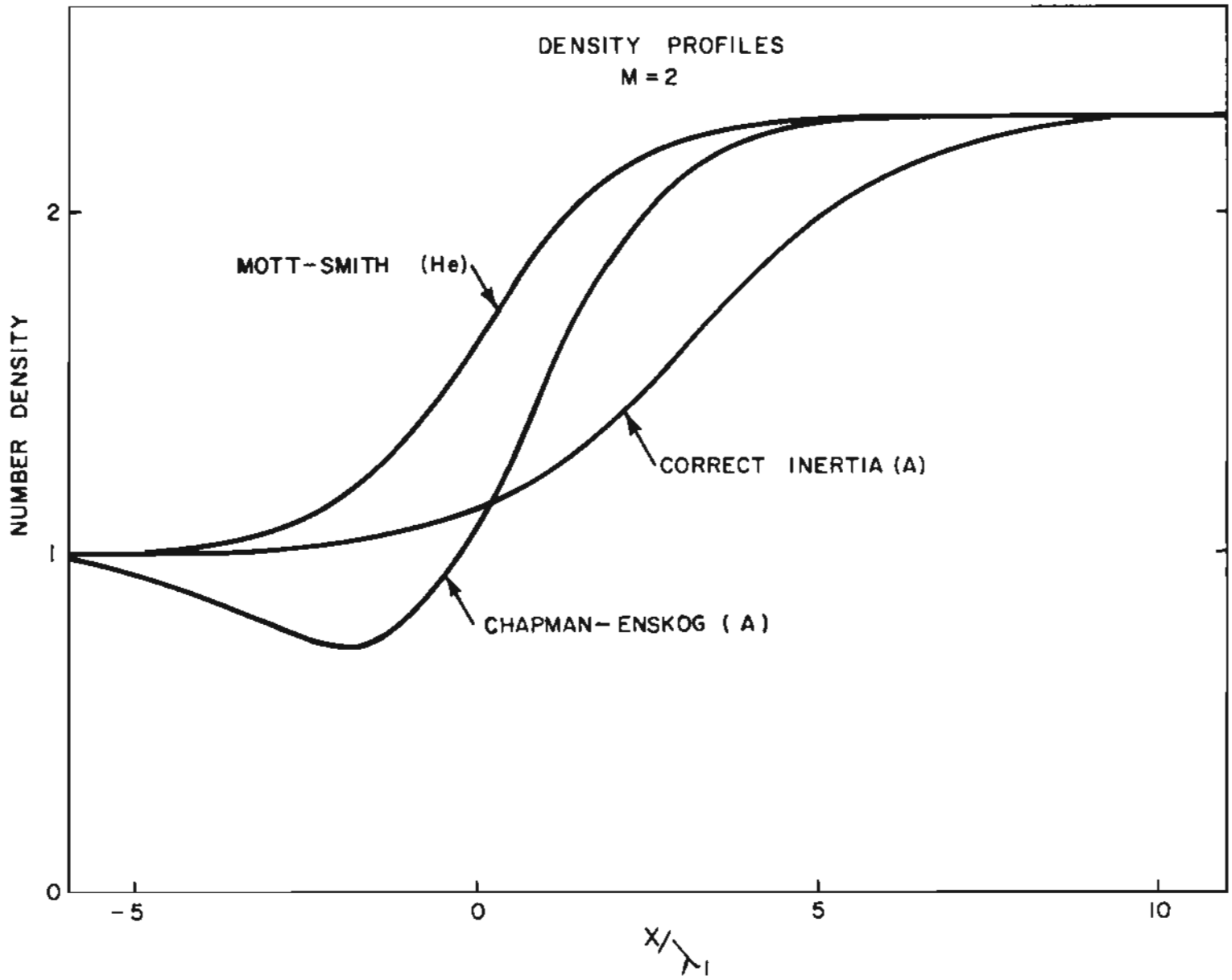

FIG. 4 ANOMALOUS DENSITY UNDERSHOOT CAUSED BY THE USE OF THE INCORRECT INERTIA TERM IN THE ARGON MOMENTUM EQUATION

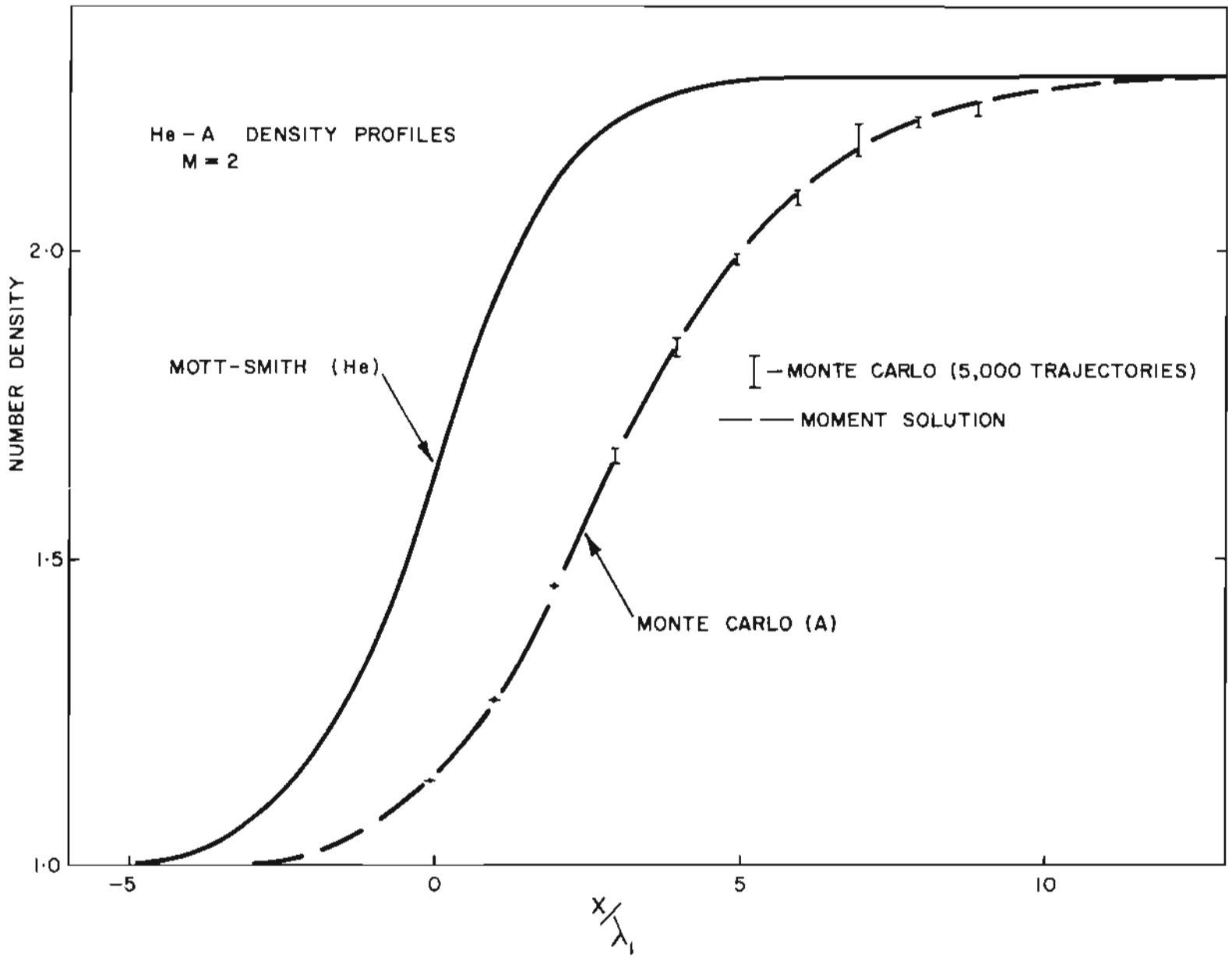

FIG. 5 NUMBER DENSITY PROFILES FOR A TRACE OF ARGON IN A MACH 2 HELIUM SHOCK

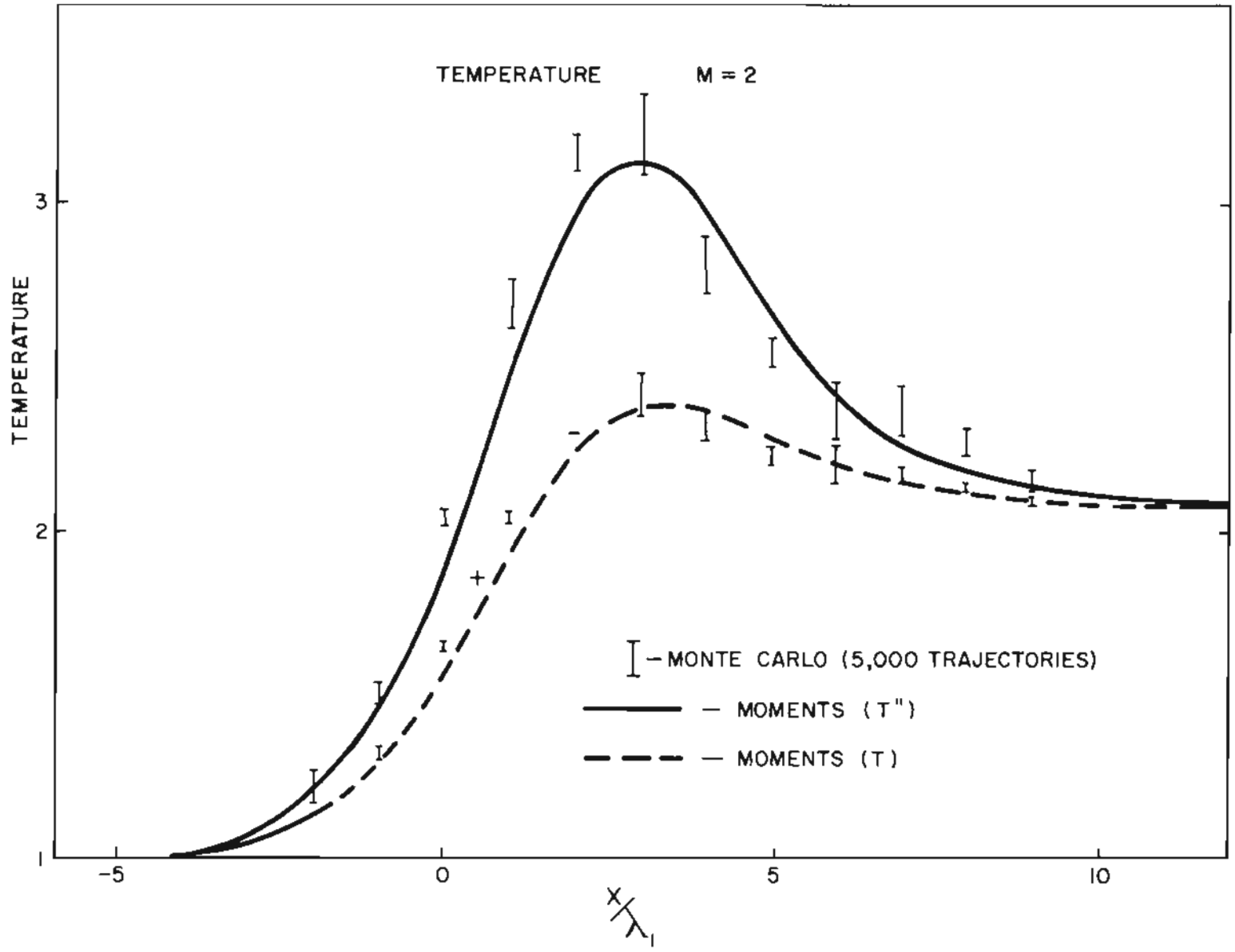

FIG. 6 TEMPERATURE PROFILES FOR A TRACE OF ARGON IN A MACH 2 HELIUM SHOCK

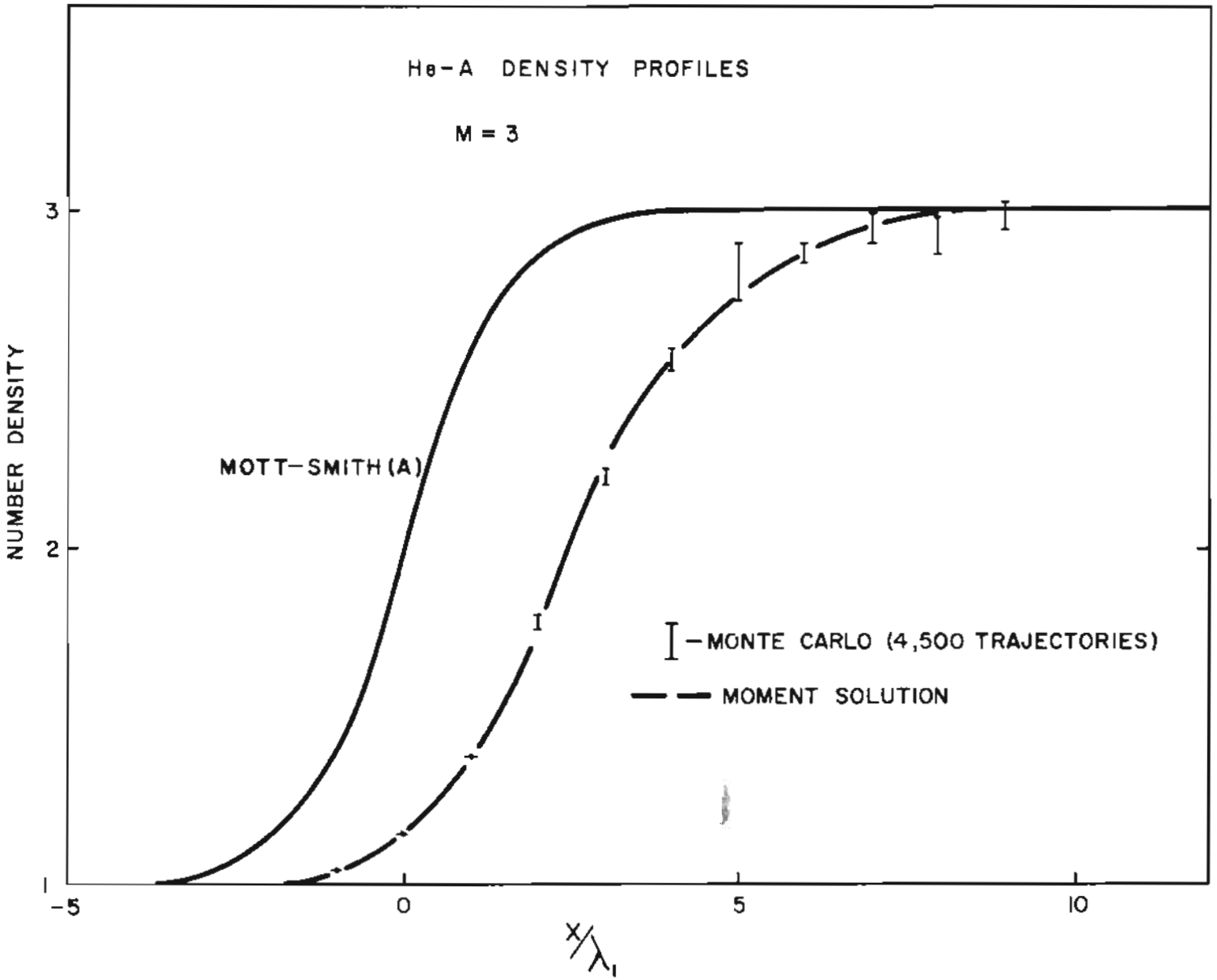

FIG. 7 NUMBER DENSITY PROFILES FOR A TRACE OF ARGON IN A MACH 3 HELIUM SHOCK

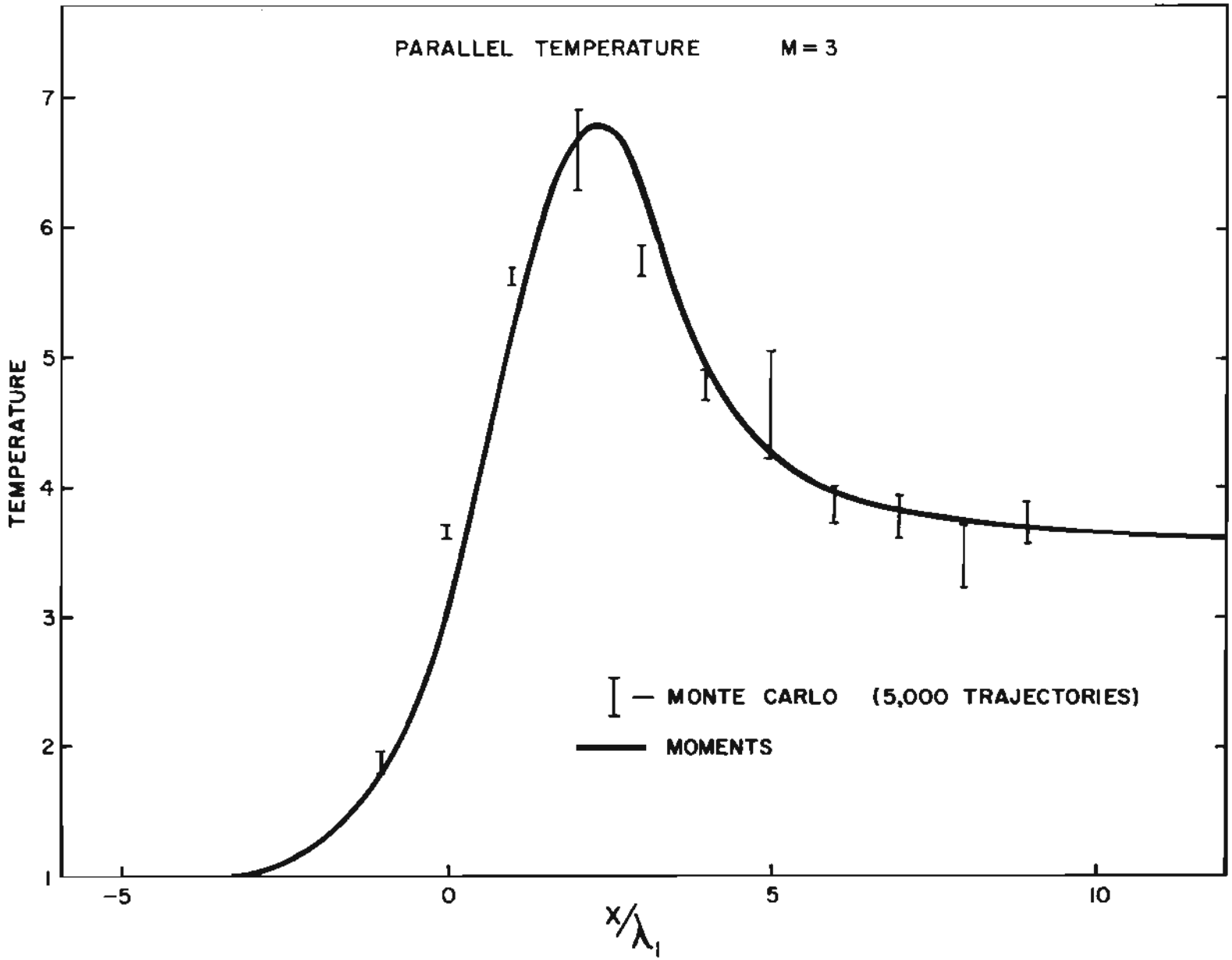

FIG. 8 TEMPERATURE PROFILE FOR A TRACE OF ARGON IN A MACH 3 HELIUM SHOCK

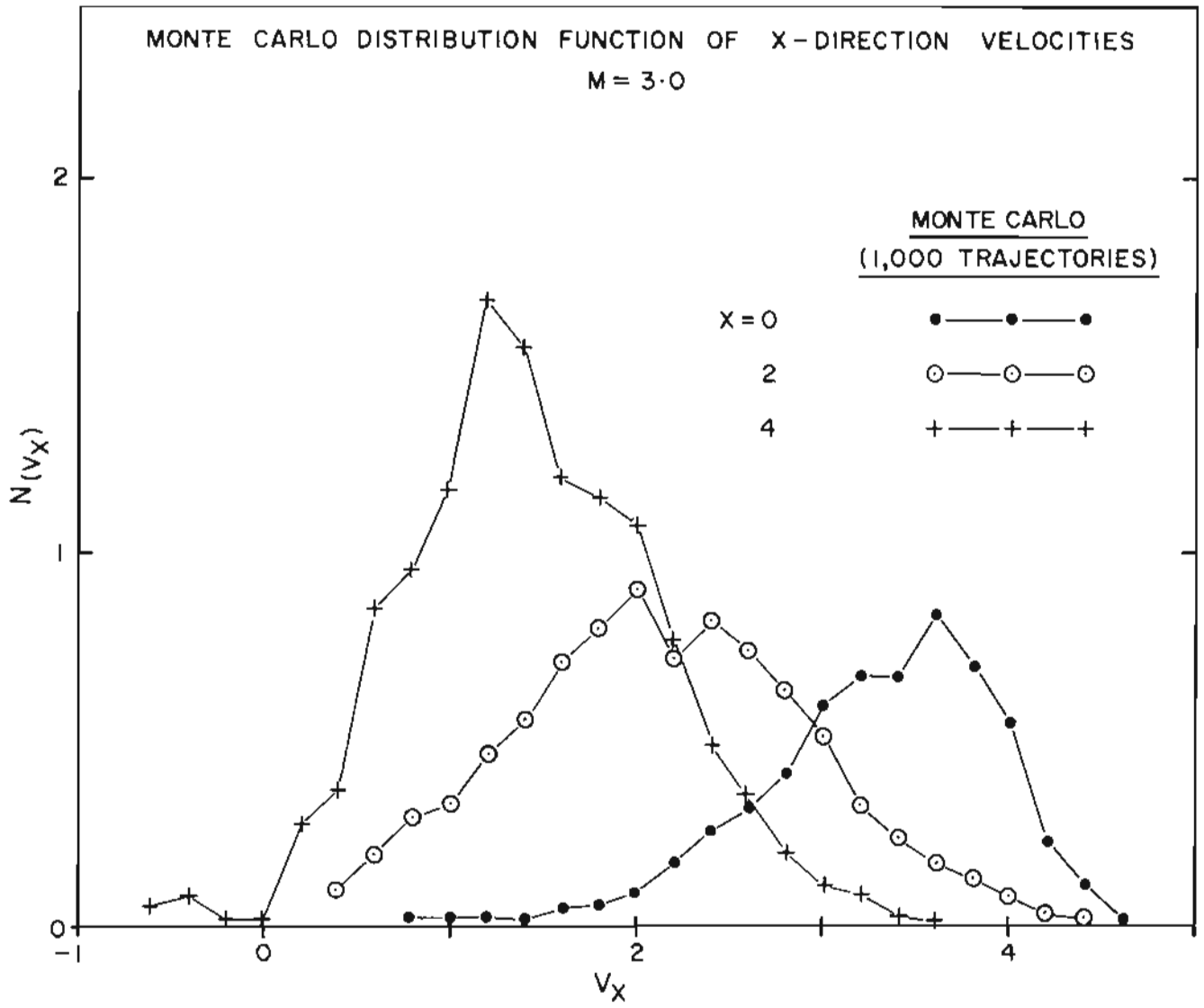

FIG. 9(a) DISTRIBUTION OF x-DIRECTION VELOCITIES FOR THE TRACE OF ARGON CALCULATED FROM THE MONTE CARLO SOLUTION AFTER 1000 PARTICLE TRAJECTORIES (HELIUM SHOCK MACH NUMBER 3).

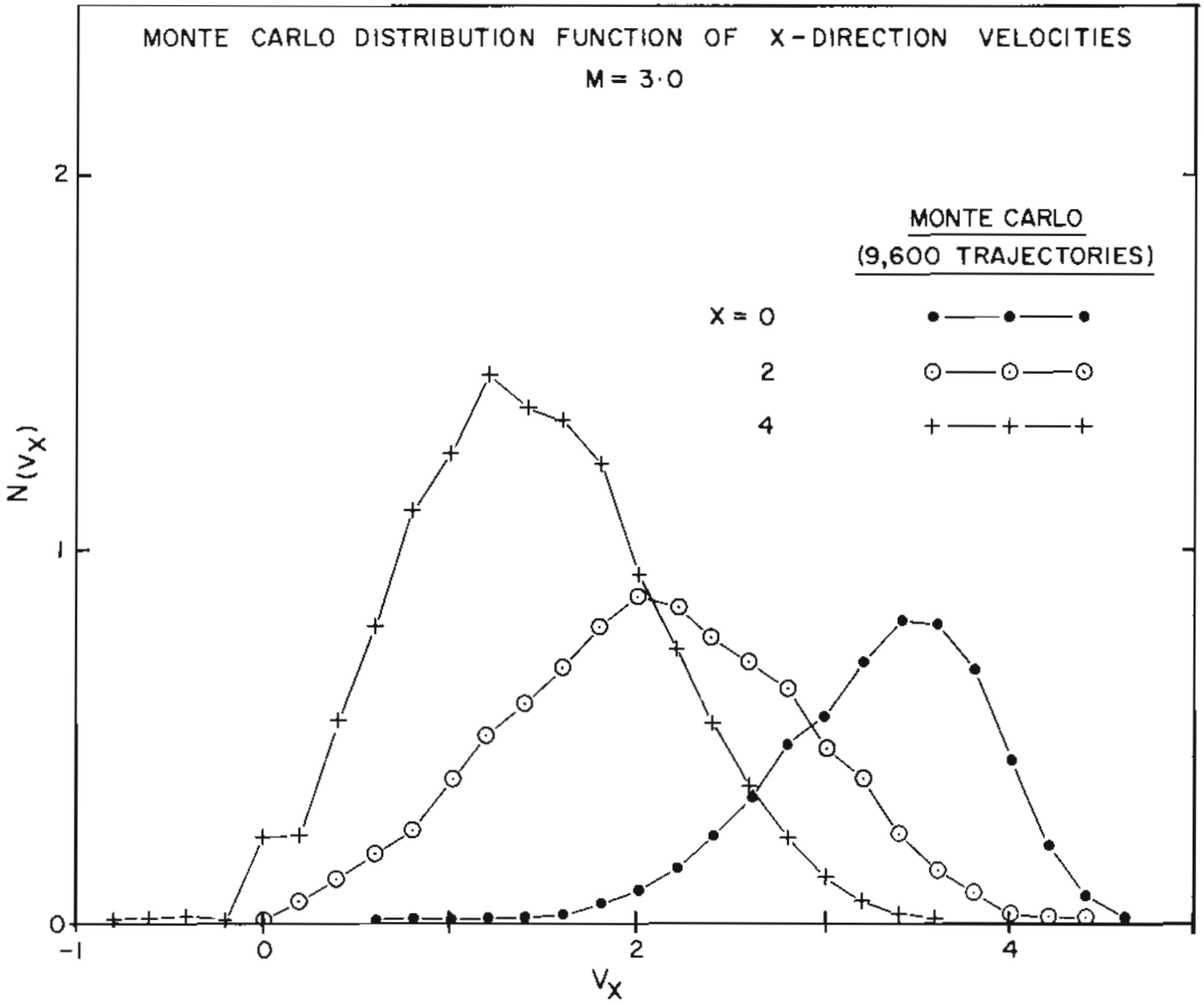

FIG. 9(b) DISTRIBUTION OF x-DIRECTION VELOCITIES FOR THE TRACE OF ARGON CALCULATED FROM THE MONTE CARLO SOLUTION AFTER 9600 PARTICLE TRAJECTORIES (HELIUM SHOCK MACH NUMBER 3)

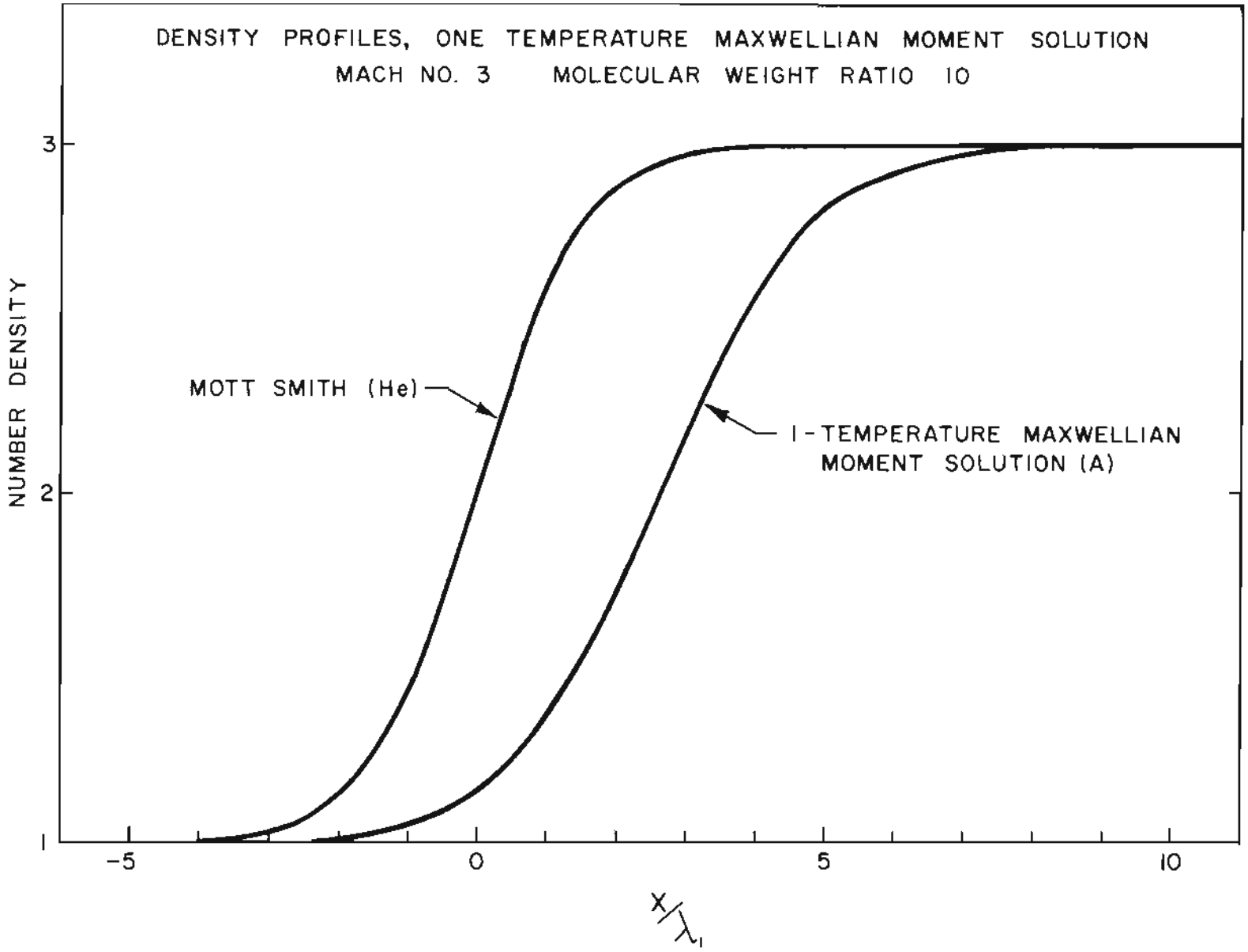

FIG. 10 THE SIMPLE MAXWELLIAN MOMENT SOLUTION DENSITY PROFILE (HELIUM SHOCK MACH NUMBER 3).

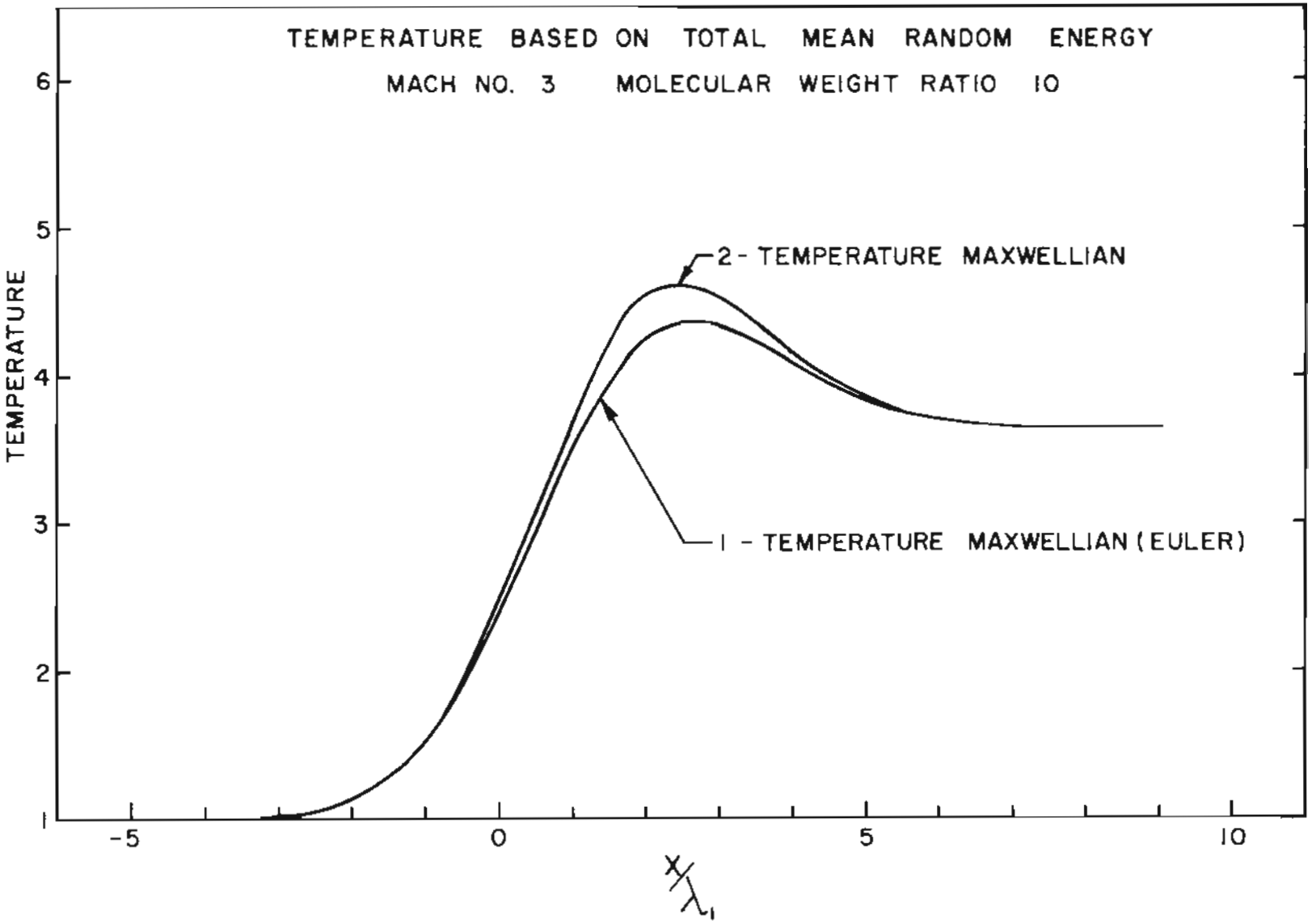

FIG. 11 COMPARISON OF TEMPERATURE PROFILES FOR THE DIFFUSING HEAVY SPECIES CALCULATED FROM THE ONE AND TWO TEMPERATURE MAXWELLIAN MOMENT SOLUTIONS

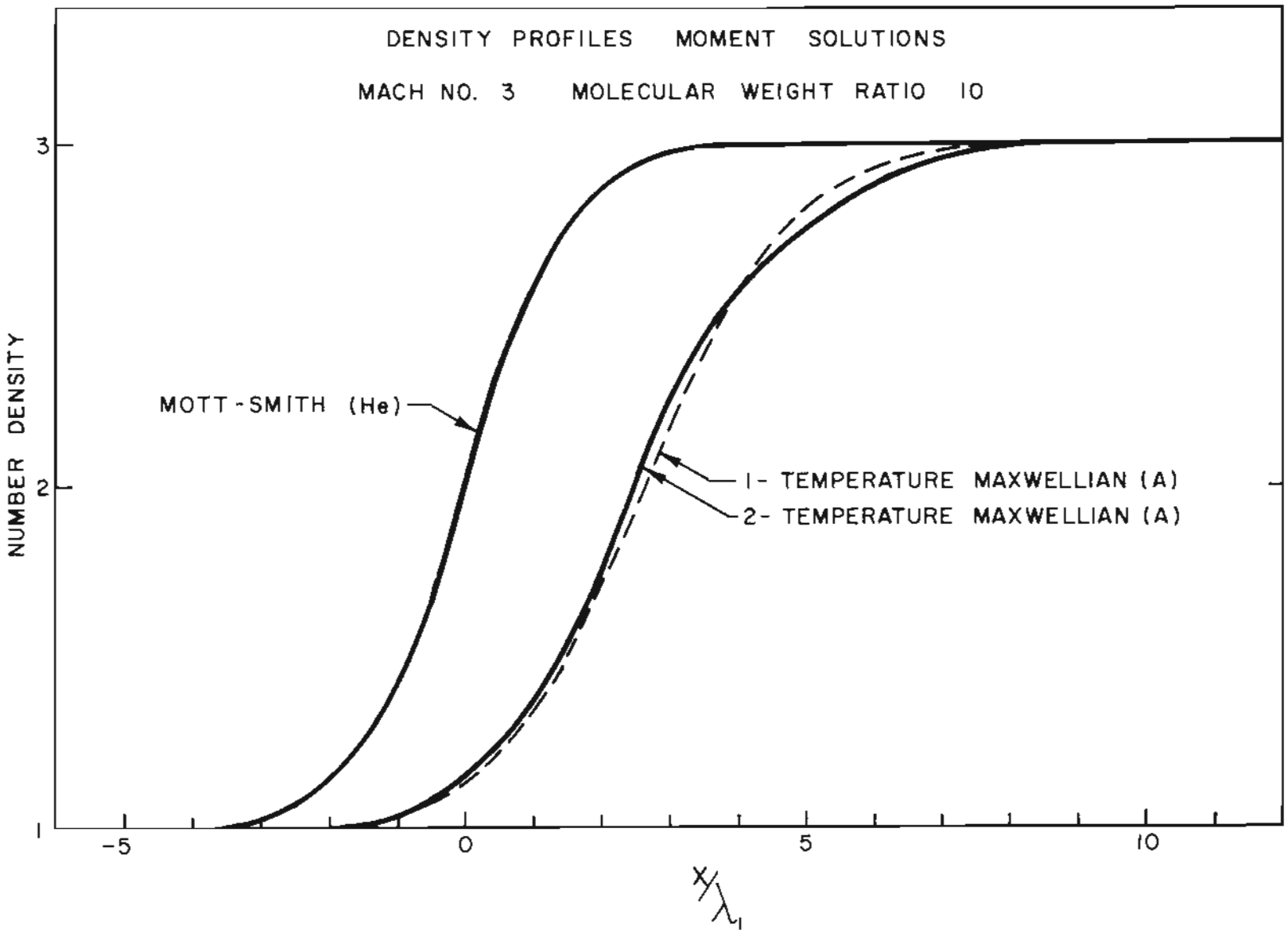

FIG. 12 COMPARISON OF THE DENSITY PROFILES OF THE DIFFUSING HEAVY SPECIES CALCULATED FROM THE ONE AND TWO TEMPERATURE MAXWELLIAN MOMENT SOLUTIONS.

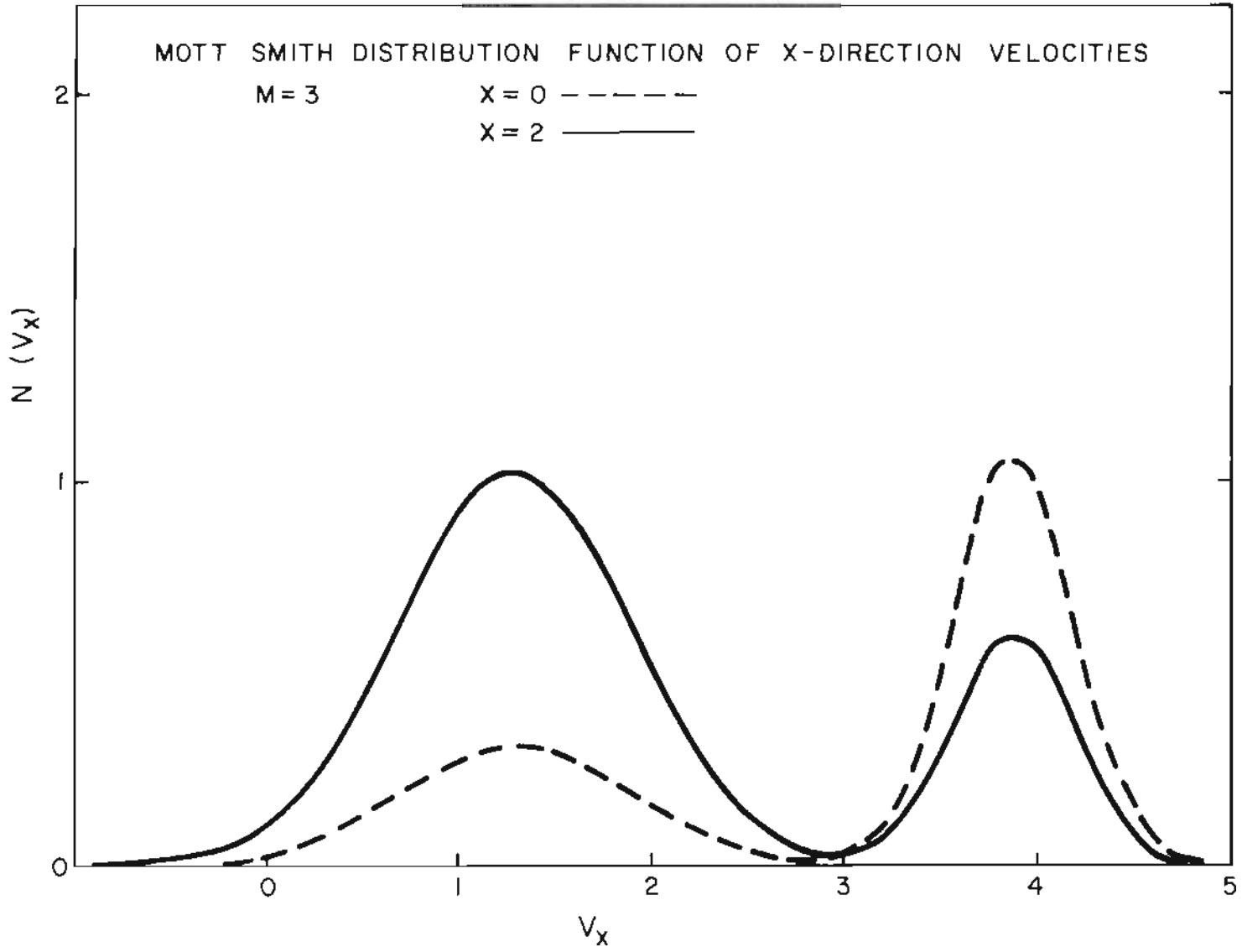

FIG. 13 DISTRIBUTION OF x-DIRECTION VELOCITIES FOR THE TRACE OF ARGON CALCULATED FROM THE SIMPLE MOTT-SMITH DISTRIBUTION FUNCTION (HELIUM SHOCK MACH NUMBER 3)

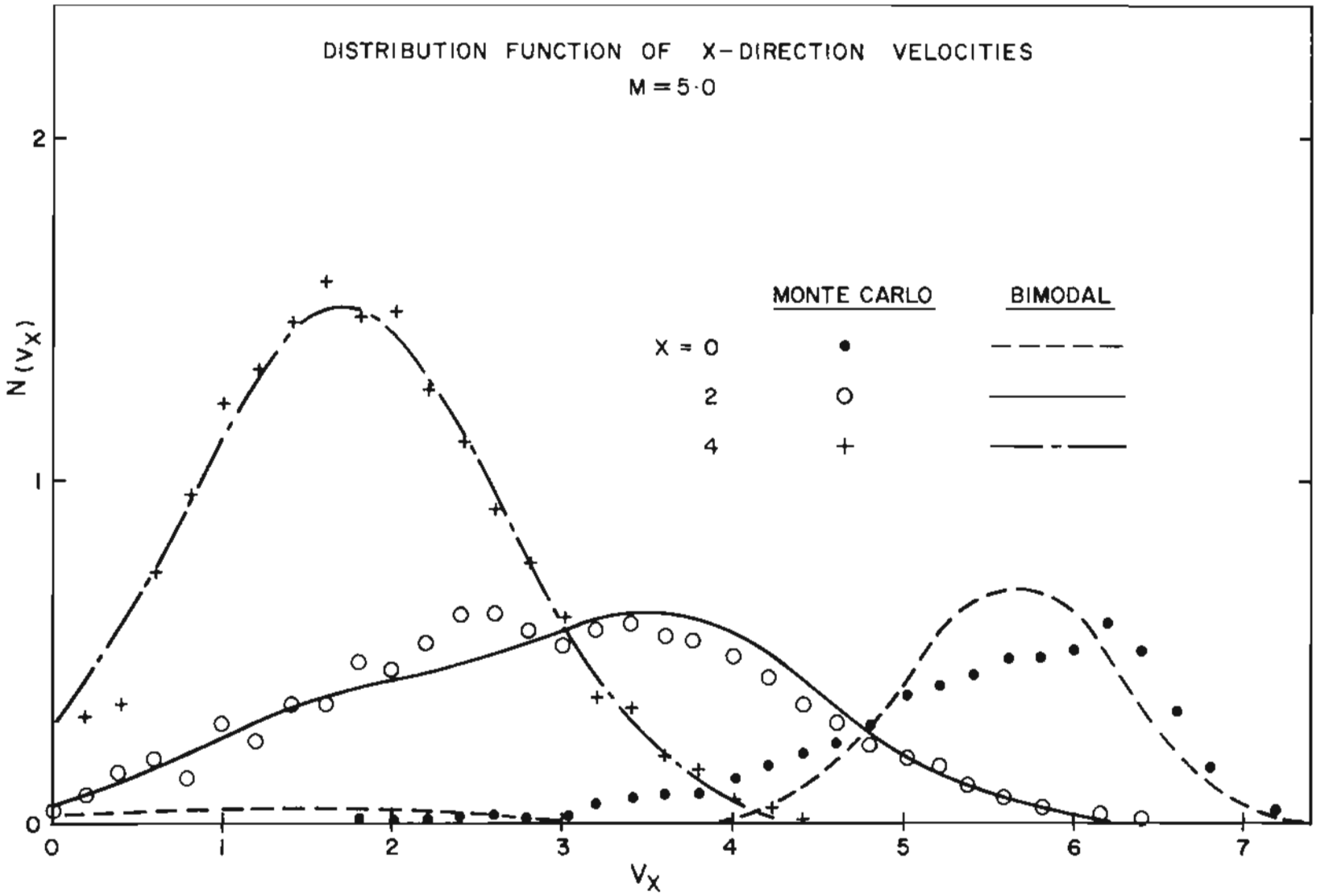

FIG. 14 DISTRIBUTION OF x-DIRECTION VELOCITIES FOR THE TRACE OF ARGON CALCULATED FROM THE MONTE CARLO SOLUTION AFTER 3600 PARTICLE TRAJECTORIES. THE DOWNSTREAM ANCHORDED BIMODAL MOMENT SOLUTION IS SHOWN FOR COMPARISON.

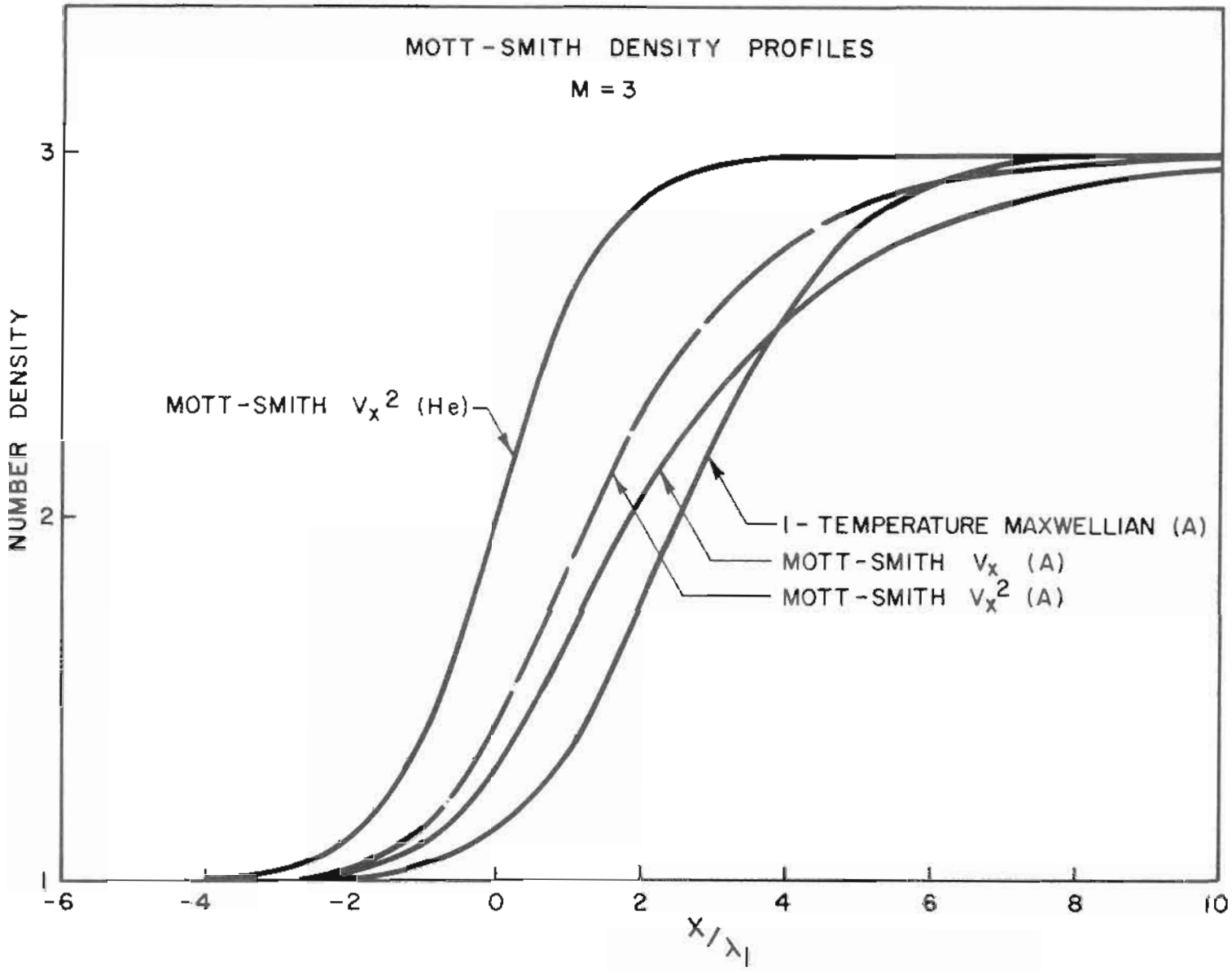

FIG. 15 COMPARISON OF THE DENSITY PROFILES OF THE DIFFUSING HEAVY SPECIES CALCULATED FROM THE SIMPLE MOTT-SMITH AND ONE-TEMPERATURE MAXWELLIAN SOLUTIONS

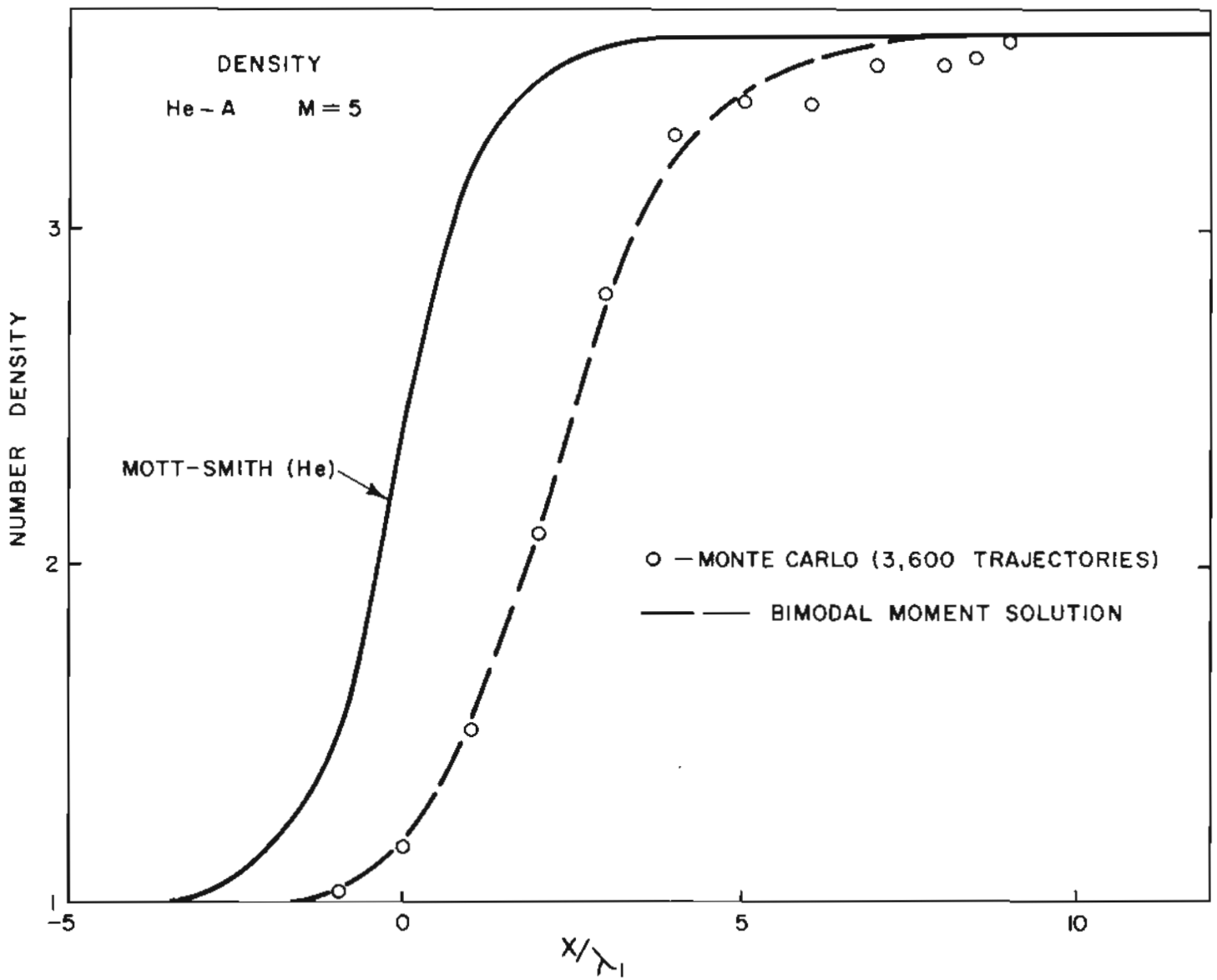

FIG. 16 COMPARISON OF THE DENSITY PROFILES OF THE DIFFUSING HEAVY SPECIES CALCULATED FROM THE MONTE CARLO SOLUTION AFTER 3600 PARTICLE TRAJECTORIES AND FROM THE BIMODAL MOMENT SOLUTION.

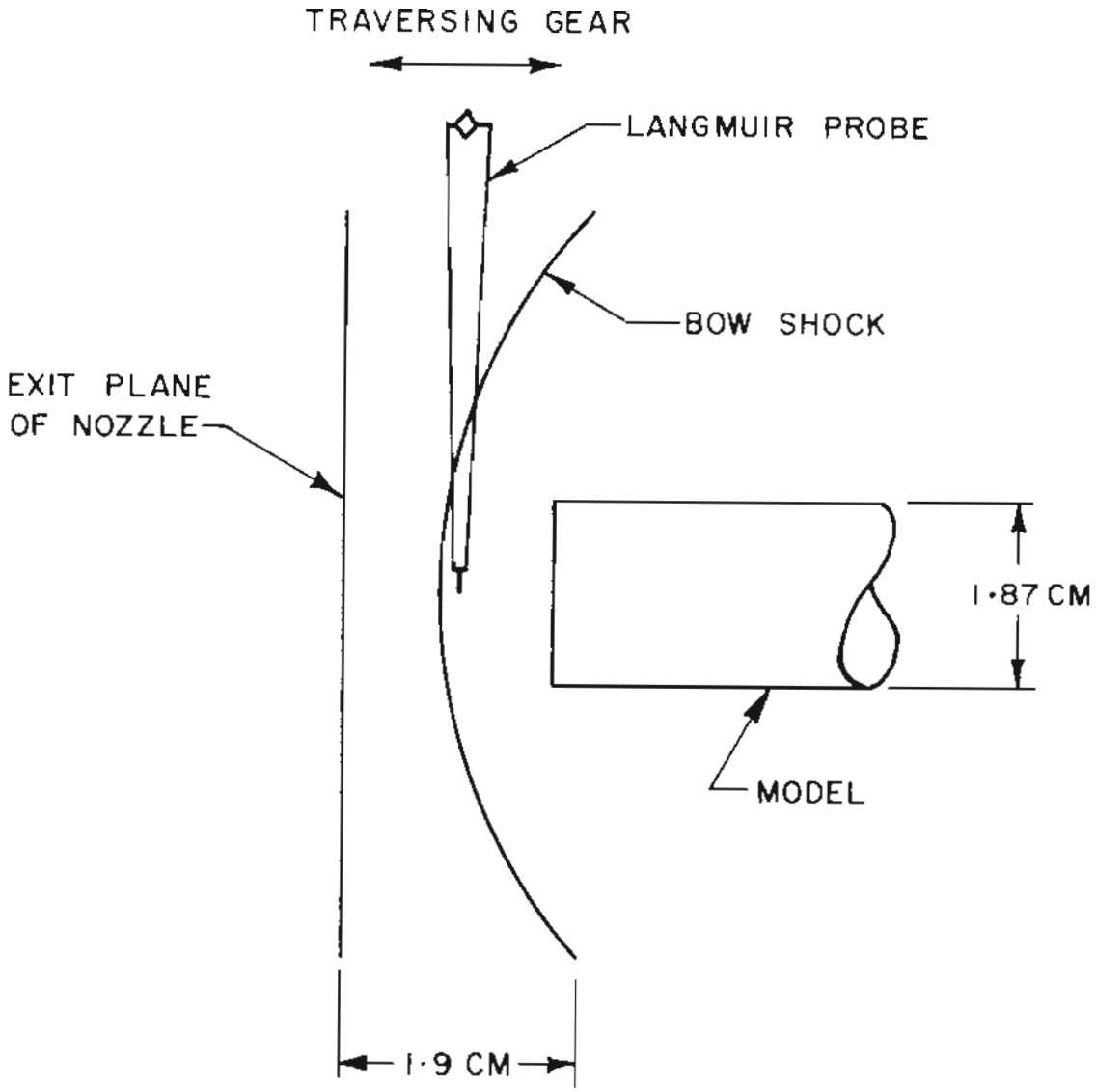

FIG. 17 SCHEMATIC REPRESENTATION OF SONIN'S SHOCK STRUCTURE EXPERIMENT.

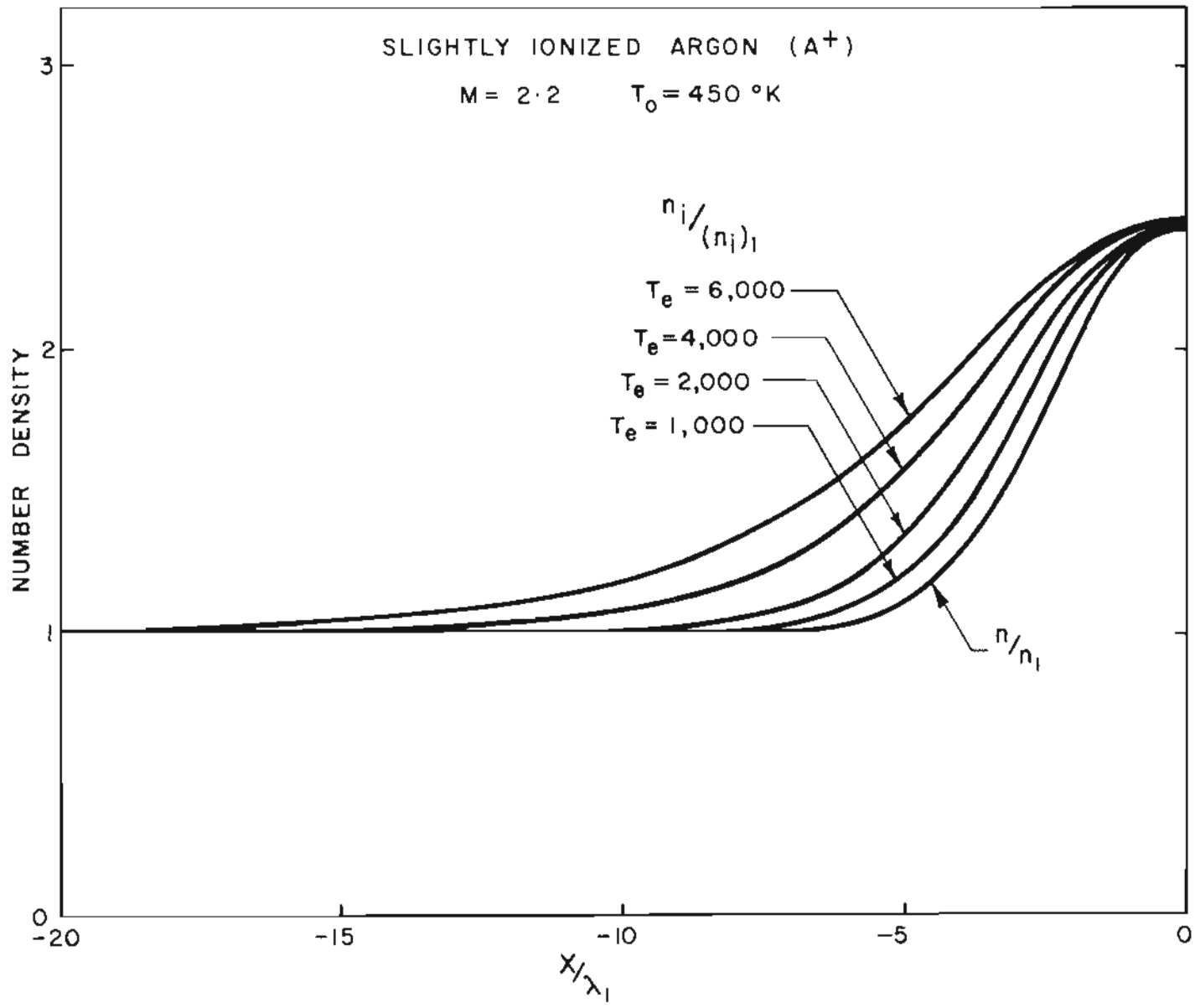

FIG. 18 DEPENDENCE OF THE ION SHOCK STRUCTURE ON ELECTRON TEMPERATURE

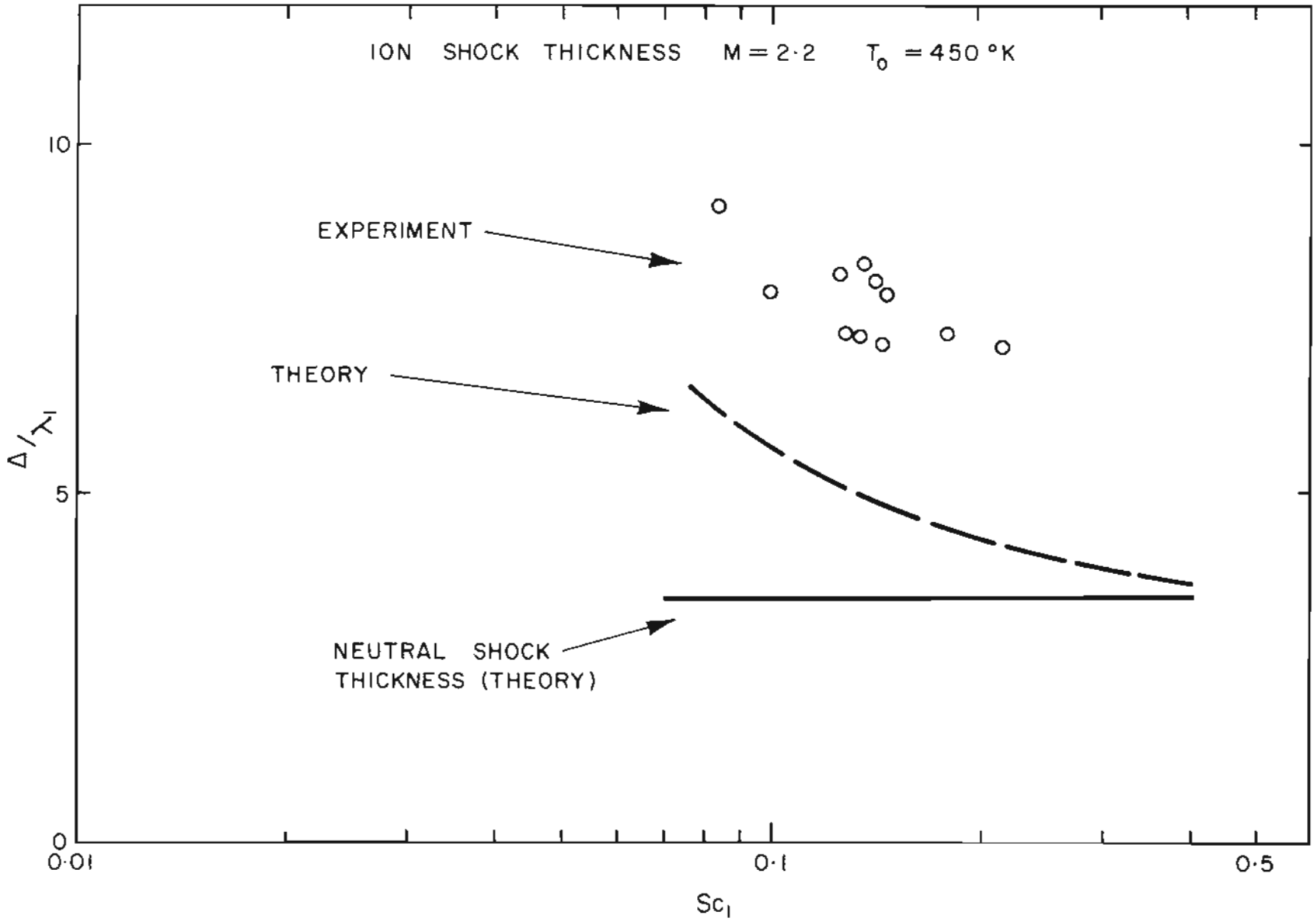

FIG. 19 COMPARISON BETWEEN EXPERIMENTAL AND THEORETICAL SHOCK WAVE THICKNESS AS A FUNCTION OF AMBIPOLAR SCHMIDT NUMBER

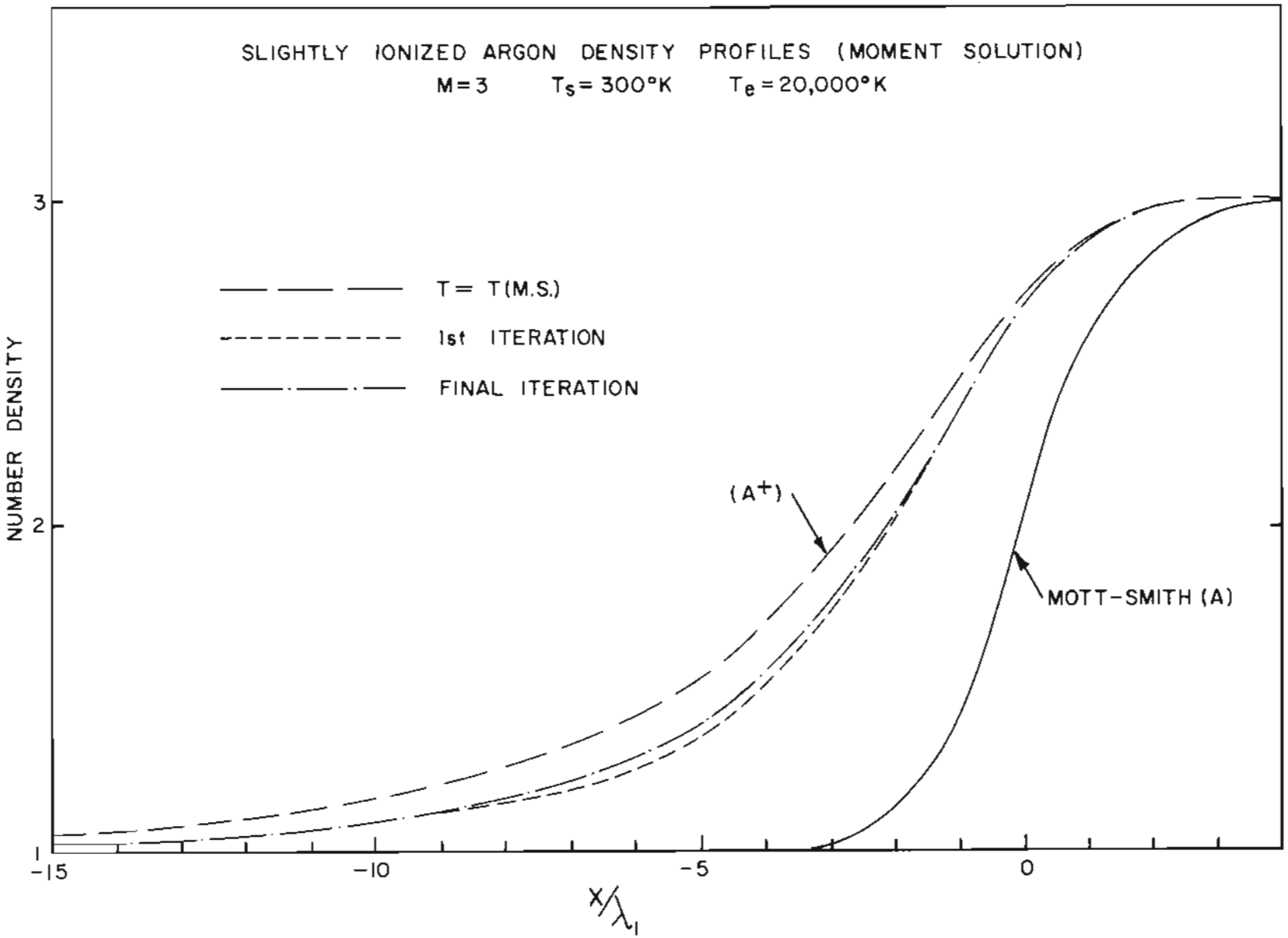

FIG. 20 CONVERGENCE OF THE ITERATIVE SOLUTION FOR THE ION NUMBER DENSITY PROFILE

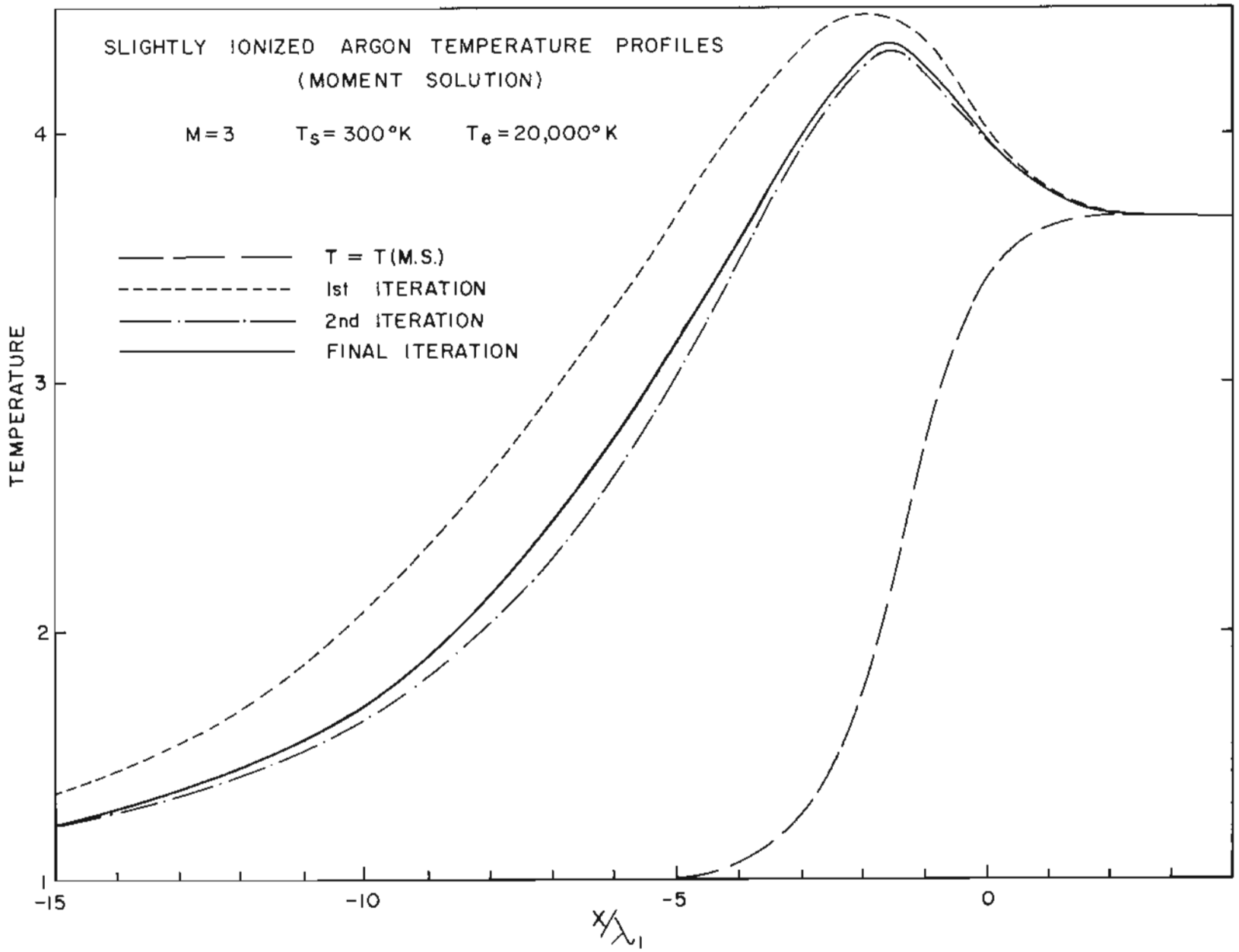

FIG. 21 CONVERGENCE OF THE ITERATIVE SOLUTION FOR THE ION TEMPERATURE PROFILE

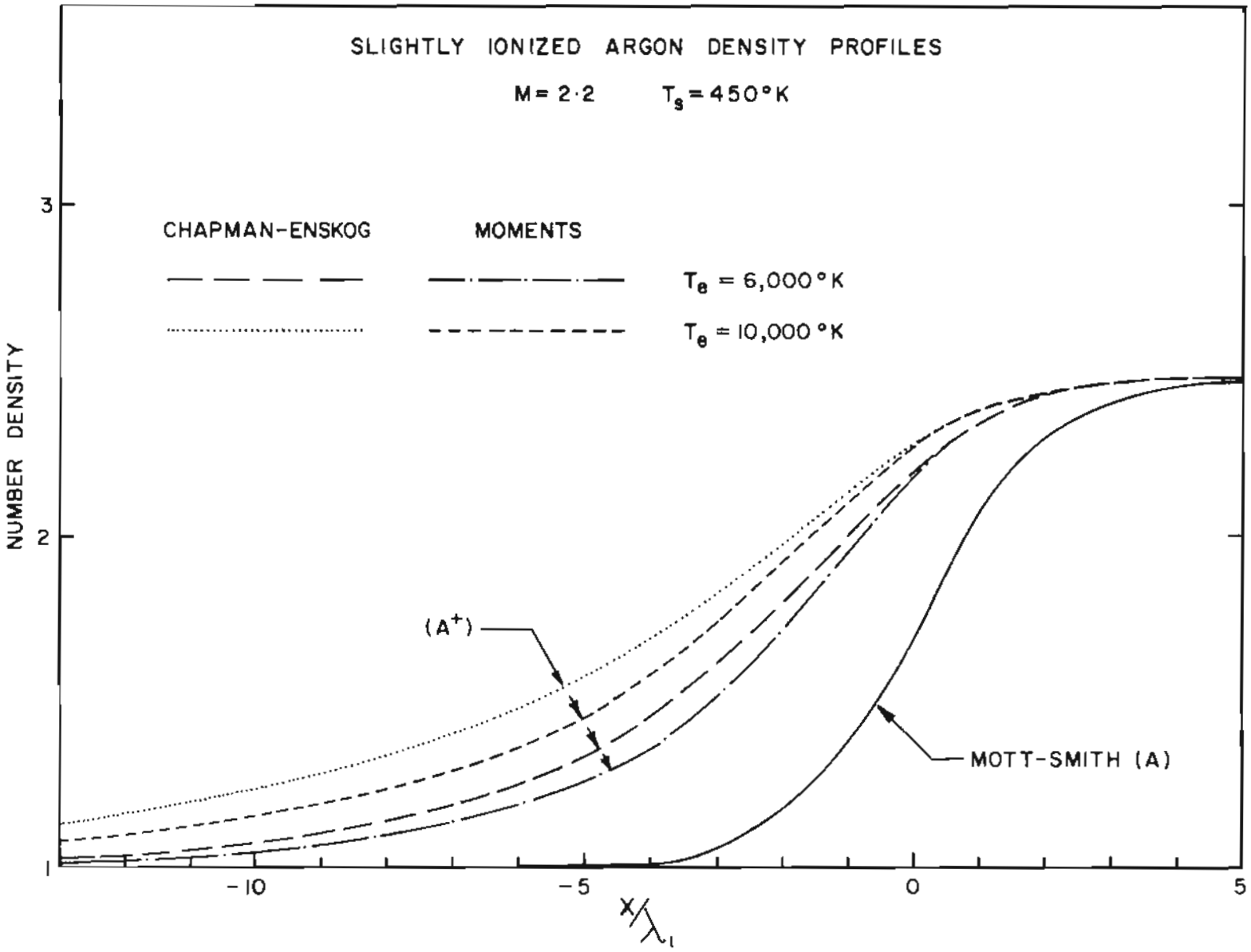

FIG. 22 COMPARISON OF THE DENSITY PROFILES OF THE SIMPLE SOLUTION OF SECTION 6.1 AND THE MOMENT SOLUTION OF SECTION 6.2

UNCLASSIFIED

Security Classification

DOCUMENT CONTROL DATA - R & D

(Security classification of title, body of abstract and indexing annotation must be entered when the overall report is classified)

1. ORIGINATING ACTIVITY (Corporate author)
University of Toronto
Institute for Aerospace Studies
Toronto, Ontario, Canada

2a. REPORT SECURITY CLASSIFICATION
UNCLASSIFIED

2b. GROUP

3. REPORT TITLE

SHOCK WAVE STRUCTURE IN GAS MIXTURES AND PLASMAS

4. DESCRIPTIVE NOTES (Type of report and inclusive dates)
Scientific - Interim

5. AUTHOR(S) (First name, middle initial, last name)

S R M Sinclair

6. REPORT DATE	7a. TOTAL NO OF PAGES	7b. NO. OF REFS
	78	24

8a. CONTRACT OR GRANT NO AF-AFOSR-276-66

b. PROJECT NO 9783-01

c. 6144501F

d. 681307

9a. ORIGINATOR'S REPORT NUMBER(S)
UTIAS REPORT NO. 130

9b. OTHER REPORT NO(S) (Any other numbers that may be assigned this report)
AFOSR-68-0576

10. DISTRIBUTION STATEMENT

1. Distribution of this document is unlimited.

11. SUPPLEMENTARY NOTES
TECH, OTHER

12. SPONSORING MILITARY ACTIVITY
AF Office of Scientific Research (SREM)
1400 Wilson Boulevard
Arlington, Virginia 22209

13. ABSTRACT This research has been concerned with a theoretical description of shock wave structure in gaseous mixtures when diffusive effects are important. The problem considered in detail is the structure of a shock wave in a helium-argon mixture in which the argon is present in very small concentration. An anomalous result cited in the literature, suggesting that the argon undergoes an initial pre-expansion before compression, has been analysed to show the theoretical origin of this effect. In view of the lack of definite experimental data with which to compare calculations for binary shock structure, an "exact" numerical experiment has been formulated. The velocity distribution of a trace of heavy gas (and its lower moments) are watched as the heavy particles pass through a Mott-Smith background shock of lighter particles. The Mott-Smith background is chosen because its bimodal Maxwellian form provides an analytical determination of the free path to the next event for the heavy test particle at any point along its trajectory. This so-called Monte Carlo solution to the idealized diffusion shock problem is exact within the limits of statistical flucuations due to the finite sample of heavy test particles, and can be used as a standard for evaluating the diffusion equations derived from various kinetic theory approximations. A number of systems of moment equations of the heavy particle Boltzmann equation have been solved and the resulting heavy particle moment profiles have been compared with those of the Monte Carlo solution. A second strong diffusion problem has been analysed from a kinetic theory point of view. It has been found experimentally that the ion density profile through a shock in a weakly ionized plasma with elevated electron temperature is much more diffuse than the neutral atom shock. The theoretical analysis shows that this strong diffusion effect can be attributed to the electrical coupling between the ions and the hotter electron gas.

DD FORM 1 NOV 68 1473

UNCLASSIFIED

Security Classification

14 KEY WORDS	LINK A		LINK B		LINK C	
	ROLE	WT	ROLE	WT	ROLE	WT
Shock Transition						
Diffusive Separation						
Shock Wave in Ionized Gas						